University of Messina

University of Reggio Calabria

DOCTORATE COURSE IN

CIVIL, ENVIRONMENTAL AND SAFETY ENGINEERING

XXXIV CICLE

Curriculum: Science and technology, materials, energy, and complex systems for distributed computing and networks (ICAR/03 - CHIM/07)

Sustainable Process for the Complete Upgrading of Orange Peel Waste into Value-Added Chemicals and Bio-Carbon Materials

Head of Doctoral School:
Prof. Gaetano Bosurgi

PhD:
Antonella Satira

Supervisor:
Prof. Paolo S. Calabrò

Co-Supervisor:
Prof. Francesco Mauriello
Prof.ssa Claudia Espro

A.A 2020/2021

A Filippo,

per avermi reso un chimico migliore

Nelle cose confuse l'ingegno si desta a nuove invenzioni.

Dal sogno dell'alchimia nacque la realtà della chimica.

Carlo Dossi, Note Azzurre, 1870/1907

Index

Abstract

This doctoral work is focused on the complete upgrading of orange peel waste (OPW) into value-added chemicals and bio-carbon materials through the development of sustainable strategies for the valorization of the citrus waste.

Chapter 1 contains a general overview of the sustainability concepts and the use of biomass for the production of various value-added products. Furthermore, an extensive overview of the chemical composition and the utilization of the OPW, along with the recent advances in the recovery and catalytic upgrading of value-added chemicals from OPW is provided.

In particular, as described in **Chapter 2**, a simple and green protocol was first investigated to obtain hydrochar and high-added value products, mainly 5-hydroxymethylfurfural (5-HMF), furfural (FU), levulinic acid (LA), and alkyl levulinates, by using the Hydrothermal Carbonization (HTC) process of the OPW. Process variables, such as reaction temperature (180-300 °C), reaction time (60-300 min), biomass: water ratio, and initial pH were investigated in order to find the optimum conditions that maximize the yields of 5-HMF and levulinates in the light bio-oil. Data obtained evidence that the highest yield of hydrochar is obtained at a 210 °C reaction temperature, 180

min residence time, 6/1 w/w orange peel waste to water ratio and a 3.6 initial pH. The bio-products distribution strongly depends on the applied reaction conditions. Overall, 180 °C was found to be the best reaction temperature that maximizes the production of furfural and 5-HMF in the presence of pure water as a reaction medium.

Chapter 3 reports the complete characterization of the hydrochar samples, carried out by various complementary techniques such as TGA, XRD, SEM-EDX, FT-IR, and BET surface area, highlights their different morphological and microstructural characteristics. These modifications are also accomplished by variations of the electrical and electrochemical properties, which are here exploited, for the first time, for the development of high performances chemical sensors based on HC as sensing element. Hydrochar derived from OPW treatment at 300 °C HC300 shows the best characteristics, and thereby is used for the fabrication of a conductometric NO_2 and electrochemical dopamine sensors. The conductometric HC300-based sensor was demonstrated to be sensitive up to a 50 ppb of NO_2 in air 100 °C. Dopamine at nanomolar concentration was detected with good performances (large linear detection range from 0 to 1000 µM, and low limit of detection (LOD) of 180 nM) on the HC300-based electrochemical sensor.

Chapter 4 is dedicated to the transformation of limonene into p-cymene over a Pd/C catalyst under both batch and continuous gas-flow conditions. A complete transformation of limonene into p-cymene is shown to be achieved at 300 °C in a nitrogen atmosphere under continuous gas-flow conditions. Based on the selectivity values obtained for p-cymene and by-products, a mechanistic scheme for the transformation of limonene into p-cymene over Pd/C catalyst is proposed. In addition, the catalytic conversion of methyl and ethyl levulinates into γ-valerolactone (GVL) by using alcohols (methanol, ethanol and 2-propanol) as the H-donor/solvent is presented. These reactions are promoted by the ZrO_2 catalyst under both batch and continuous gas-flow

conditions. Under batch conditions, ethyl levulinate provides the highest yield to GVL, with 2-propanol which are found to be the best H-donor molecule. The reactions occurring under continuous gas-flow conditions were found to be much more efficient, providing excellent yields in GVL with ethanol as the H-donor/solvent. These experiments clearly show that the high reducing activity of alcohols is the main factor driving the CTH process, while the tendency to attack the esteric group is the key step in the formation of transesterification products.

In the last part, presented in **Chapter 5**, final conclusions of this PhD thesis are described.

AIM of the thesis

Citrus fruits are among the most worldwide cultivated fruits. The global orange production is estimated up 2.5 million tons from the previous year to ~ 48.6 for the 2020/21 [FAS-USDA, 2021], and the citrus processing industry yearly generates huge amounts of agricultural waste, in the form of peel, pulp, and segment membranes, from the extraction of citrus juice in industrial plants, and citrus peel waste alone accounts for almost 50% of the wet fruit mass. The considerable volume characterizes the exhausted citrus peel as well as the high biodegradability that involves high rates of fermentation processes. Therefore, the direct disposal of this secondary product, without previous proper processing, causes serious environmental issues and economic loss for the citrus industry [Raimondo et al., 2018]. Different potential ways for the recovery and utilization of these wastes have been proposed in the past years. Fermentation aimed to bio-ethanol extraction, flavonoids and chemicals recovery, use as organic soil fertilizer, or as animal feed to cite a few are some of the main utilization [Zema et al., 2018].

This research project is inserted in this scientific and technological context and focuses on the development of innovative strategies for the valorization of citrus waste as a useful example for generating new market and non-market values (Scheme 1). In this regard, the research activity was focused

first on the investigation of the optimum conditions that maximize the yields of high-added value products, mainly furfural (FU), 5-hydroxymethylfurfural (5-HMF) and levulinates, by using the hydrothermal carbonization of the OPW, which is among the most promising thermochemical technologies for the energy valorization of the agro-industrial waste.

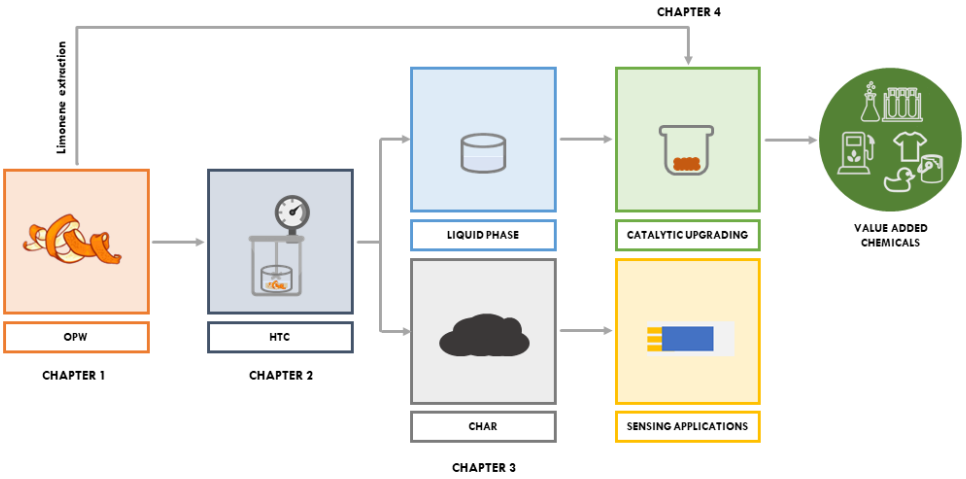

Scheme 1. Schematic representation of the research project.

Then, the second aim of this doctoral work was the preliminary study of the possible application of the obtained hydrochar, a promising material that has a huge potential to be used in a wide range of applications, for the development of chemo- and bio-sensors.

The last part of this doctoral study is dedicated to the development of a clean process to transform limonene, the principal component of essential oils obtained from the rinds of various citrus fruits, widely used in cosmetic and perfume industries, into p-cymene, a value-added product used in the chemical industry, by using the commercial Pd/C catalyst, easily reused and recovered. On the other hand, the research activity is also concerned with the evaluation of the catalytic conversion of methyl and ethyl levulinate into γ-valerolactone (GVL), commonly used, as an intermediate, in fine chemicals synthesis, and as a starting material for the production of bio-based polymers

and resins, with particular attention to the optimization of operating parameters. These reactions were performed by using alcohols as reducing agents and were promoted by the ZrO_2 catalyst.

References

FAS-USDA (Foreign Agricultural Service-United States Department of Agriculture). Citrus: world markets and trade, **2021**. Available online: https://apps.fas.usda.gov/psdonline/circulars/citrus.pdf.

Raimondo, M.; Caracciolo, F.; Cembalo, L.; Chinnici, G.; Pecorino, B.; D'Amico, M. Making Virtue Out of Necessity: Managing the Citrus Waste Supply Chain for Bioeconomy Applications. *Sustainability* **2018**, *10*, 4821.

Zema, D.A.; Calabrò, P.S.; Folino, A.; Tamburino, V.; Zappia, G.; Zimbone, S.M. Valorisation of citrus processing waste: A review. *Waste Management* **2018**, *80*, 252-273.

Chapter 1

General Introduction and Scientific Background of the PhD Thesis

1.1 The Sustainability concept

1.1.1. Agenda 2030 and 12 green chemistry principles

In recent decades, the scientific research has increasingly focused on protecting the environment and reducing pollution with the aim of using renewable sources and reducing waste substances that have a harmful environmental impact. This prompted the great representative heads of state of the United Nations in 2015 to enter into an universal action plan aimed at a sustainable development and the prosperity of the planet. This plan is called *Agenda 2030* that is based on 17 objectives summarized in Figure 1.1, and 169 indivisible goals [SSDGs, 2019]. These SDGs are tangible objectives aimed to improve the management of economic and environmental resources through

cooperation between states *win-win* that allows enormous gains to be obtained for all countries of the world, with a horizon that reaches up to 2030. The UN defines sustainable development as **a development that satisfies the needs of the present without compromising the ability of future generations to meet their own needs**.

Figure 1.1. The United Nations Sustainable Development Goals [SSDGs, 2019].

In this context of sustainability, there is the need to redirect industries, mainly chemical ones, on paths of the eco-sustainability: a sustainable development that requires chemistry to play a primary role in the conversion of old technologies into new *clean* processes and in the design of new products and new processes that are increasingly eco-compatible by preventing environmental pollution [Sheldon, 1997].

The term *green* once linked only to the term sustainable, has now been expanded to regulate economic and social dynamics such as the reduction of carbon dioxide emissions, the reuse of waste materials, the use of softer chemical-energy processes. Hence the term Green Chemistry constitutes a different way of approaching the work of the chemist, both at an academic and

industrial level. Green Chemistry is therefore governed by 12 principles [Anastas and Warner, 1998]:

1. **Prevent**: designing chemical syntheses to avoid waste, disposing of waste or reusing it;
2. **Atomic economy**: designing synthesis so that the final product contains the maximum percentage of starting materials, thus maximizing the economy so that no atom is wasted;
3. **Less dangerous chemical syntheses**: designing syntheses that use or generate substances with minimal or no toxicity to humans or the environment;
4. **Designing safer chemicals**: developing chemicals that are fully effective but have little or no toxicity;
5. **Safer solvents and reaction conditions**: use solvents, separating agents or other auxiliary chemicals that are harmless to health;
6. **Energy requirement**: perform energy-saving chemical reactions, conducted at ambient temperature and pressure;
7. **Renewable raw materials**: use starting materials that are renewable rather than exhaustible;
8. **Chemical derivatives**: avoid the use of protective groups or any temporary changes, since the derivatives require the use of additional substances that generate waste;
9. **Catalysis**: minimize waste by using catalytic reactions. Catalysts are effective in small quantities and can perform a single reaction many times. They are preferable to stoichiometric reagents, which are used in excess and perform a reaction only once;
10. **Design of chemical products to be degraded after use**: design chemical products that reduce non-harmless substances after use so that they do not accumulate in the environment;

11. **Analyze in real time to prevent pollution**: include real-time monitoring and control during syntheses to minimize or eliminate the formation of by-products;
12. **Minimize the risk of accidents**: design chemical products and their physical forms (solid, liquid or gaseous) to minimize the potential for chemical accidents including explosions, fires and the release of substances into the environment.

1.1.2 Bio-based economy in Europe: state of art and future perspectives

According to the 7th principle of Green Chemistry, renewable sources of raw materials should be preferred as starting material to exhaustible ones: renewable sources are often agricultural products, citrus waste or waste from other processes. Sources of exhaustible raw materials are often fossil resources (oil, natural gas or coal) or residues from mining activities. Today, about three-quarters of the world's energy is provided by fossil fuels such as coal, oil, and natural gas [Kircher, 2019], which account for 81% of the total supply of primary energy, while nuclear power accounts for 5% and renewable energy sources for 14%. Between these last ones, biomass represents about the 70% [Popp et al., 2020]. In the chemical sector, oil and natural gas account for 11% and 8% of the global primary demand, respectively. However, half of the energy inputs for the industry are used as raw material for chemicals [REN21, 2019].

The growing demand for these non-renewable energy sources does manifest itself at a time when natural reserves are running out: it has been estimated that the world oil reserves may be sufficient to guarantee energy supplies and production of chemicals for the next 40 years [Popp et al., 2020]. Furthermore, the price of emissions allowances traded on the ETS (emissions trading system, the system setting the carbon price in the European Union)

has increased from €8/tonn of CO_2 equivalent at the beginning of 2018 to around €60 more recently (European Emission Allowances, 2021). Beyond the market changes, the rise in prices could also reflect an increase in energy demand caused by the stalled economic recovery due to the pandemic coronavirus (COVID-19). So, biomass is becoming a very valid alternative source for the production of energy, generating fewer greenhouse gas emissions than fossil fuels, because CO_2 released is consumed in the growth process of the biomasses themselves [Tuck et al., 2012].

The EU and the USA have introduced limits on food-based biofuels. Although only 2% of the global earth is used for the production of raw materials from the biofuel industry, the *fuel versus food* debate indicates that biomass used for industrial purposes is a sensitive issue in modern society. The demand for some commodities (e.g. corn, oilseeds, sugarcane, vegetable oil) is relatively high: 20% of the global sugarcane, 12% of the global vegetable oil, and 10% of the global production of coarse grain is used to produce biofuels [Popp et al., 2020].

The term biomass represents a broad concept that includes agricultural waste (e.g. cereal residues, seed crops), agro-food waste, lignocellulosic residues, organic waste (e.g. animal manure), and aquatic organisms (e.g. algae). In addition to biomass, other types of renewable energy sources, such as solar, wind, and water, will play a key role in reducing the dependence on fossil fuels. From a quantitative point of view, the production of fuels from renewable sources certainly is a more interesting goal to achieve than the production of chemicals; this results obviously if we consider that 85% of crude oil is used for the production of fuels and that only 10% is used in developing Chemistry. Unfortunately, however, the cost of using biomass is much higher than fossil fuels. However, the prices of bio-based carbon and fossil-based carbon, as well as the costs of processing bio-based materials with corresponding fossil-based materials, cannot be precisely specified and

depend on raw materials and molecular economy of the processes to the final products. Fossil fuels and basic chemicals are produced from mineral oil refining which results in very high carbon efficiency and rather low labor intensity. On the contrary, biomass requires multiple processing steps, therefore a higher cost and a higher labor requirement [Sheldon, 2016].

In the energy and chemical fields, innovative biotechnology projects have reduced dependence on petroleum and fossil fuels with a positive impact on the environment. In addition, the circular economy and the bioeconomy are converging through the integration of the economic aspects of the circular economy and the sustainable development of the bioeconomy.

1.2 Upgrading of lignocellulosic residues and waste

1.2.1 The lignocellulosic biomasses chemistry and upgrading

The lignocellulosic biomass, which is the most abundant and bio-renewable biomass on earth, is exclusively derived from residues or waste, inedible raw materials, and collected from non-cultivable lands. In fact, the lignocellulosic biomass is readily available worldwide from various waste streams, including agriculture, forestry, and the paper industry. [Pauly and Keegstra, 2008]. Therefore, many studies have shown that the lignocellulosic biomass holds an enormous potential for the sustainable production of biofuels and bio-chemicals [Somerville et al., 2010; Taarning et al., 2011]. Furthermore, the three main constituents of lignocellulose (Figure 1.2), which are cellulose, hemicellulose, and lignin, can be transformed into platform chemicals derived from the biomass with variable compositions and functionalities [Yan et al., 2015].

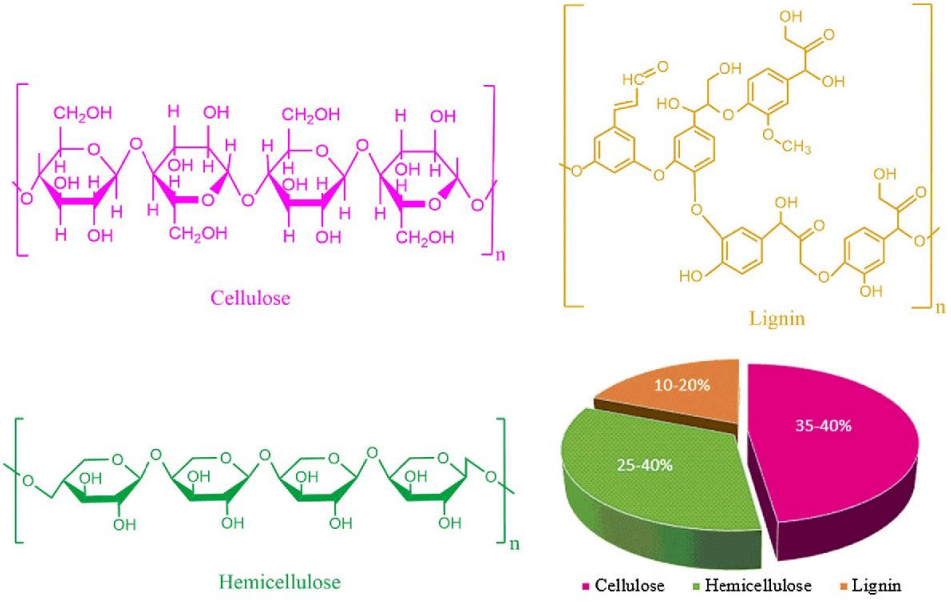

Figure 1.2 Lignocellulose composition: cellulose, hemicellulose and lignin [Amin et al., 2017].

The chemical structure of lignocellulosic biomasses allows the production of a wide spectra of platform chemicals as reported in Figure 1.3.

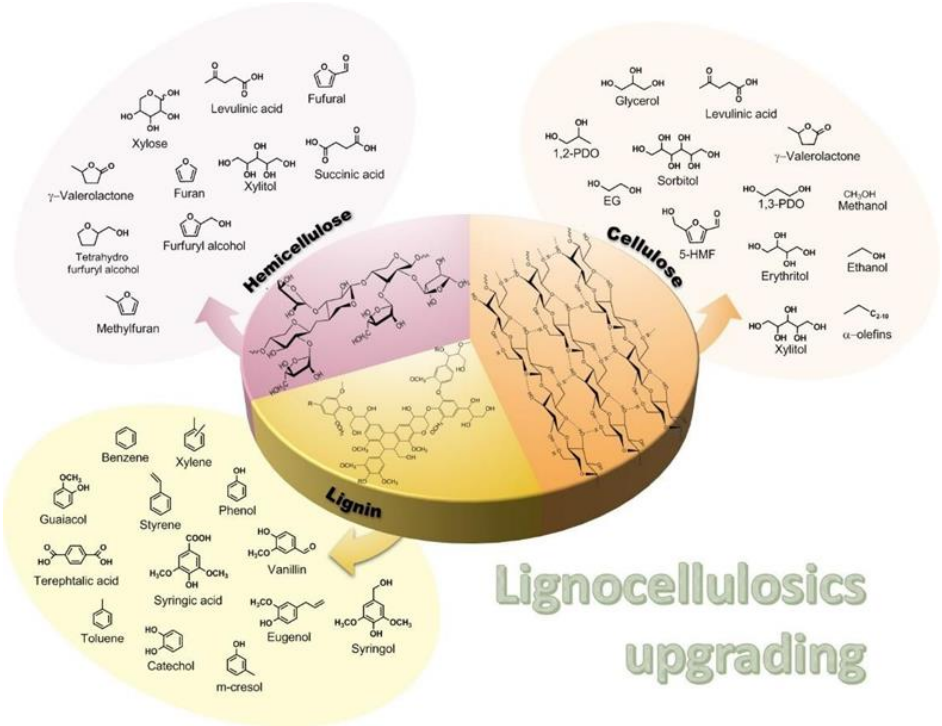

Figure 1.3. Chemical structure of cellulose, hemicellulose, lignin, and related derivable molecules [Espro et al., 2018].

Several pretreatment methods have been developed to access the carbohydrate portion of the lignocellulosic biomass. There have been excellent reviews that provide an account of these pretreatment strategies [Agbor et al., 2011]. Cellulose and hemicellulose allow the production of C5-C6 sugars that can be easily converted into aliphatic acids, ethers, esters, polyols, and alcohols, while lignin is a source of aromatic compounds [Espro et al., 2018].

Cellulose is the major component of lignocellulosic biomass and it is considered to be the strongest potential candidate for the substitution of petroleum-based polymers owing to its eco-friendly properties like renewability, bio-compatibility, and bio-degradability [Ahn et al., 2012]. It is a linear polymer consisting of β-D-glucopyranose units linked via β-1,4-glycosidic bonds, with cellobiose as the fundamental repeating unit glucosidic units, and an average molecular weight of around 100,000 [Chen et al., 2014]. The β-D-glucopyranose units of cellulose are also engaged in the formation of intra- and inter- molecular hydrogen bonds, which involve their hydroxyl groups respectively in the same chain and in the proximate one. This feature maintains the structure of cellulose as a *planar sheet*, which can be packed as well through hydrogen bonds and a large number of Van der Waals weak interactions (Figure 1.4). Therefore, the conversion of cellulose into added-value chemicals and/or fuel components is one of the core technologies in the modern bio-refinery. The crystalline structure of cellulose is responsible for its low solubility in water and its elevated mechanical and chemical stability. The degree of crystallinity, as the degree of polymerization, depends on the kind of biomass and it is generally in the range of 27-63% [Klemm et al., 1998]. The first step of the cellulose valorization is based on its depolymerization into oligomers and glucose followed by several types of catalytic reactions such as hydrogenation, oxidations, and esterification for the manufacture of chemicals

such as C6–C2 polyols, levulinic acid, and 5-hydroxymethylfurfural, among others [Delidovich and Leonhard, 2014].

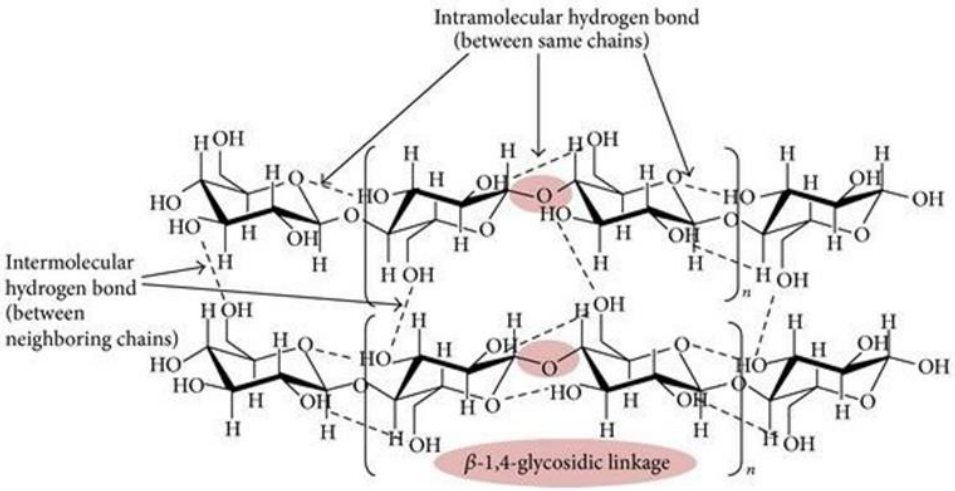

Figure 1.4. Chemical structure of cellulose.

Hemicellulose is the third most abundant biopolymer in nature after cellulose and lignin, representing 20-35% in weight of the lignocellulosic biomass, with a heterogeneous chemical structure of pentoses, hexoses, and sugar acids (Figure 1.5) [Scheller et al., 2010]. The polymerization degree of hemicelluloses is in the range of 100-300 units [Mota et al., 2018], which is much lower than that of cellulose, but it can present a high degree of more or less complex substitutions. Hemicellulose is amorphous, with little physical strength, thus it is easily hydrolyzed by dilute acids or bases, as well as by hemicellulase enzymes. The chemical hydrolysis of hemicelluloses into xylose and arabinose is generally afforded in high yields and low costs. Xylose, in particular, is largely used in modern biorefineries to produce furfural (2-furaldehyde), with a world production of about 200,000 tonnes per year, which is the key precursor of important building blocks such as furfuryl alcohol, 2-methylfuran, 2-methyltetrahydrofuran and levulinic acid [Li et al., 2016].

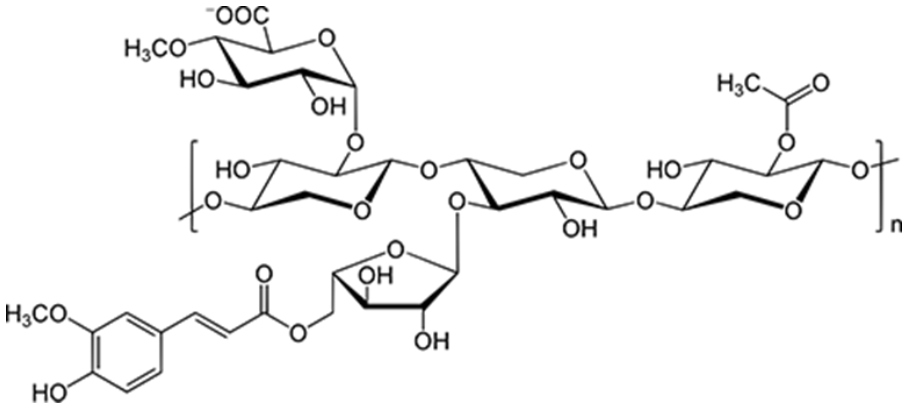

Figure 1.5. Chemical structure of hemicellulose.

Lignin is the second most abundant biopolymer in the world, corresponding to 15-40% of dry weight in lignocellulosic biomass, and it is responsible for hydrophobicity and structural rigidity. It is well-known that lignin plays a negative role in the conversion of cellulose, whose extent is influenced by several factors such as total lignin content, lignin composition, and structure [Zoghlami and Paës, 2019]. In fact, lignin can physically limit polysaccharide accessibility to hydrolytic catalysts, acting as a physical barrier that blocks the access to the cellulose. Lignin, unique among other biomass components, is characterized by an aromatic sub-structure with a large amount of etheric C–O bonds (Figure 1.6) [Chen, 2014].

The native constituents of lignin are therefore of particular interest for a lignocellulosic biorefinery aimed at the sustainable production of green aromatic compounds. The research on the sustainable production of chemicals from lignin has developed rapidly in the last years [Xu et al., 2014; Robinson et al., 2016]. Currently, industrial processes are limited to the production of vanillin and *lignin kraft* (about 60 kt/year) but research on the sustainable production of chemicals from lignin is developing rapidly in recent years [Xu et al., 2014; Deuss and Barta, 2016]. In this regard, one of the major challenges is the low cost-effective catalytic depolymerization of lignin preserving its aromatic nature [Sergeev and Hartwing, 2011].

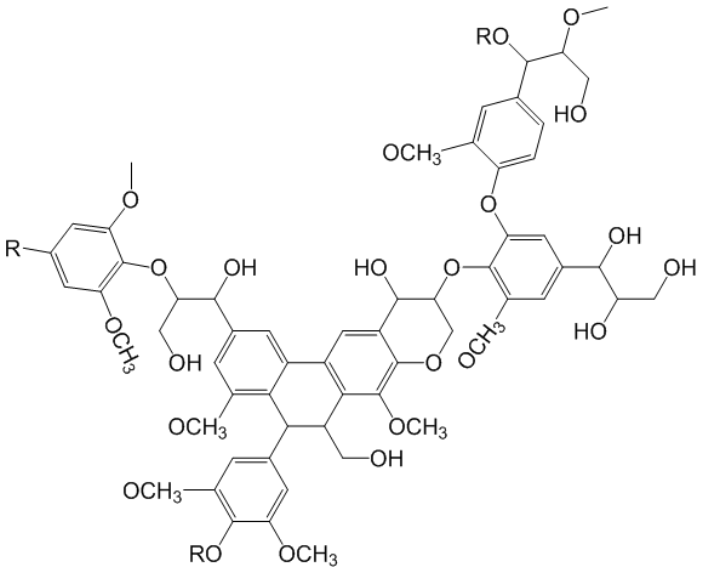

Figure 1.6. Chemical structure of lignin.

1.2.2 Hydrothermal processes for the valorization of lignocellulosic biomass

Thermochemical treatments employ heat to promote the chemical transformation of biomass into energy and chemical products [Demirbaş, 2001]. Recently, thermochemical conversion processes (pyrolysis and hydrothermal carbonization) are gaining more attention to manage the lignocellulosic biomass, and to produce valuable end-products.

Among several, pyrolysis is generally defined as the thermal decomposition process of lignocellulosic waste in the absence of oxygen to inhibit any oxidizing reaction, leading to three types of products: the solid char (biochar), the liquid phase (bio-oil), and the syngas consisting of CO_2, CO, H_2, and CH_4 [Patel et al., 2016]. Depending on the conditions of the process, pyrolysis can be further divided into six subcategories: fast pyrolysis, slow pyrolysis, intermediate pyrolysis, flash pyrolysis, vacuum pyrolysis, and ablative pyrolysis. Carbonization is also an extension of the low heating speed

pyrolysis process in which the main product is a carbon-based solid material with a lower yield of liquids and gases [Strezov et al., 2017].

Hydrothermal carbonization (HTC) is an aqueous carbonization method in which wet biomass is placed in a closed container and heated to the typical temperature of 180-250 °C, under autogenous pressure for a period of time (several minutes to several hours) which depends on the desired output of the process [Peterson et al., 2008]. The main product of the HTC process is a highly carbonized and densified material named hydrochar, possibly used in a wide range of applications, for example as a soil improver, biocatalyst, in materials and in water treatment [Bargmann et al., 2014]. The other products of the HTC are liquid bio-oil and gaseous volatile vapors (mainly CO_2).

Despite the different technologies potentially suitable for transforming the lignocellulosic waste into fuels, the hydrothermal carbonization is advantageous in terms of energy needs since it does not require the drying of the raw material as pre-treatment [Fang et al., 2018].

Biochar and hydrochar are both carbon-rich solid fuels obtained from various types of biomass through pyrolysis and hydrothermal carbonization processes, respectively. Both processes allow a sustainable transformation of the waste biomass into a quickly and efficiently resource, thus contributing to carbon sequestration and climate change mitigation, although the HTC process has the advantage of operating at relatively low temperatures than the pyrolysis process [Beesley et al., 2011].

Bio-oil is a dark brown red liquid, with a characteristic smoke smell and a chemical composition closely related to the starting raw material [Han et al., 2019]. It can be used efficiently as biofuel or for the production of chemicals and carbon materials [Tabanelli et al., 2019; Fasolini et al., 2019; Weldekidan et al., 2018; Hu and Gholizadeh, 2020]. The main compounds present in the bio-oil, reported in Figure 1.7, derive from cellulose and hemicellulose

fragmentation and lignin depolimerization. The mixture includes various organic compounds (20-30 wt%), water (19-20 wt%), water-soluble oligomers and water-insoluble oligomers (43-59 wt%) [Tabanelli et al., 2019].

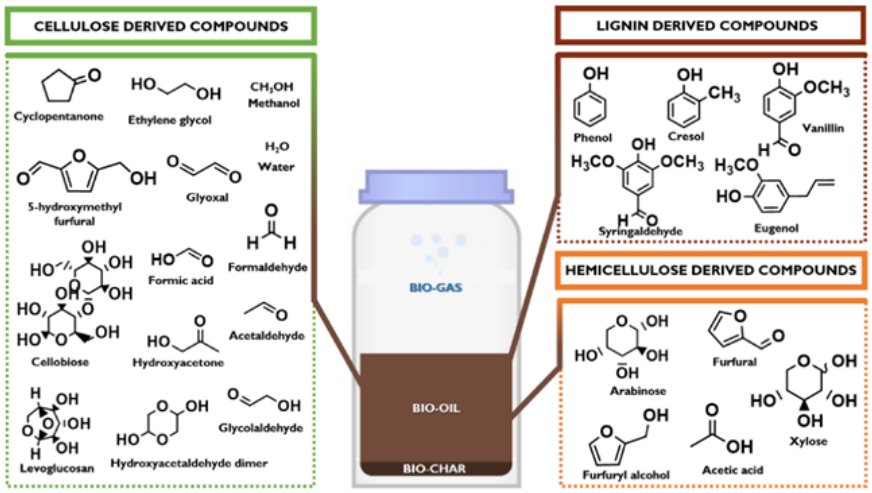

Figure 1.7. A simplified chemical composition of bio-oil: main lignocellulose-derived compounds.

Many of the compounds that are formed, such as acetic acid, propionic acid, lactic acid, formic acid, 5-hydroxymethylfurfural, and levulinic acid, can subsequently be converted into a number of high-value-added chemicals in biorefineries [Funke and Ziegler, 2010; Hoekman et al., 2013]. The production of a group of chemicals instead of a single compound has also been the focus of several studies, such as phenolic compounds production that can be used as a raw materials for the production of binders via crosslinking reactions [Maneffa et al., 2016; Mirkouei et al., 2017; Velez et al., 2018].

1.2.3 Sustainable production and catalytic upgrading of chemicals from lignocellulosic biomass

Researchers at the Pacific Northwest National Laboratory (PNNL) recently conducted an extensive study to identify valuable sugar-based building blocks from the lignocellulosic biomass [Werpy and Petersen, 2004]. A long list of thirty platform chemicals was obtained as sustainable

alternatives to the fossil-derived molecules. The list was further reduced to twelve by evaluating the potential markets of the interesting chemicals and their derivatives and the complexity of the synthetic pathways. One of these promising top-twelve building blocks is levulinic acid (LA) which is a versatile platform chemical for the industrial production of various added-value commercial products, such as plasticizers, fuels and oil additives, solvents, polymers, biodegradable surfactants, pharmaceutical products and herbicides [Cao et al., 2019; Chen et al., 2018]. Moreover, LA can be esterified into levulinate esters (LEs), which represent promising liquid biofuels to be used as additives to gasoline, diesel and biodiesel and as intermediates in the flavouring and fragrances production. Furthermore, it can be transformed into succinic acid, diphenolic acid and γ-valerolactone through oxidation, condensation and hydrogenation reactions, respectively [Chen et al., 2017].

Accordingly, furfural (FU) and 5-hydroxymethylfurfural (HMF) are valuable platform compounds for preparing several high-value biobased chemicals and materials. For example, HMF can be transformed to useful building block intermediates such as 5-arylaminomethyl-2-furanmethanol, 5-hydroxymethylfuroic acid, furfuryl alcohol, LA, levulinate esters [Hu et al., 2017] and 5-ethoxymethyl furfural [Kumari et al., 2018]. Similarly, furfural can be converted to valuable chemicals such as furfuryl alcohol, tetrahydrofuran, 2-methyltetrahydrofuran, methyl furfural, dimethylfuran maleic anhydride, and 1,5-pentanediol. These industrially relevant platform compounds have shown a great potential in replacing fossil derived molecules in the synthesis of industrial polymers. However, for their economic production, it is necessary the development of advanced approaches that result in the conversion of biomass-derived sugars to the sustainable production of high-yield furfurals [Mittal et al., 2020].

The conversion of typical lignocellulosic biomass to innovative platform molecules is shown in Scheme 1.1.

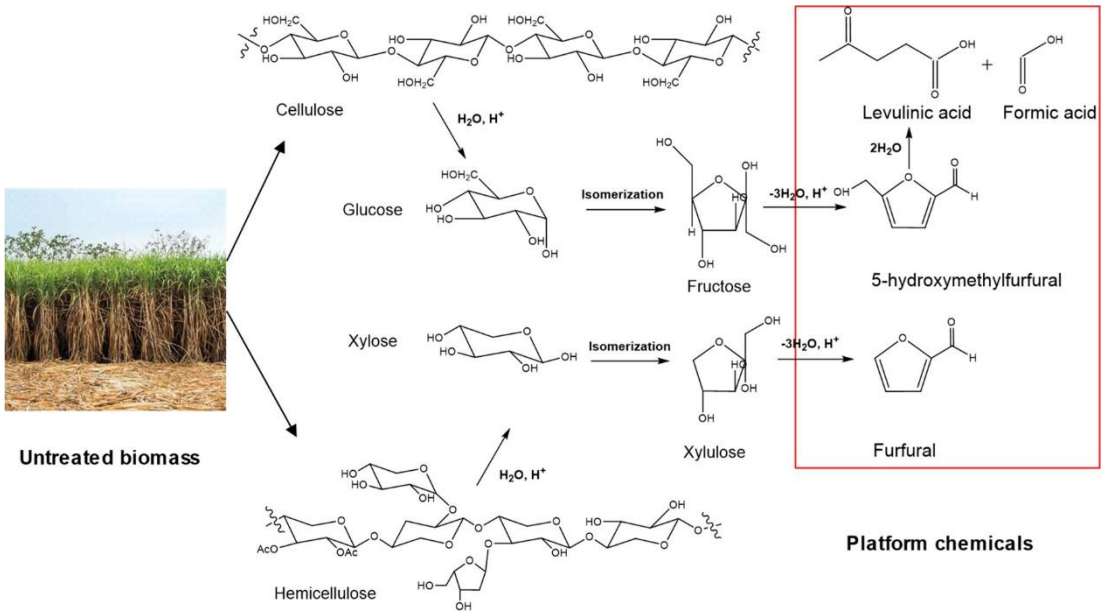

Scheme 1.1. Simplified reaction scheme for the conversion of lignocellulosic biomass to added value products [Mittal et al., 2020].

These platform chemicals could be subsequently converted into liquid fuels and value-added chemicals using heterogeneous catalytic processes such as oxidation, hydrogenation, and hydrogenolysis, among others. Catalytic transfer hydrogenation/hydrolysis (CTH) over non-precious metal catalysts has recently sparked considerable research interest due to the ability of most organic molecules to donate hydrogen to dissolve biomass and eliminate the serious problem that results from the mild mass transfer properties of H_2 in most organic solvents [Xu et al., 2020]. Furthermore, the CTH process is performed even under milder conditions, and the cost of a lignocellulose-based biorefinery can be reduced by eliminating the use of an expensive infrastructure necessary for the transportation, storage, and use of an explosive gas such as H_2 [Srivastava et al., 2020].

Useful chemicals such as methyl furfural (MF) and dimethylfuran (DMF) can be produced by FU and 5-HMF via catalytic hydrogenolysis on catalysts of noble metals and non-precious metals supported using external H_2 or H-

donor solvents. However, these transformations are usually performed at higher temperatures than generally used for the transformation of 5-HMF and FU into industrially relevant chemicals via hydrogenation [Wang et al., 2019].

On the other hand, γ-valerolactone (GVL) shows great potentials and has been the central focus of several research studies since it has numerous industrial applications. For instance, GVL can be used directly as a green solvent for various important chemical reactions or as a fuel additive to enhance the fuel combustion process, as well as a precursor for the synthesis of bio-based polymers, liquid fuels, and valuable chemicals [Yan et al., 2015]. Traditionally, GVL can be produced via hydrogenation of LA followed by dehydration over noble metal catalysts by using high-pressure H_2 gas [Wright and Palkovits, 2012].

Recently, many studies have shown that LA conversion to GVL can also take place over non-precious metal catalysts using H-donor molecules [Dutta et al., 2019]. In addition, LEs were identified as interesting starting materials for the production of GVL since offering the advantage of a non-corrosive environment due to their acid-free characteristics and lower boiling points compared to LA. Therefore, the use of LEs can help significantly to reduce the cost of GVL production in bio-refinery setups [Srivastava et al., 2020].

Innovative catalytic approaches to produce eco-friendly chemicals and fuels have created significant interest and opportunities for the production of value-added chemicals from the lignocellulosic biomass. Moreover, mild operating temperatures such as ambient temperature or 100 °C based CTH processes over inexpensive transition metal catalysts for the sustainable production of novel biofuels and chemicals needs to be developed.

1.3 Orange peel waste (OPW)

1.3.1 Chemical composition of OPW

Orange trees are citrus plants belonging to the Rutaceae family. The orange fruit is believed to have been originated in Asia, particularly in the southern China, northeast India and probably in Indonesia. Bitter oranges were introduced to Italy by crusaders in the 11th century. Sweet oranges were unknown until the late 15th or 16th century, when Italian and Portuguese traders brought oranges trees into the Mediterranean area. Spanish travelers introduced them to the American continent. In 1493, on his second travel, Christopher Columbus may have planted the fruit at Hispaniola. At that time oranges were mainly used for medicinal purposes, but soon they were used as a luxury food for wealthy people [Annamalai, 2004; Berti et al., 2018].

The orange fruit accounts for about 50-60% of the total citrus production, although also other species (e.g. lemon, lime, mandarin, and grapefruit) play also an important role in the agro-industrial sector [Satari et al., 2018; Zema et al., 2018]. Orange is widely produced and processed worldwide for the manufacture of different products including orange juice and generally is associated with the production of relatively high amounts of orange peel [Gavahion et al., 2019]. In addition to the orange juice, other products, including jams, orange blossoms, orange blossom honey, flavoring agents for beverages, and sweet orange essential oil (D-limonene is the primary constituent), are used as food products [Ferguson, 1990; Wilkins et al., 2007].

Figure 1.8 shows the section and the structure of an orange. It is possible to see how the peel is composed of two parts: the albedo (mesocarp) and the flavedo (exocarp). Albedo is the inner part of the peel and is rich in pectin [Mamma et al., 2014]. The albedo derives its name from the Latin (albzls = white) and has an ivory or light yellow color. The thickness and the spongy consistency of the albedo depend on the examined species. The flavedo, so

called for the presence of flavonoid compounds, is the outer part of the peel and it is rather thin, having a changing pigmentation depending on the cultivars or the variety. The flavedo consists mainly of a cellulosic material but also contains essential oils, paraffin waxes, steroids and triterpenoids, fatty acids, pigments (carotenoids, chlorophylls), bitter principles (limonene), and enzymes [Dugo, A. Di Giacomo 2002, Citrus; Liu et al., 2006].

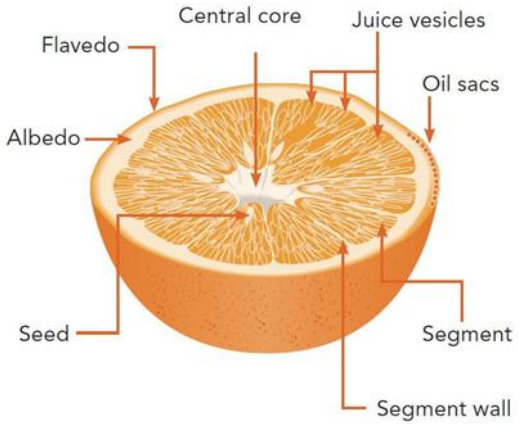

Figure 1.8. Structure and section of an orange [The Orange Book, Tetra Pak 2004].

According to the Food and Agriculture Organization (FAO) of the United Nations, the sweet orange (*Citrus sinensis*), with an annual production rate of about 70 million tons [FAO STAT, 2018], is one of the most appreciated citrus fruits not only for its fragrant taste but also for the content of many nutrients including vitamin C, A and B, some mineral salts containing calcium, phosphorus, potassium, dietary fiber and many healthy phytochemical products including flavonoids, amino acids, triterpenes, phenolic acids and carotenoids [Rezzadori et al., 2012; Guimarães et al., 2010; Gonçalves et al ., 2017]. Vitamin C is important to fight infections and strengthens the immune system. It also supports the healing of the mucous lining by stimulating the formation of procollagen [Sood et al. 2009]. There is an extensive research on the bioactive compounds of orange and orange juices and even on orange peels, due to health benefits such as a reduced risk of oxidative damage and

diseases related to free radicals (different types of cancer, cardiovascular or neurological diseases, etc.) [Tütem et al., 2020].

The main varieties of oranges include common oranges, which account for about 66% of the entire production of oranges, navel oranges, blood oranges and acid-free oranges. The Valencia and Hamlin varieties belong to the category of common oranges. Valencia oranges represent the most important crop in California, Texas and South Africa, while Hamlin oranges are a small sweet, smooth variety, having very few seeds and juicy and grows grown mainly in Florida [Kimball et al. 1999; Sauls, J.W. et al. 1998].

In order to exploit the maximum value from the waste peel, the knowledge of the chemical composition of orange peels is essential. The quantitative composition is given in detail in Table 1.1. The orange peel is abundant in insoluble carbohydrates (cellulose, hemicellulose, lignin, and pectin), soluble sugars, starch, ashes, proteins and fats [Rivas et al., 2008]. The unidentified small amounts, reported in the table, include organic acids such as citric acid, malic acid, malonic acid, and oxalic acid, collectively accounting for about 1%, and vitamins [López et al., 2010].

Table 1.1. The chemical composition of orange peel [Rivas et al., 2008].

Component	% (dry basis)
Soluble sugar	16.90
Cellulose	9.21
Hemicellulose	10.50
Lignin	0.84
Pectin	42.50
Starch	3.75
Ash	3.50
Protein	6.50
Fat	1.95
Others	4.35

Bampidis and Robinson reported the dry matter (DM) content of the orange peel (Table 1.2) having, predominantly, an organic composition containing proteins and many other short-chain organic acids (not more than four carbon atoms) [Bampidis and Robinson, 2006]. Table 1.3 shows the heavy metals (Cr, Cd, Ni, Pb and Zn) contained in the orange peel waste, that have to be removed during the disposal. The pH value of the orange peel waste is 3.4 and should be neutralized during composting and microbial conversion processes [Siles et al., 2016]. However, the physico-chemical composition of oranges depends on the variety, growing conditions, ripening stage, and climatic conditions [Salunkhe et al., 1995; Kale et al., 1995].

Table 1.2. The chemical composition of the orange peel [Bampidis and Robinson, 2006].

Component	g/Kg (dry basis)
Organic matter	975
Crude protein	58
Neutral detergent fibre	129
Lactic acid	23.0
Acetic acid	20.0
Propionic acid	0.3
Isobutyric acid	0.6
Calcium	7.3
Phosphate	1.7

Table 1.3. The chemical composition of the orange peel (mean value ± standard deviation) [Siles et al., 2016].

Parameter	mg/Kg (dry basis)
pH	3.42 ± 0.02
Cr	1.6 ± 0.7
Cd	4.9 ± 0.8
Ni	6.1 ± 1.3
Pb	< 1.0
Zn	4.5 ± 0.4

The largest orange-producing country is Brazil followed by the US, with 7.5 million tons of oranges (the 70% of which grows in Florida), and China with an upward trend of 7 million tons per year [FAO 2014; AIJN, 2014]. In the European Union, the cultivation of oranges is mainly concentrated in Mediterranean countries such as Italy, Spain and Greece, for a total annual production of about 6.0 million tons [Negro et al., 2016].

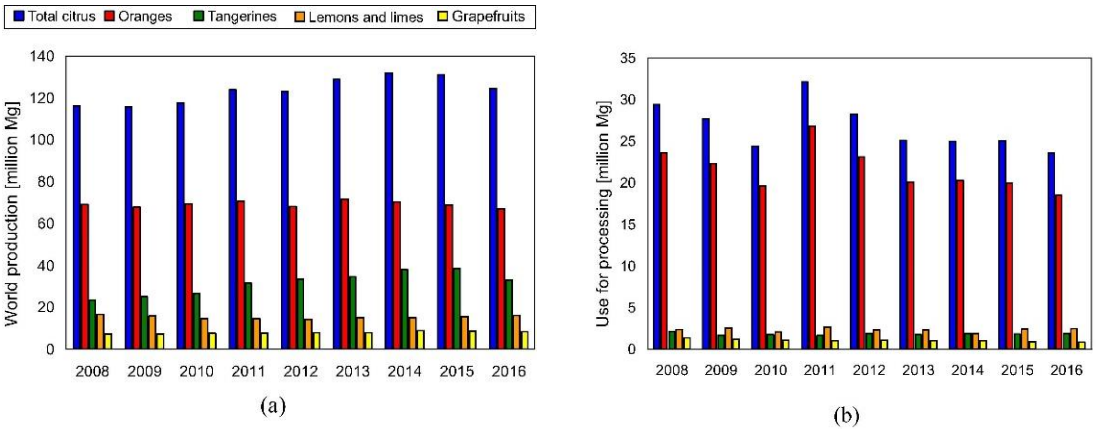

Figure 1.9. Produced and processed citrus fruits in the World (a and b) [FAOSTAT, 2017].

In 2016, more than 124 million Mg (Mg is the SI unit equivalent to one tonne) of citrus fruits were produced (Fig. 1.9a). Generally, about the 50-60% is consumed as fresh fruit within the production areas while the remaining 40-50% is used for industrial processing (Fig. 1.9b). [FAOSTAT, 2017; Satari et al., 2018; Sharma et al., 2017; Sharma et al., 2019].

The citrus industry produces large quantities of waste water and solid/semi-solid residues (citrus peel waste) after processing. Orange peels and orange pulp are the waste of oranges: in particular, orange peels account for the 60-65%. Annual world production of citrus fruit waste is likely to be close to 10 million Mg. The peculiar characteristics of citrus processing residues, such as low pH and high concentrations of organic compounds, entail considerable constraints for their management due to both economic and environmental factors. In particular, the content of phenolic compounds

and the presence of essential oils are the main problem for biological management options due to their antimicrobial properties [Calabrò et al., 2016; Battista et al., 2020]. The disposal of citrus peel waste requires high costs and traditional disposal strategies, such as incineration or landfill, are currently insufficient and problematic in terms of environmental impacts and energy efficiency [Satari et al., 2018; Wei et al., 2017]. In order to minimise operating costs and to prevent environmental damage, several uses of residues from the citrus processing industry have been assessed in recent decades. These consider citrus processing residues as a valuable resource to be reused in the bioeconomy rather than a waste to be disposed of in landfills [Zema et al., 2018].

The orange peel has a considerable economic value and one of the most precious and abundant products is its essential oil. According to the Association of Official Agricultural Chemists (AOAC), the raw orange peel has 1.45 ± 0.16 ml of essential oil per kg. The essential oil produced by orange peel is a low-cost material and includes many components used in the synthesis of certain drugs, food chemicals, detergents and cosmetics [Espachs-Barroso et al., 2005; López et al., 2010]. In fact, the orange peel essential oil can include more than 200 compounds depending on the cultivar, orange maturity, type of extraction and separation processes [Reverchon, 1997]. About 90–95% of the essential oil includes terpenes. However the main peculiarity charachterizing the essential oil presence is mainly due to oxygenated derivatives of terpenes. In addition, nitrogenous or sulfuric compounds may also be present in the oil. On the other hand, terpenes generally decompose under the influence of heat, light and/or air [Diaz et al., 2005].

In recent years, since the orange processing waste contains a huge amount of moisture (about 80%), a great interest in their use as a raw material for thermochemical processes to produce value-added products is increasing. In fact, hydrothermal carbonization (HTC), a thermochemical conversion

process, could represent a promising treatment technique for wet lignocellulosic biomass waste, overcoming the disadvantages of the conventional thermochemical process since humidity is not an impediment and is even used as a mean of reaction for hydrothermal reactions [Zhang et al., 2018; Burguete et al., 2016].

On this account, if the great potential relative to the exploitation of agro-industrial processing residues by green economy programmes is realised, negative impacts of citrus processing industries on the environment could be reduced. [Zema et al., 2018].

1.3.2 The OPW valorization system

Applications, using the entire orange peel without differentiating the individual constituents, are the easiest way to process the raw material since they require little infrastructure or investment and greatly increase the value of the waste material [López et al., 2010]. On the other hand, conversion processes, in biorefineries, have recently been proposed for a more profitable and environmentally friendly use and lead to production of new useful products. Below both uses (direct use and uses in biorefinery) will be discussed [Zema et al., 2018].

Animal feed

The solid waste, generated during the orange juice production can be reused directly as an animal feed supplement to provide extra nutrients for animals. This traditional use of orange peel as feed for animals is preferable in areas having a high density of livestock since its transport to breeding can involve considerable costs. In fact, the fresh and dry citrus waste can provide extra fibers for ruminants by promoting microbial growth and lactation. Up to 20 % of the animal feed could be replaced by this waste use in combination with the cereal straw. In addition, the increase in body weight in cattle is much greater when fed with orange scraps than with starch-rich feed [Bampidis et

al., 2006; Zema et al., 2018]. The dry or fresh citrus waste is also a good source of nutrients for non-ruminants such as pigs and rabbits. It is noteworthy that the insilation of the citrus waste, before supplying feed to animals, is also a common practice [Wadhwa et al., 2013]. The high amount of moisture from this waste promotes its decomposition, so the direct reuse of orange wastes as animal feed usually requires immediate drying to prevent its deterioration and to prolong its lifespan, although this would inevitably lead to an increase in the price of the product. Moreover, poor storage could lead to uncontrolled production of methane [Joshi et al., 2005]. Further, depending on the composition of the waste, the concentration of indigestible components may change. Therefore a microbial pre-treatment is needed to improve the digestibility and bioavailability of nutrients in the feed [Villas-Bôas et al., 2003]. Thus, the traditional exploitation of the orange peel waste, as animal feed, has several limitations and an increasing research into alternative applications by producing high-value products is actually going on [López et al., 2010].

Organic fertilizer

A different application of the waste orange peel is its conversion into fertilizers by using the composting technique. This is a process involved in the biological decomposition of the organic matter under controlled and aerobic conditions. Compost is characterized by a high level of organic carbon and vital minerals for crops [Epstein, 2017]. Some studies have shown the improvement of the content of organic substances and soil nutrients by using the orange peel for the production of compost. Therefore it is also advisable on agricultural lands close to the citrus processing industries. This treatment was successfully performed using calcium hydroxide, generally used for composting acid substrates, to adjust the pH (6.3) and the modify both the C/N ratio (24:1) and the moisture content (60%) of the citrus waste. After a short latency phase followed by a rapid increase of the temperature and a final

phase of gradual cooling, the biochemical process, related to the composting of the orange peel waste, can be completed within 3 months [Van Heerden et al., 2002; Zema et al., 2018]. Alternatively, according to Golueke, the C/N ratio of the waste and the pH value should be between 25-35 and 6.0-7.5 respectively, for a rapid and complete humification of the organic substrate [Golueke, 2017].

Composting of the municipal solid waste, including the orange waste, can increase the soil pH compared to that of inorganic fertilizers. Compost, derived from fruit and vegetable wastes, is also an ideal source of phosphorus (for both potatoes and sweet corn) and nitrogen, providing an alternative to inorganic and minerals nitrogen fertilizers [Mkhabela et al., 2005; Nevens et al., 2003]. However, this method of processing requires a long period of pre-treatment due to the content of many fibers that are difficult to be bio-degraded. The disadvantage of this treatment is mainly due to the emission of unpleasant odors and to contamination by pathogens due to microbial transformation that can have negative impacts on the environment and human health [Ajila et al., 2012].

Pectin extraction

Pectin is a complex carbohydrate, a polymer of α-galacteronic acid with a variable number of methylester groups [Liu et al., 2006], and is commercially produced from orange peels in the form of white or light brown powder [Putnik et al. 2017]. Pectins are extracted from citrus peels through various operations including washing the peel with water, acid hydrolysis, filtration and final precipitation by isopropanol or ethyl alcohol. In order to avoid risks to the human health and the environment, the pectin extraction is usually carried out using water as solvent [Sharma et al., 2017]. During the pectin extraction from orange peels, several factors influencing the process, include pH, temperature, solvent used for extraction, extraction time, agitation rate and solid liquid ratio [Fakayode and Abobi, 2018]. More recently, other

methods for pectin extraction have been introduced, such as ultrasonic extraction [Zhang et al., 2013], microwave assisted extraction [Fishman and Cooke, 2009], enzyme extraction [Ptichkina et al., 2008], and the supercritical fluid extraction [Ueno et al., 2008]. According to several researchers, the amount of pectin contained in orange peels is about 30% on a dry basis [Rouse and Crandall, 1976; May, 1990, and Khan et al. 2015]. To recover pectin from the flavedo and the albedo of the orange peel waste, Liu et al. used different extraction techniques and water as solvent (with an optimal ratio of 1:12.5), and reported that the total yield of pectin from the dried peel is 2,2 %, increasing on using the Soxhlet method [Liu et al., 2006].

Citrus pectins have gelling, thickening and stabilizing properties, therefore they are widely used in the food industry because they favour a desirable consistency of food and drink [Satari and Karimi, 2018] as well as in pharmaceuticals and cosmetics, although 75% of the pectin produced is used in the preparation of jams, jellies and similar products. In addition, for their biodegradability, biocompatibility, edibility and chemical versatility, pectins are also a suitable substrate for the manufacture of edible active films with different applications in food packaging [Espitia et al., 2014]. However, pectin production is economically unsustainable for orange peel waste, due to the lower gelling capacity of the derived pectins [Zema et al., 2018].

Flavonoids extraction

Flavonoids are phenolic compounds present, in high quantities, in citrus peel waste [Satari and Karimi, 2018] and show various bioactivities including antioxidant, anti-inflammatory, anti-carcinogenic and anti-atherosclerosis activities [Hu et al., 2003; Kitts, 2006; Pan et al., 2010]. The total content of flavonoids in orange peel is within the range of 14.0-31.9 mg/g [Chen et al., 2017]. These compounds can be found, in different forms, in citrus fruits (flavanones, flavones and anthocyanins) [Cook and Samman, 1996; Peterson and Dwyer, 1998; Tripoli et al., 2007]. The most important flavonoids are

naringin, neoeriocitrin, experidine, diosmin, rutin, naringenin, eriodittol, esperetin, apigening, luteolin, diosmetin, caerapferon, quercetin and tangeretin [Benavente-García et al., 1997].

Raw flavonoid extracts are often used in pharmaceutical formulations due to their biological properties and ability to have antiperoxidizing effects on lipids [Marín et al., 2002]. In fact, several studies have shown that flavonoids exhibit antiallergic and anticancer properties, and regulate the synthesis of prostaglandins, natural and effective compounds against inflammatory states and in other physiological processes such as platelet aggregation. Experidine, nobiletin, naringin and especially tangeretin have been studied for their ability to block metastatic cells in their initial phase, typical of the more advanced stages of primary tumor progression [Benavente-García et al., 1997]. The most important flavones are rutin and diosmin which, together with experidine, have an effective pharmacological action especially for vascular pathologies and thrombotic diseases [Zema et al., 2018]. Nobiletin and tangeretin, in addition to their antioxidant and anti-inflammatory effects, can be used as drugs for the treatment and prevention of neurodegenerative diseases such as Alzheimer's and Parkinson's disease [Braidy et al., 2017]. Anthocyanins, present in Italian orange varieties such as Moro, Tarocco and Sanguinello, have a high antioxidant activity since they act as scavengers of free radicals, produced during the oxidative cellular metabolism and can damage lipids, proteins and DNA of membrane cells [Proteggente et al., 2003; Rapisarda et al., 1999; Terao, 1999; Yao et al., 2004]. Currently, flavonoids in citrus fruits can be obtained by various extraction techniques including conventional solvent extraction (e.g. ethanol, methanol and water), and novel ultrasound-assisted, microwave-assisted, supercritical and subcritical extraction, and high-hydrostatic-pressure for extraction [M'hiri et al., 2014]. Xu et al. reported a hot water extraction process that produces a total phenolic content and antioxidant activity similar to those obtained by methanol extraction [Xu et al., 2007], while Ho and Lin investigated a heat treatment that

increases the flavonoids content and anti-inflammatory activity of the orange peel extract [Ho and Lin, 2008].

Ethanol production

Bioethanol deriving from biomass fermentation, from long time, has been used worldwide as a solvent, perfume, aroma, medicine and heating fuel. In recent years, the fuel demand for renewable sources deriving products has increased considerably due to growing concern about high oil and natural gas prices, and the dependence of the United States and European Union countries on imports of hydrocarbons from a limited number of countries, and for global warming. On this regard, the second generation technology allows the production of bioethanol from lignocellulosic materials, allowing benefits in terms of reducing greenhouse gas emissions [Lynd et al., 2005].

Recently it has been shown that the orange peel is a good source for producing ethanol through a simple process that hydrolyzes pectin, cellulose and hemicellulosic polysaccharides to monomeric sugars, suitable for alcoholic fermentation using saccharomycetes [Kimball, 1999; John et al., 2017]. Hydrolysis and enzymatic fermentation can traditionally be performed through separate or integrated processes [Satari and Karimi, 2018]. Three enzymes including pectinase, cellulase and beta-glucosidase were used in a pre-hydrolysis process, and the maximum concentration of ethanol was reached when the amounts of enzymes were greater than 25 IU/g of dried peel for the enzyme pectinase, 0,02 IU/g dried peel for the enzyme cellulase and 13 FPU/g dried peel for the enzyme beta-glucosidase, with an initial pH value of 6,0 [Grohmann et al., 1994; Wilkins et al., 2007]. According to Grohmann and Baldwin, the combination of cellulase and pectinase was more effective for hydrolyzing the orange peel waste than the individual use of these enzymes [Grohmann and Baldwin, 1992].

Pre-treatment methods for orange peel waste hydrolysis are simpler than those required for the usual lignocellulosic biomasses, due to the low lignin content of the citrus peel. Hydrothermal pre-treatment is mainly aimed to remove or lower limonene and other chemicals that are shown to be inhibitory to produce bioethanol [Satari and Karimi, 2018]. In fact, the main limiting factor of the process is the essential oil content which should not have a concentration greater than 0.08-0.12% to avoid inhibition of microorganisms. The essential oil presence prevents, in fact, alcoholic fermentation due to its toxicity to many microorganisms [Kimball, 1999; Wilkins et al., 2007]. Koutinas et al. reported the minimum inhibitory concentration of the essential oil to be 0.01% (v/v) for ethanol fermentation of orange peel waste by the bacterium Pichia kudriavzevii KVMP10 [Koutinas et al., 2016]. Other pre-treatments, relative to citrus waste, include steam explosion and acid hydrolysis, although these last two pre-treatments are quite expensive [John et al., 2017].

After the pre-treatment, the hydrolyzed product is fermented by specific yeasts to produce bioethanol. The yeasts used in ethanol fermentation are Kluvyeromyces marxianus, Escherichia coli KO11 and Saccharomyces cerevisiae that is the most effective in converting the orange peel into ethanol (40.90 g/L) compared to the other two enzymes [Grohmann et al., 1994; Wilkins et al., 2007].

The production of bioethanol from the citrus waste requires a very large investment [Sánchez-Segado et al., 2012] and is not energy efficient as the production of methane (biogas) by anaerobic digestion. For instance, it is worth to underline that methane production can afford over 700 kWh per tonne of waste while the energy yield of bioethanol production is only about 300 kWh per tonne [Ruiz et al., 2014].

Anaerobic digestion

The anaerobic digestion is a valid alternative for the valorization of the citrus waste as it allows the biological conversion of an organic material into a biogas, formed by a mixture of methane (50-70%) and carbon dioxide (30-50%) [Wheatley, 1990; Bozym et al., 2015]. This process is technically feasible, ecological and energy efficient, although the citrus essential oil, known as anti-microbial agent, can inhibit the biomass activity [Ruiz and Flotats, 2016; Forgács et al., 2012; Martín et al., 2010]. Lane reported an essential oil inhibitory concentration above 2.5 mg/L [Lane, 1984] while Ruiz and Flotats reported that the inhibitory effect of D-limonene is mainly due to the presence of p-cymene, over a concentration of 200 mg/Kg [Ruiz and Flotats 2016]. Two possible options can be evaluated to overcome this limitation and significantly improve the efficiency of the waste treatment: the co-management of the orange peel waste with other substrates or their pre-treatment before the anaerobic digestion by distillation, aeration, solid-state fermentation, biological removal, burst of steam excretion with a solvent [Anjum et al., 2017; Forgács et al., 2012; Martín et al., 2013; Calabrò et al., 2018; Ruiz and Flotats, 2014].

The methane yield of the agro-industrial waste depends on many factors including pH, temperature, nutrient availability for microorganisms, citrus cultivars and mineral ion content [Zema et al., 2018; Bozym et al., 2015]. The research has shown that a citrus processing plant, which handles 600 Mg of fruit daily, can produce enough biogas, from waste streams, to meet the demand for electricity and fuel, while the excess electricity generated by biogas can also be sold [Koppar e Pullammanappallil, 2013]. Gunaseelan found that methane yields and velocity vary among species and parts of the fruit. Specifically, in batch tests of 100 days at 35 °C, the methane yields from sweet orange peel waste and pressings were respectively 0.46 and 0.50 m^3/kg of volatile solids (VS) added [Gunaseelan, 2004].

Zema et al. evaluated the methane production through a semicontinuous anaerobic digestion of the industrial orange peel waste under mesophilic and thermophilic conditions. Under mesophilic conditions, the highest daily yield of specific methane was achieved with an organic load rate (OLR) of 1.0 g_{VS}/L·d and an essential oil presence of 47.6 mg/L·d. Under thermophilic conditions, the total production of methane, equal to 0.12 m^3/kg VS added, was about the 25% of that obtained in mesophilic conditions, equal to 0.46 m^3/kg VS added [Zema et al. 2018].

Therefore, the increasing development of biogas production from waste and organic residues suggests the future use of the citrus peel waste, that shows a higher methane potential production than other crop substrates [Calabrò et al., 2018; Gunaseelan, 2004; Plöchl and Heiermann, 2006]. However, the problems associated with the seasonal production of the citrus peel waste and the toxicity due to essential oils for microorganisms still need to be overcome. On this account, optimizing conservation techniques and new simplified pre-treatment techniques for the D-limonene removal are probably the most promising options for the sustainable anaerobic digestion of citrus waste [Zema et al., 2018]. In addition, the resulting large amount of digestate and effluent, containing phytotoxic compounds, pathogens and heavy metals, requires a careful treatment [Nkoa, 2014].

1.4 Recovery and catalytic upgrading of value-added chemicals from OPW

1.4.1 Recovery and catalytic upgrading of d-limonene

The chemical conversion (upgrade) of the lignocellulosic biomass and wastes for the production of fuels and chemical building blocks, the so-called "biorefinery", has been widely explored in the last two decades [Zhou et al., 2011; De et al., 2015]. Modern biorefineries already use cellulose, hemicellulose

and lignin (the three-key components of lignocellulose) as starting feedstocks for the preparation of furans, polyols, acids and aromatics [Ruppert et al., 2012; Xu et al., 2020; Xu et al., 2020].

In this context, limonene (1-methyl-4-(1-methyl phenyl) cyclohexene), the main constituent of citrus essential oil (around 68–98% w/w) is industrially derived from the citrus industry in solving orange processing waste [Ozturk et al., 2019]. An optically active cyclic monoterpene that exists in two enantiomeric forms, *R*-limonene (the predominant isomeric form in citrus varieties, also known as *d*-limonene) and *S*-limonene (the less common isomer found in mint oils) [Erasto and Viljoen, 2008; Ciriminna et al., 2014; Mahato et al., 2017; Uwidia et al., 2020], limonene is generally adopted as a flavor and fragranze additive in the cosmetic and perfume industries due to its pleasant citrus smell, and in the food industry as a flavor and preservant, avoiding alterations of the organoleptic properties. Moreover, it is also extensively adopted as an ingredient in household cleaning products, as wetting and dispersing agent in manufacturing resins, in the production of varnishes, in germicide treatments for wastewaters [Veillet et al., 2010] and as insect control. In this regard, limonene represents an efficient alternative to halogenated carbon hydrates or conventional degreasing agents. Likewise, due to its elevated apolar solvent properties, limonene is a versatile compound used as a green solvent for the extraction of natural products, replacing toxic oil-based solvents such as *n*-hexane [Rubulotta et al., 2017; Aissou et al., 2017; Lohrasbi et al., 2010]. For example, it was recently proven to have a unique ability to recover marine oils rich in omega-3 lipids, vitamin D and carotenoids from shrimp and anchovy leftovers [Ciriminna et al., 2019; Ciriminna et al., 2019; Pagliaro et al., 2021]. These uses are particularly important in light of its anticancer, anti-tumoral and anti-diabetic properties [Negro et al., 2016; Santiago et al., 2020]. The industrial demand of limonene largely exceeds its supply, limited by the yearly global production of orange crops. As a result, the price of orange essential oil (EO) has increased to such an extent that it is

now a primary source of revenue for the orange juice industry [Ciriminna et al., 2014; 360 Market Updates].

Due to its versatile chemistry, when the supply of the terpene obtained via bacterial fermentation will replace limited supply from citrus processing waste, limonene will replace a number of aromatic intermediates currently produced from oil [Ciriminna et al., 2014; Martin-Luengo et al., 2008; Swift, 2004]. For example, 1,2-limonene oxide obtained via catalytic selective oxidation readily reacts with carbon dioxide to form biobased polycarbonates of exceptional optical and mechanical properties, with some important reviews published in recent years on this subject [Parrino et al., 2018; Ciriminna et al., 2018; Cagnoli et al., 2005]. Likewise, limonene can be used as a substrate for the production of p-cymene, a fine chemical intermediate in several industrial chemical processes [Martin-Luengo et al., 2010; Buhl et al., 1999]. In fact, p-cymene is involved in the synthesis of fragrances, perfumes, flavors, fungicides, pesticides and pharmaceutical products [Negro et al., 2016]. At the same time, in the perfume industry, it is used as a raw material for the production of key intermediates including p-cresol that is used, for example, in the production of antioxidants such as butylated hydroxytoluene (BHT) [Sanches-Silva et al., 2007; Tavera Ruiz et al., 2019; Eggersdorfer, 2012]. Moreover, p-cymene can be added to inks, adhesives, paints and pigments and is widely used for the manufacture of some products that are normally obtained from petroleum-based compounds. Finally, p-cymene can be transformed into aromatic monomers, including terephthalic acid and dimethyl styrene, or used as starting substrate for the synthesis of non-nitrate mosses (i.e., tonalide).

The current industrial route to p-cymene using the Friedel-Crafts alkylation of benzene with methyl and isopropyl halides or of toluene with 2-propanol generates a large amount of byproducts. Moreover, the use of large quantities of hazardous acid catalysts gives rise to safety, corrosion, handling

and waste disposal problems. In further detail, the FC alkylation is performed at high temperatures (200-450 °C) in the presence of $AlCl_3$, BF_3 or H_2SO_4 as catalysts, producing significant amounts of by-products (especially o- and m-cymene along with other multiple alkylation products) with an overall yield of p-cymene that usually does not exceed 50%. Finally, since the conventional p-cymene production occurs in a liquid phase, the separation of the reactants from the catalyst is an energy-intensive process [Bueno et al., 2008; Kamitsou et al., 2014; Makarouni et al., 2018]. Alternative methodologies for the production of p-cymene have been widely investigated, including the use of renewable limonene, also considering that a relatively low amount of p-cymene (4000 tonnes) is manufactured yearly [Marchese et al., 2017; Fiege, 2012; Ghiaci et al., 2007; Corma et al., 2007; Retajczyk and Agnieszka Wróblewska, 2019].

Extraction methods for the recovery of limonene

Extraction techniques are the first step in any treatment of citrus fruits and medicinal plants. The extraction has a significant and crucial role in the final result and can be per- formed with different technologies [Azmir et al., 2013]. Recently, eco-friendly unconventional extraction methods, such as microwave-assisted extraction (MAE), ultrasonic-assisted extraction (UAE), supercritical fluid extraction (SFE) and enzyme-assisted extraction (EAE) [Lefebvre et al., 2021], which reduce time and the use of chemical solvents improving the yield and quality of the extracted essential oil, have been developed. At the same time, conventional extraction methods, such as hydrodistillation (HD), cold press (CP) [Ferhat et al., 2016] and solvent extraction, are still considered reference methods [Azmir et al., 2013].

Table 1.4 summarizes the recovery of limonene from different species of citrus by means of conventional and novel extraction technologies. The amount of limonene recovered strongly depends on the extraction technique and on the type of citrus fruit used. Indeed, as shown in Table 1.5, the

maximum yield of about 94–96% has been reached for the orange peel [González-Rivera et al., 2016; Bustamante et al., 2016], while lower values were obtained for clementine and grapefruit. A lower extraction efficiency resulted also from the lemon, with a yield of limonene that did not exceed the 70% [Teigiserova et al., 2021].

The limonene recovery from citrus has been, so far, widely achieved by using conventional solvent extraction with different types of various solvents such as n-hexane, dichloromethane, diethyl ether and ethyl acetate. Among the several solvents used, n-hexane, due to its low boiling point, highly hydrophobic character and excellent solubilizing ability, was found to be the most efficient extracting agent [Nguyen, 2012; Liu and Mamidipally, 2005]. Besides the type of the starting citrus fruit, the solvent extraction efficiency depends also on the operating parameters, such as extraction temperature, cycle number and substrate–solvent ratios. Battista et al. recently reported the recovery of limonene from the orange essential oil (OEO), extracted from orange peels (Ops) by means of a Soxhlet n-hexane extraction under optimized reaction parameters (85 °C; solvent/OPs ratio equal to 2:1) allowing higher OEO yields of 1.31% to be reached with a limonene content of about 90% [Battista et al., 2020]. At the same time, the high-pressure–high-temperature extraction (HPTE) process, using hexane, in an agitated reactor, has been successfully used by Lopresto et al. to recover d-limonene from lemon fruits, highlighting that the high temperature excites the analyte solubilisation by increasing both solubility and mass transfer rate, thus enhancing the extraction efficiency [Lopresto et al., 2014; Paini et al., 2016].

As shown in Figure 1.10, the non-conventional HTPE processes, carried out at 150 °C and 6 bar pressure with a matrix/solvent ratio equal to 1:4 during an extraction time of only 30 min, lead to a yield in d-limonene three times higher (2.97% vs. 0.95%) compared to that of the classic Soxhlet extraction performed for 4 h at 68 ◦C and 1 bar pressure with a matrix/solvent ratio 1:25

[Lopresto et al., 2014]. However, due to its high toxicity, the use of hexane has been severely limited by various regulations, such as the REACH (EC 1907/2006) and the IPPC (96/61/EC), pushing the scientific research towards the use of green solvents, as an alternative to n-hexane, without compromising the yield of oil [Kumar et al., 2017].

On this account, the use of green solvents obtained from the biomass (i.e., bio-based solvents) or nontoxic and biodegradable environmentally friendly petrochemical solvents could represent a valid alternative to replace hazardous volatile organic solvents, not only in terms of environmental and healthy impact, but also in terms of extraction efficiency.

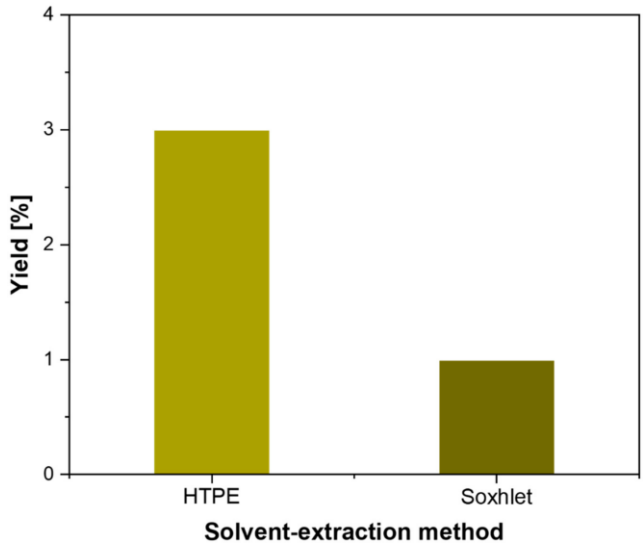

Figure 1.10. Comparison between non-conventional high-pressure–high-temperature extraction (HPTE) and conventional Soxhlet extraction [Lopresto et al., 2014].

Ozturk et al., evaluated the performance of several bio- solvents, demonstrating how the use of cyclopentyl-methyl and 2-methyl-tetrahydrofuran, operating at T= 70 °C, t= 150 min and substrate/liquid ratio equal to 1:10, allows us to obtain a better performance of recovery and reuse in consecutive extraction cycles, and limonene extraction yields up to 80% and 40% respectively, in comparison with the conventional hexane extraction methodology [Ozturk et al., 2019].

The cold press, one of the ancient essential oil extraction methods and already integrated into most of the modern juice production systems, is based on the use of needles to tear the oil glands in the peels [Negro et al., 2016; Mahato et al., 2019] and the use of a mechanical pressure to release the oils [Teigiserova et al., 2021]. It has the major advantage of minimizing the degradation of the essential oil constituents [Karaman et al., 2015], with the oil expeller pressed at low temperature and pressure. Additionally, the resulting oil is 100% pure and retains most of the volatile compounds and waxes, which are important for their aromatic properties [Rassem et al., 2016]. Although the cold press extraction provides an inexpensive opportunity compared to conventional methods, as the equipment is very simple and does not require heat supply, usually it has the lowest yield of essential oil extraction compared to the most recent extraction techniques, such as hydro (HD) and steam (SD) distillation. Therefore, in recent years, the number of reports based on the cold press extraction of limonene was very limited.

Ferhat et al., in a comparative study of essential oil extraction from fresh citrus peels by conventional hydrodistillation (HD), cold pressing (CP) and innovative microwave-accelerated distillation (MAD), obtained, via cold press extraction, a yield of 73.75% from whole fresh lemon (*Villa Franca*, *Citrus limon* (*L.*) *Burm cultivar*), while, starting from whole fresh grapefruit (*Marsh Seedless*, *Citrus deliciosa Ten C. tangerine cultivar*) and whole fresh orange (*Valencia cultivar Citrus sinensis* (*L.*) *Osbeck*; *Bouquetier de Nice* (*Citrus paradisi*) *cultivar*), a yield of ca. 95–96% was reached. Such results further highlight the fundamental role played by the type of the starting fruit on limonene yields, since a higher amount from oranges (around 95%) is obtained, while it is significantly less from lime and lemon fruit (around 70%). In any case, Ferhat et al., in the same study, showed that the innovative microwave process offers substantial advantages over conventional processes, in terms of both shorter distillation time (30 min vs. 3 h for hydrodistillation and 1 h for cold pressing),

and improved yields (0.24% vs. 0.21% for hydrodistillation and 0.054% for cold pressing) [Ferhat et al., 2016].

As mentioned above, hydrodistillation (HD) is a classic method for the extraction of aroma-producing compounds that does not involve the use of organic solvents. It is performed before the dehydration of citrus materials, and it is generally widely used. Three main types of HD processes can be listed: (i) water distillation, (ii) steam distillation and (iii) water–steam distillation. HD requires long extraction times and cannot be widely used for thermolabile compounds extraction, such as terpenic compounds, due to the volatility of some components, possibly lost at high extraction temperatures [Mahato et al., 2017; Azmir et al., 2013; Zema et al., 2018]. The technique shows a simple apparatus based on the evaporation of a solution containing immiscible liquid compounds at a boiling temperature lower than the one of each component [Zema et al., 2018; Ferhat et al., 2007]. Starting from fresh orange peels, Ruiz et al. achieved a maximum extraction efficiency of limonene, above 44%, for the treatment at the higher steam flowrate (16 mL min−1) and the longest contact time (180 min) [Ruiz et al., 2016], according to the results previously obtained by Cannon et al. [Cannon et al., 2013]. The extraction efficiency of limonene, obtained by Martin et al. by steam distillation at lab scale, with a distillation time ranging from 0 to 6 h, was above 70% [Martin-Luengo et al., 2010], while, using the same technique, Uwidia et al. reached limonene yields above 95% [Uwidia et al., 2020]. In any case, the limonene extraction efficiency obtained in the above studies cannot be directly compared owing to the different operating conditions.

Microwave-assisted extraction (MAE) is a green and versatile extraction technology usable starting from several raw materials and providing both faster extraction and lesser solvent consumption [Lee et al., 2016]. Recently, MAE has been largely used also for the extraction of pectin and betanin from the peel of red and green *Opuntia ficus*-indica fruits with high efficiency

[Ciriminna et al., 2019]. MAE shows many advantages, such as a less solvent volume, faster extraction, mass transfer intensification and protection of thermolabile compounds from high temperatures. The temperature is the main control parameter. Moreover, MAE allows a better extraction efficiency of oxygenated compounds to be obtained compared to the classical hydrodistillation (HD), since the absence of solvent reduces the thermal and hydrolysis reactions, thus hindering the degradation of the oxygenated compounds [Lefebvre et al., 2021]. In recent years, coupling MAE with other technologies, such as microwave-assisted hydro distillation (MADH) [Negro et al., 2016] and microwave Steam Distillation (MSD) [Mahato et al., 2017], is of particular interest due to the reduced time of the extraction process and its allowing the recovery of essential oil without causing any change in the composition of the oil gas. On this account, Bustamante et al. studied the upscaling of the MAHD process for the extraction of the essential oil from citrus peel, developing a two-step process, where the microwave energy was supplied, with intermittent power, during the extraction time, obtaining a substantial saving in energy costs and a significant increase in the extraction efficiency. Indeed, as can be observed in Figure 1.11, the energy efficiency of the applied microwave energy decreases as the extraction time increases, confirming that short irradiation times are required to reach a significant extraction efficiency [Bustamante et al., 2016].

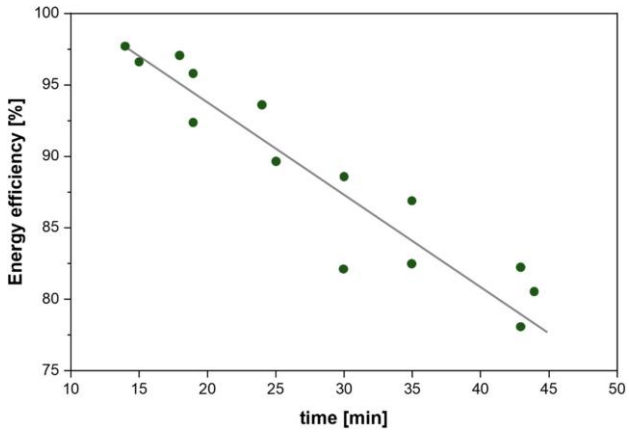

Figure 1.11. MAHD energy efficiency (%) at different extraction times [Bustamante et al., 2016].

One of the most innovative approaches is solvent-free microwave extraction (SFME), a combination of microwave heating and dry distillation, performed at atmospheric pressure without using solvents or water. This technique affords similar yields as the traditional steam distillation with a considerably shorter extraction time and without the post-treatment steps [Teigiserova et al., 2021; Boukroufa et al., 2017]. The SFME extraction process was performed by Ciriminna et al. for the isolation of essential oils from different parts of the fruit: outer skin (exocarp), peel (exo- and mesocarp) and waste (exo-, meso- and endocarp), starting from three types of citrus fruits, orange, lemon and grapefruit, grown in Sicily. Numerous compounds have been identified in EOs with very high yields compared to other industrial methods (0.4% vs. 0.05–0.25%), with limonene as the main constituent (50–80%) in most cases [Ciriminna et al., 2019].

Ultrasound (US) technology has been also applied for the recovery of essential oils [Lefebvre et al., 2021]. The use of ultrasound has the advantage of being fast, simple and low cost [Alves Filho et al., 2020] and is based on milder extraction operative conditions [Negro et al., 2016]. The control and optimization of process parameters (e.g., time, temperature, pressure, speed and power) make this method useful not only for the limonene extraction but also for the selective extraction of different compounds from citrus and plants [Alves Filho et al., 2020]. According to Aliaño-González et al., the technique exploits the energy of ultrasounds for the extraction of different organically derived raw materials [Aliaño-González et al., 2020]. US was successfully used to intensify the extraction of d-limonene from the *Citrus limetta* (sweet lime) peel by Khandare et al. As evidenced in Figure1.12, the ultrasound-assisted extraction (EAU) under optimized conditions allows yields to be achieved similar to those obtained by using Soxhlet, close to 100%, in very short extraction times, due to the physical and structural changes on the substrate surface and the consequent improvement of extraction efficiency [Khandare et al., 2021].

Table 1.4. Comparison of different extraction methods for the recovery of limonene.

Citrus Peel Waste	Extractive Method	Limonene (% in EO)	Extraction Conditions	Ref.
Orange peel fresh	SFME	94.6	Solvent-free, 30 min	[Ferhat et al., 2016]
	MAHD	80.0	Water, 60 min, 100 °C	[Ciriminna et al., 2017]
Orange peel fresh (after juicing)	HD	96.8	Water, 240 min, 100 °C	[Bustamante et al., 2016]
	MAHD	97.4	Water, 240 min, 100 °C	[Bustamante et al., 2016]
	MAHD	80.0	Water, 80 min, 100 °C	[Ciriminna et al., 2017]
Orange peel thawed	HD	94.4	Water, 155 min	[González-Rivera et al., 2016]
	MAHD	94.7	Water, 76 min	[González-Rivera et al., 2016]
	SFME	95.2	Solvent-free, 5 min	[González-Rivera et al., 2016]
	US-MWHD	95.0	Water, 60 min	[González-Rivera et al., 2016]
Orange whole fresh	CP	96.0	Water, 90 min	[Ferhat et al., 2016]
Lemon peel fresh	SFME	74.0	Solvent-free, 30 min	[Ferhat et al., 2016]
	MAHD	50.0	Water, 80 min, 100 °C	[Ciriminna et al., 2017]
Lemon peel fresh (after juicing)	MAHD	68.4	Water, 240 min, 100 °C	[Bustamante et al., 2016]
	MAHD	65.0	Water, 70 min, 100 °C	[Ciriminna et al., 2017]
Lemon flavedo peel fresh	HD	72.9	Water, 180 min	[Ferhat et al., 2007]
	HD	93.0	Water, 180 min	[Ferhat et al., 2016]
	MAHD	30.0	Water, 60 min, 100 °C	[Ciriminna et al., 2017]
Lemon whole fresh	CP	73.8	Water, 90 min	[Ferhat et al., 2016]
Grapefruit peel fresh	SFME	91.6	Solvent-free, 30 min	[Ferhat et al., 2016]
	MAHD	45.0	Water, 70 min, 100 °C	[Ciriminna et al., 2017]
Grapefruit peel fresh (after juicing)	MAHD	89.2	Water, 240 min, 100 °C	[Bustamante et al., 2016]
Grapefruit flavedo peel fresh	HD	92.6	Water, 180 min	[Ferhat et al., 2016]
Grapefruit whole fresh	CP	94.5	Water, 90 min	[Ferhat et al., 2016]

On this account, Pingret et al. designed and developed the sono-Clevenger process, a new procedure employing the US technology for the extraction of essential oils from orange peels. Compared to the conventional Clevenger technique, this advantageous alternative provides a substantial reduction of the extraction time without interfering with the composition of target compounds [Pingret et al., 2014].

González-Rivera et al. studied the solvent-free, microwave-assisted extraction (SMWAE) and the simultaneous ultrasonic and microwave irradiation hydrodistillation (US–MWHD). The cavitation effect of US favors the breakage of the internal cell membranes rushing the extraction of limonene and promoting the volatilization of compounds with higher boiling point, such as valencene.

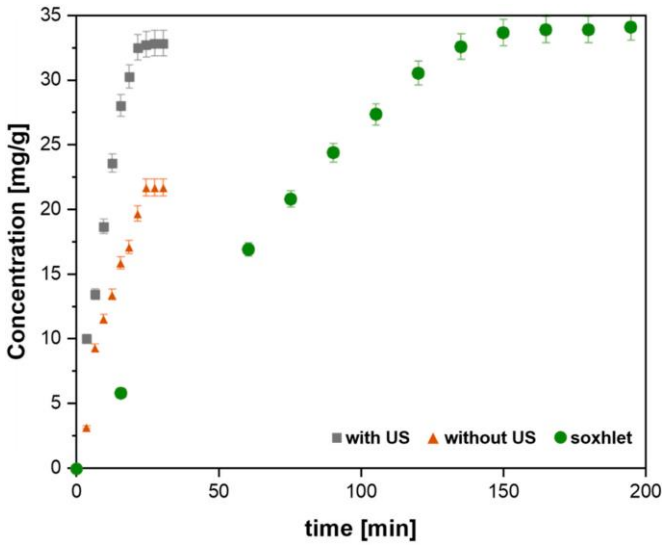

Figure 1.12. Comparison of ultrasonic-assisted extraction (UAE) with conventional extraction methods. [Khandare et al., 2021].

Indeed, the amount of limonene and myrcene, the two main compounds of the orange peel EOs, increases over time and reaches a limit value at the end of the process (Figure 1.13), resulting in a limonene content above 95% and a higher amount of valencene. Since the valencene amount in the orange EOs, due to its aromatic and flavoring characteristics, contributes to an increase in

its quality and commercial value, it is evident that the US-MWHD cavity-less configuration can be considered not only a faster method, compared with the microwave coaxial hydrodistillation (MWHD) and conventional hydrodistillation (CH), but also the best way to obtain the highest quality of EO (Figure 1.14) [González-Rivera et al., 2016].

The extraction by supercritical fluid (SFE) has been extensively studied and is generally considered a non-traditional eco-friendly extraction technique [Khaw et al., 2017], using CO_2 as green and renewable solvent. Although many other solvents can be used for plant extraction (such as propane), CO_2 is considered an ideal solvent for SFE. The critical temperature of CO_2 is slightly higher than the room temperature, and the low critical pressure allows it to operate at moderate pressures, generally between 100 and 450 bar [Azmir et al., 2013; Lefebvre et al., 2021]. Therefore, limonene's extraction by the traditional hydrodistillation technique may be replaced by the supercritical fluid extraction (15 MPa, 40 °C), which offers the possibility to save time and represents an eco-friendly alternative method [Lopresto et al., 2019]. Several researchers, by using supercritical CO_2 to investigate the extraction of volatile components from the orange peel, showed that the concentrations of limonene and linalool depend significantly on the applied process parameters [Jokić et al., 2020]. The optimization of process conditions for supercritical CO_2 extraction plays a key role for the selectivity of the extracted components and their subsequent application in the food industry [Lopresto et al., 2014]. Finally, it is worth mentioning that, in recent years, the use of the supercritical CO_2 (SC-CO_2) as a solvent and hydrotropic extraction tool has been evaluated to extract limonoids from the citrus waste, allowing yields up to 13 times higher to be obtained than the traditional cold-pressing technique, recovering the 100% limonene yield. However, it is impossible to compare the efficiency of this technique with others, as the yield depends on the amount of CO_2 used [Teigiserova et al., 2021; Mira et al., 1999].

A recent study employed the enzymatic pre-treatment of cellulose for the extraction of essential oils from three different citrus peels [Chávez-González et al., 2016]. Compared to conventional methods, the use of assisted enzymes allows an increase in essential oil yield by 2- and 6-fold for orange peel and grapefruit, respectively. The enzymatic treatment has the advantage of reducing the overall viscosity, which facilitates the breaking of an emulsion for the recovery of the oil from the aqueous phase [Putnik et al., 2017].

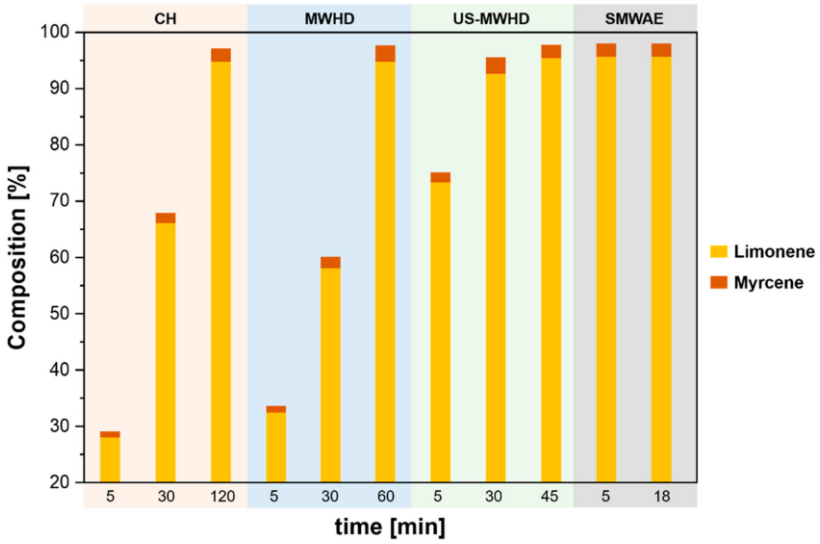

Figure 1.13. Chemical composition of the orange peel essential oils (Eos) obtained by conventional hydrodistillation (CH), solvent-free, microwave-assisted extraction (SMWAE), ultrasonic and microwave irradiation hydrodistillation (US–MWHD) and MWHD at different extraction times with a composition higher than 2% [González-Rivera et al., 2016].

The preliminary steps play an important role during the extraction of compounds from the biomass. Among these, drying and grinding are two factors that predominantly affect the final yield. Generally, dehydration involves the removal of the bound water from the peel by increasing the porosity of the cellular matrix, thereby facilitating diffusion rate and promoting the contact with enzymes, consequently enhancing the overall process [Nadar et al., 2018]. Most important, the enzyme-assisted extraction can be coupled with other techniques (e.g., microwave-assisted, ultrasound-

assisted, supercritical fluid and high-pressure) to increase the overall yield of the limonene.

Upgrading of limonene into p-cymene over heterogeneous catalysts

Limonene tends to turn into monocyclic terpenes (terpinenes and terpinolenes) that can dissociate into menthenes and cymenes as final products [Corma et al., 2007]. Indeed, in an alternative process, p-cymene can be produced via isomerization or hydrogenation, as well as by the direct dehydrogenation of limonene [Yılmazoğlu and Akgün, 2018].

Reports on the transformation of limonene into p-cymene by homogeneous catalysts are quite limited since low yields and separation drawbacks generally occur, thus driving the interest towards heterogeneous systems (Table 2), able to ensure good performances and, at the same time, an easy separation from the post-reaction mixture [Bueno et al., 2008; Shokouhimehr, 2015].

In an interesting approach, Catrinescu et al. used several metal-modified bentonites as catalysts at 150 °C for 15 min in the presence of n-dodecane as solvent. The results show that the nickel-modified bentonites are the most active with respect to analogous Al- and Cr-based catalysts [Catrinescu et al., 2006].

The catalytic conversion of limonene to p-cymene was also performed by Martin-Luengo et al., using sepiolite, a clay (hydrated magnesium silicate) of natural and economic origin, as a catalyst by microwave irradiation. High conversion of limonene to p-cymene, under solvent-free conditions, was achieved using a modified catalyst with Na, Ni, Fe or Mn oxides. Modification of the catalyst with nickel allows the complete conversion of limonene with a selectivity of 100% to p-cymene, after 20 min of reaction [Martin-Luengo et al., 2010]. The same research group as before used mesoporous silica-alumina

supports as catalysts with a SiO_2 content ranging from 1% (SIRAL 1) to 40% (SIRAL 40) [Martin-Luengo et al., 2008].

Both the limonene conversion and the p-cymene selectivity linearly increase with the silica content with SIRAL 20 and SIRAL 40 catalysts, leading to complete conversion of limonene into p-cymene.

In another approach, limonene was previously isomerized into α-terpinene, γ-terpinene and terpinolene and then converted into p-cymene over the H-FER (T) (ferrierite from Tosoh in which the Si/Al ratio amounts to 8.9) catalyst at 65 °C. At this temperature, after a reaction time of 60 min, a 38% limonene conversion was gained. Interestingly, limonene transformation was not observed over H-FER (Z) ferrierite catalysts characterized by Brønsted sites with higher acid strength [Rachwalik et al., 2012].

The dehydrogenation of limonene to p-cymene was explored by Cui et al. using a Pd/HZSM-5 catalyst under both inert (N_2) and reductive (H_2) reaction conditions. Due to the endothermic nature of dehydroaromatization reactions, an increase in the reaction temperature is beneficial to the shift of the equilibrium toward p-cymene production both in the presence and in the absence of added hydrogen (Figure 1.14).

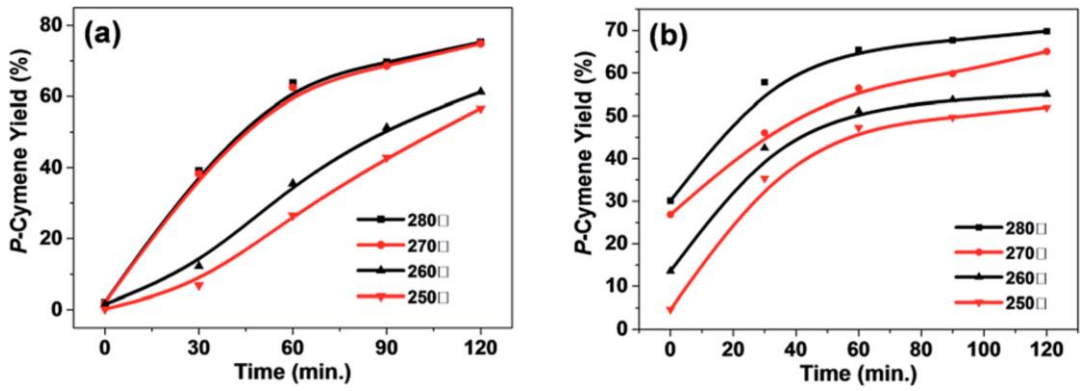

Figure 1.14. Conversion of limonene into p-cymene over the Pd/HZSM-5 catalyst as a function of time (**a**) in absence of added hydrogen and (**b**) under inert atmosphere [Cui et al., 2016].

Table 1.5. Conversion of Limonene into p-cymene promoted by heterogeneous catalysts.

Catalyst	Limonene Conversion (%)	p-Cymene Yield (%)	Reaction Conditions	Ref.
Ni-SD	96	17	Batch, n-dodecane, 150 °C, 15 min	[Catrinescu et al., 2006]
H-FER (T)	38	n.d.	Batch, 65 °C, 60 min	[Rachwalik et al., 2012]
SIRAL 20	100	100	Batch, microwave, 175 °C, 10 min	[Martin-Luengo et al.,2008]
SepNi	100	100	Batch, microwave, 210 °C, 20 min	[Martin-Luengo et al., 2010]
Pd/HZSM-5 (258)	100	82	Batch, n-dodecane, 260 °C, 2 h, 8 bar N_2	[Cui et al., 2016]
Ti-SBA-15	99	56	Batch, 160 °C, 23 h	[Retajczyk and Wróblewska, 2019]
TECHNOSA-H2	98	65	Batch, tetraethylene glycol dimethyl ether, 140 °C, 7 h, N_2	[Lycourghiotis et al., 2018]
TiO_2	100	90	Continuous flow, 300 °C, 6 h, H_2	[Kamitsou et al., 2014]
Pd/Al_2O_3	100	80	Continuous flow, SC-ethanol, 300 °C, 30 s, 6.5 MPa	[Yılmazoğlu and Akgün, 2018]

The addition of hydrogen leads to a lower selectivity to p-cymene, since it increases the hydrogenation rate on the double bonds, facilitating the isomerization reaction of limonene and preventing its reverse reaction [Cui et al., 2016]. Most important, it was proved that the first step in the conversion of limonene into p-cymene is the isomerization, followed by a sequential dehydrogenation process.

Retajczyk et al. carried out studies on the limonene isomerization process using Ti- SBA-15 and Ti-MCM-41 as catalysts, performing the limonene isomerization without any organic solvents [Retajczyk and Agnieszka Wróblewska, 2019]. The conversion of limonene increases by increasing both the reaction temperatures as well as the reaction time (Figure 1.15).

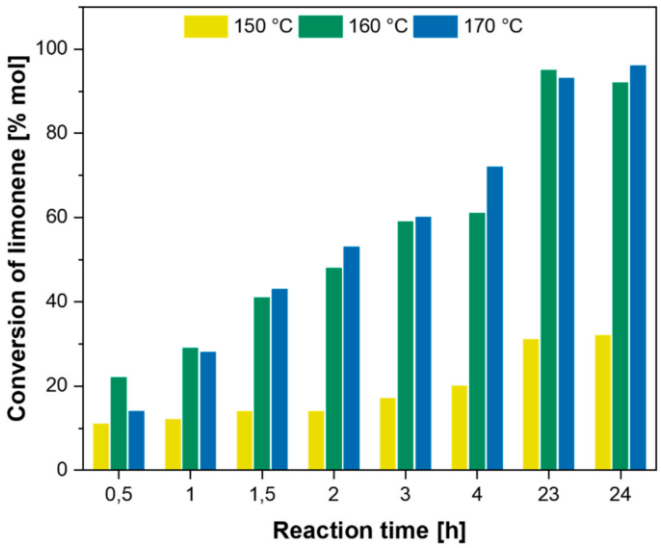

Figure 1.15. Temperature effect on the isomerization of R-limonene [Retajczyk and Wróblewska, 2019].

Results clearly show that, under the same processing conditions (temperature 160 °C, catalyst content 15% wt, for 23 h), the different mesoporous silica structures of MCM and SBA give rise to different yields of p-cymene (29% with a limonene conversion of 92% for Ti-MCM-41 and 56% with a limonene conversion of 99% for Ti-SBA-15).

A 2-step mechanism was proposed by Makarouni et al., starting from the limonene isomerization over activated natural mordenites and then its isomerization into p-cymene in a non-catalytic process, using atmospheric oxygen as a green oxidant (Figure 1.16).

The acid treatment with sulfuric acid aqueous solutions of natural mordenite causes the removal of sodium oxide from its micropores, which drastically increases the specific surface and acidity, making natural mordenite very active in the catalytic transformation of limonene into p-cymene and causing a significant enhancement in both the limonene conversion and in the amount of p-cymene obtained in the reaction mixture. A rather high p-cymene yield (63%) at 140 °C, with a limonene/catalyst ratio of 15 and a reaction time of 7 h, was obtained [Eggersdorfer, 2012]. Another achievement of the same group was the use of aqueous solutions of various acids (CH_3COOH, HCl, H_2SO_4, HNO_3) to further improve the surface area and the acidity of natural mordenite with a significant increase in the conversion of limonene to p-cymene up to 65% [Lycourghiotis et al., 2018].

It is generally accepted that the addition of a transition metal to supports like silica, alumina, silica–alumina mixed oxides, zeolites and natural clays generally improves the catalytic performance as a consequence of the dual functionality exhibited by metal-modified catalysts. In the case of the conversion of limonene into cymene, acid sites are responsible for the isomerization step, while metallic sites can promote the dehydrogenation reaction [Kamitsou et al., 2014; Roberge et al., 2001].

On this account, several Cr_2O_3, CuO, ZnO, ZrO_2, MgO, La_2O_3, TiO_2 and Pd supported on C catalytic systems have been successfully used for the dehydrogenation of terpenes [Swift, 2004], improving the p-cymene selectivity by up to 97% [Yılmazoğlu and MesutAkgün, 2018].

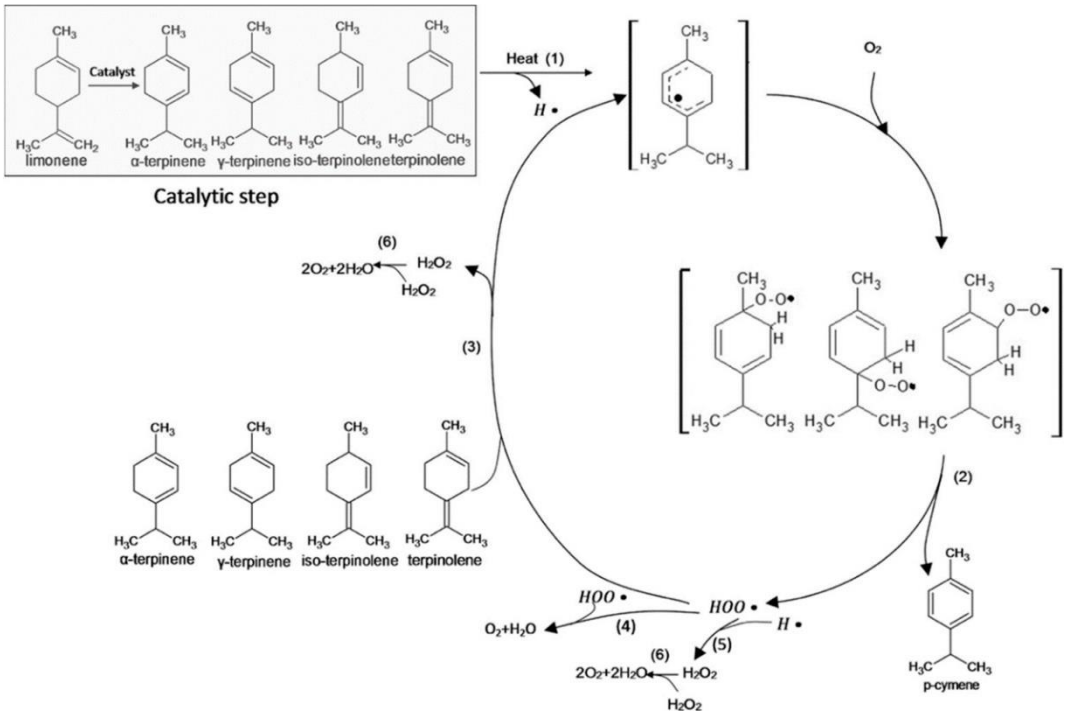

Figure 1.16. The reaction mechanism of the two-step conversion of limonene into p-cymene [Makarouni et al., 2018].

Kamitsou et al. recently reported an almost complete transformation of α-limonene into p-cymene (90% yield at 300 °C) over the TiO_2 catalyst in a helium atmosphere. Titanium oxide is a very stable catalyst, and its high catalytic performance could be attributed to a good acidity/reducibility balance, allowing the Ti (IV)/Ti (III) transformation during the reaction, thus positively promoting the limonene conversion. At the same time, by using the CaO catalyst, the production of p-cymene takes place directly via limonene dehydrogenation, with a conversion rate of up to 98% and a selectivity of about 100% [Kamitsou et al., 2014].

The transformation of limonene over different heterogeneous catalysts (Pt/Al_2O_3, Ni/Al_2O_3, and Pd/Al_2O_3) and in supercritical conditions of ethanol and 2-propanol was investigated by Yılmazoğlu et al. When the Pd/Al_2O_3 catalyst was used, the limonene was completely converted with an overall p-cymene yield of 80% [Yılmazoğlu and MesutAkgün, 2018].

In a very interesting approach, Zhang and Zhao proposed d-limonene as a hydrogen- donor molecule for the deoxygenation of fatty acids into alkanes and arenes (these can be used as bio-jet fuel) in the presence of the bimetallic Pd-Ni/HZSM-5 catalyst [Zhang and Zhao, 2015; Zhang and Zhao, 2016]. Palladium promotes the conversion of limonene into p-cymene and H_2, which is the reducing agent also for the hydrodeoxygenation of stearic acid to alkanes over Ni and Pd-Ni sites (Figure 1.17).

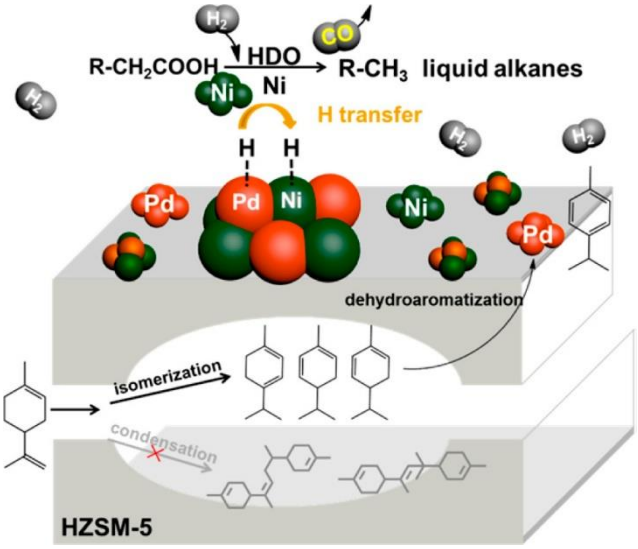

Figure 1.17. Brief description of individual steps for stearic acid and limonene coactivation using the bimetallic Pd-Ni/HZSM-5 catalyst [Zhang and Zhao, 2016].

This kind of approach is of particular significance since catalytic transfer hydrogenation/hydrogenolysis reactions are getting increasing attention in the reductive upgrading of lignocellulosic biomasses and their relative macromolecules and derived molecules [Tabanelli et al., 2019; Mauriello et al., 2018; Paone et al., 2020; Paone et al., 2020; Paone et al., 2016; Malara et al., 2020; Gumina et al., 2018], thus opening new opportunities for the use of limonene as a green and renewable H-donor solvent.

1.4 Production of levulinic acid and alkyl levulinates

Levulinic acid, also known as 4-oxopentanoic acid or γ-ketovaleric acid, is a low molecular weight fatty acid containing a carbonyl group. The name *levulinic acid* (LA) comes from *levulose*, which is obtained from the reaction of fructose with hydrochloric acid. The global interest in this molecule stimulated the need to develop easier synthesis strategies, favoring the yield increase related to the intensification of a rapid process [Raspolli Galletti et al., 2020]. Levulinic acid and its derivatives are resources that can be used in various applications in addition to the already known use as bio-fuels [Corma et al., 2011] or ecological fertilizers, and are intermediate compounds in the production of high-performance materials, both in the chemical and pharmaceutical industries. Figure 1.18 shows a summary of the potential derivatives of LA.

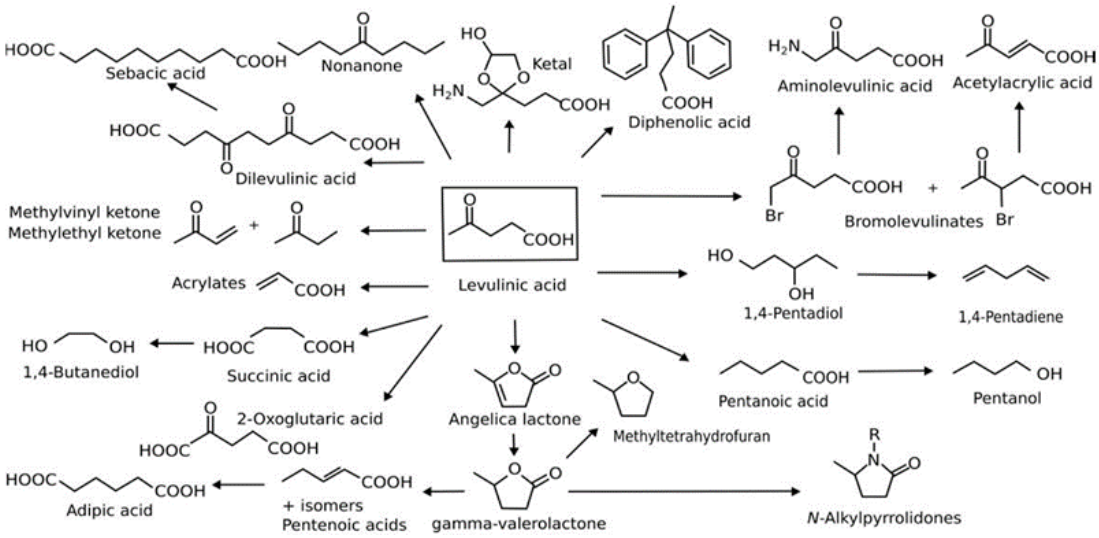

Figure 1.18. Chemical structure of the main molecules derived from LA [Antonetti et al., 2016].

Furthermore, LA derivatives can be easily obtained by esterification with acid catalysts [Badgujar and Bhanage, 2020]. Among these derivatives, alkyl levulinates (ALs) stand out because they have some advantageous characteristics compared to LA. For instance, the reaction between the esters

of levulinic acid and alcohol leads to the formation of ketals that can be used as new green surfactants [Freitasa et al., 2016]. Furthermore, the moderate reactivity of the carboxylate group leads to the possibility of being exploited as more selective starting raw materials towards the final products of interest [De María, 2016]. A further advantage is given by the lower boiling point compared to LA which can guarantee rapid separation by distillation [Shrikhandea et al., 2020].

In most of the studies in which LA and ALs were obtained, monosaccharides as starting materials (mainly glucose and fructose) were used. Strong acids, such as sulfuric or hydrochloric acid, have been used as catalysts to convert sugars into LA and formic acid in an aqueous solution [Garves, 1998]. Recent studies have shifted interest in the enhancement of biomass as feedstock from which is possible to obtain high yields of levulinic acid. The most important and attractive raw material is the lignocellulosic biomass due to its high availability and its high content of cellulose, hemicellulose, and lignin [Frigo et al., 2014].

Typically, ALs are produced by two different methods from cellulosic raw materials. The first method is a two-step process of LA production carrying out cellulose hydrolysis and following the esterification of LA with ethanol or methanol to obtain ethyl and methyl levulinate respectively [Tiong et al. 2018]. However, this process has the drawback of requiring an additional step to purify the LA produced. Another process is a method in situ where the reagent, the catalysts, and the solvent are put together in a reactor to simultaneously perform hydrolysis and esterification [Maciel Filho, 2017]. Since in situ process offers the advantage of being simpler than the two-step process and of reducing the risk of polymerization of the intermediates with glucose, many recent studies have evaluated the production of LA esters with enzymes or solid catalysts used in the in-situ process [Zhou, et al. 2020].

According to world citrus production, the annual world offer of OPW should be around 115, 6 tons [FAO, 2020], therefore the orange peel waste land at 55% of the total citrus waste and could be used as a source for the production of levulinic acid and its esters. Undried citrus peel has never been used for the production of ALs. A recent study shows that the moisture in citrus peels can be exploited to form an immiscible phase with co-solvent and increase the ALs yield [Yang et l., 2018].

Therefore, the target is to promote the market of these bio-products by the development of new one-pot and green production processes by using waste biomass as raw material, including orange peel waste instead of traditional fossil sources [Seggiani, 2012].

Catalytic upgrading of levulinic acid and alkyl levulinates into γ-valerolactone

A huge number of catalytic strategies has been developed to convert the lignocellulosic biomass into platform molecules, including γ-valerolactone (GVL) which has recently attracted considerable attention due to the promise for potential industrial applications [Yan et al., 2015]. GVL proved to be an efficient fuel additive for gasoline and a green solvent especially useful in biomass valorization [Gallo et al., 2013]. Furthermore, GVL can be transformed to butenes through ring-opening and decarboxylation, and the resulting butenes can be upgraded to yield liquid hydrocarbon fuels suitable for diesel, and aviation kerosene [Bond et al., 2010]. GVL can also be utilized as a low-cost precursor for the production of various polymeric monomers, as well as for the production of derivatives such as methyltetrahydrofuran, alkanes, and 1,4-pentandiol, and valuable bio-oxygenates [Lange et al., 2010].

Biomass-derived GVL is a key derivative of LA and is typically synthesized by the reduction and subsequent intramolecular dealcoholization of LA and its esters, [Wright et al., 2012]. These are intermediate molecules

generated by acid-catalyzed hydrolysis and from the alcoholysis of various carbohydrate fractions of lignocelluloses, respectively (Scheme 1.2) [Hu et al., 2013; Kuwahara et al., 2017].

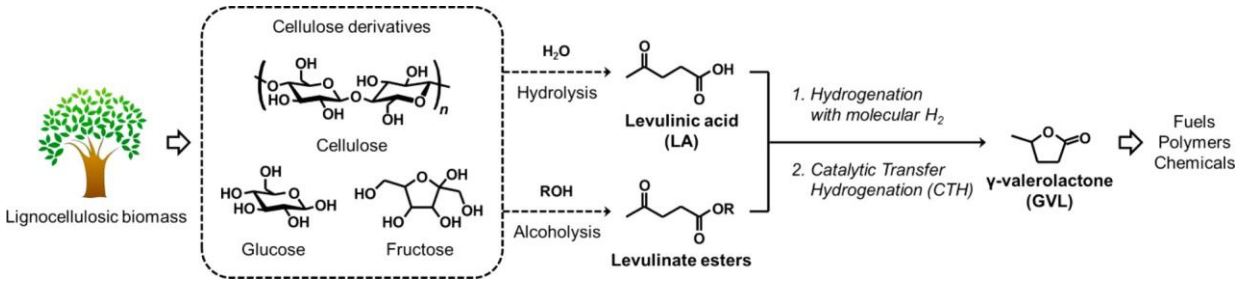

Scheme 1.2. Production of γ-Valerolactone (GVL) from Lignocellulosic Biomass [Kuwahara et al., 2017].

For the catalytic hydrogenation of LA to GVL, hydrogenation using molecular H_2 catalyzed by homogeneous and heterogeneous noble metal catalysts such as ruthenium (Ru), palladium (Pd), iridium (Ir), and platinum (Pt), has been the most important approach [Dutta et al., 2019].

Although this approach can produce high GVL yields, the expensive precious metal catalysts and operational problems associated with the use of pressurized H_2 limit the large-scale application. The CTH process using alcohols as H-donors molecules has been proposed as an innovative approach for scalable GVL production with economic competitiveness and sustainability because the reaction occurs under moderate conditions without the need for H_2 gas or noble metal catalysts, and alcohols are used as low-cost and renewable H-donors [Assary et al., 2013].

Furthermore, the alcohol media derived from the previous alcoholysis process can potentially be used as different hydrogen sources, thus leading to an energy-saving and cost-effective GVL production process [Kuwahara et al., 2014]. Although several catalysts are known to be active for CTH reactions, Zr-based catalysts, such as ZrO_2, have been reported as efficient heterogeneous

catalysts for GVL synthesis from LA and ALs via the CTH process due to their amphoteric nature [Chia and Dumesic, 2011].

This opens up new perspectives of these materials as heterogeneous catalysts for the selective transformation of biomass feedstocks in biorefinery process.

1.5 Conclusions

This chapter contains a general overview of the sustainability concepts and the use of biomass for the production of various value-added products. The developed conversion technology concerns the valorization of biomass. In fact, HTC is regarded as a critical method to convert waste into useful hydrochar and bio-oil which could be used in a wide range of applications. Subsequently, an overview of interesting chemical intermediates is provided, such as furfural, 5-hydroxymethilfurfal, and levulinic acid, for their further (catalytic) processing to high added value end-products.

Specifically, in the case of the orange peel waste, the current management including traditional treatment methods and biorefinery treatment methods were reviewed. The advantages and disadvantages of the different treatment methods were also outlined in the review.

In addition, citrus wastes are a good but intrinsically limited source of limonene. In this account, recent advances in the extraction of limonene from citrus processing waste were also highlighted with particular attention to the benign-by-design extractive process and its catalytic dehydrogenation for the production of p-cymene.

Among the conventional recovery technologies, cold press extraction provides good yields and ease of applicability. Accordingly, it is the industrial state of the art technology. Amid the new, solvent-free extraction technologies,

the highly reproducible, versatile and simple microwave-assisted extraction is one of the more relevant alternatives. Other environmentally friendly methods include supercritical fluid and ultrasound extraction. All these methods are likely to find application when the microbial production of limonene by converting virtually unlimited raw materials such as sugars will be industrialized [Ren et al., 2020], in order to magnify its production and meet the so far largely unmet market demand for limonene.

At the same time, the development of new green pathways for p-cymene production from limonene is an excellent alternative to the traditional method of obtaining p-cymene via Friedel-Crafts alkylation of toluene with isopropene. The most recent investigations found that supercritical alcohols favoring the catalytic processes by enriching both the solubility and the diffusivity are the most interesting solvents.

In order to realize the complete valorization of a low-cost lignocellulosic biomass, the production of GVL from levulinic acid derived from biomass and its esters through a CTH process is also highlighted. The use of non-noble metals such as Cu and Zr represents a greener route of GVL production than the conventional practice using noble metals such as Pd and Ru, considering their higher abundance and milder reaction conditions needed, without employing H_2.

References

Agbor, V.B.; Cicek, N.; Sparling, R.; Berlin, A.; Levin, D.B. Biomass pretreatment: fundamentals toward application. *Biotechnol. Adv.* **2011**, *29*, 675-685.

AIJN, **2014**. Available from: http://aijn.org/files/default/aijn2014-full.pdf.

Aissou, M.; Chemat-Djenni, Z.; Yara-Varòn, E.; Fabiano-Tixier, A.-S.; Chemat, F. Limonene as an agro-chemical building block for the synthesis and extraction of bioactive compounds. *Comptes Rendus Chim.* **2017**, *20(4)*, 346-358.

Ajila, C.M.; Brar, S.K.; Verma, M.; Rao, U. (**2012**). *Sustainable Solutions for Agro Processing Waste Management: An Overview*. Berlin: Springer-Verlag Berlin.

Aliaño-González, M.J.; Jarillo, J.A.; Carrera, C.; Ferreiro-González, M.; Ángel Álvarez, J.; Palma, M.; Ayuso, J.; Barbero, G.F.; Espada-Bellido, E. Optimization of a Novel Method Based on Ultrasound-Assisted Extraction for the Quantification of Anthocyanins and Total Phenolic Compounds in Blueberry Samples (Vaccinium corymbosum L.). *Foods* **2020**, *9*, 1763.

Alves Filho, E.G.; Sousa, V.M.; Rodrigues, S.; de Brito, E.S.; Fernandes, F.A.N. Green ultrasound-assisted extraction of chlorogenic acids from sweet potato peels and sonochemical hydrolysis of caffeoylquinic acids derivatives. *Ultrason. Sonochem.* **2020**, *63*, 104911.

Ahn, Y.; Lee, S.H.; Kim, H.J.; Yang, Y.-H.; Hong, J.H.; Kim, Y.-H.; Kim, H. Electrospinning of lignocellulosic biomass using ionic liquid. *Carbohydr. Polym.* **2012**, *88 (1)*, 395–398.

Anastas, P.T.; Warner, J. C. Green chemistry: Theory and practice. New York: Oxford University Press **1998**, 10-55.

Anjum, M.; Khalid, A.; Qadeer, S.; Miandad, R. Synergistic effect of co-digestion to enhance anaerobic degradation of catering waste and orange peel for biogas production. *Waste Manag. Res.* **2017**, *35*, 967-977.

Annamalai, P. Citrus yield mapping system using machine vision. University of Florida 2**004**.

Antonetti, C.; Licursi D.; Fulignati, S.; Valentini, G.; Raspolli Galletti, A.M. New frontiers in the catalytic synthesis of levulinic acid: from sugars to raw and waste biomass as starting feedstock. *Catalysts* **201**6, *6(12)*, 196.

Assary, R.S.; Curtiss, L.A.; Dumesic, J.A. Exploring Meerwein-Ponndorf-Verley reduction chemistry for biomass catalysis using a first-principles approach. *ACS Catal.* **2013**, *3*, 2694-2704.

Azmir, J.; Zaidul, I.S.M.; Rahman, M.M.; Sharif, K.M.; Mohamed, A.; Sahena, F.; Jahurul, M.H.A.; Ghafoor, K.; Norulaini, N.A.N.; Omar A.K.M. Techniques for extraction of bioactive compounds from plant materials: A review. *Journal of Food Engineering* **2013**, *117*, 426-436.

Badgujar, K.C.; Badgujar, V.C.; Bhanage, B.M. A review on catalytic synthesis of energy rich fuel additive levulinate compounds from biomass derived levulinic acid. *Fuel Process. Technol.* **2020**, *197*, 106213.

Bampidis, V.; Robinson, P. Citrus by-products as ruminant feeds: A review. *Animal Feed Science and Technology* **2006**, *128(3-4)*, 175-217.

Bargmann, I.; Rillig, M.C.; Kruse, A.; Greef, J.M.; Kucke, M. Effects of hydrochar application on the dynamics of soluble nitrogen in soils and on plant availability. *J. Plant Nutrit. Soil Sci.* **2014**, *177(1)*, 48-58.

Battista F.; Remelli G.; Zanzoni S.; Bolzonella D. Valorization of Residual Orange Peels: Limonene Recovery, Volatile Fatty Acids, and Biogas Production. *ACS Sustainable Chemistry & Engineering* **2020**, *8(17)*, 6834-6843.

Beesley, L.; Moreno-Jiménez, E.; Gomez-Eyles, J.L.; Harris, E.; Robinson, B.; Sizmur, T. A review of biochars' potential role in the remediation, revegetation and restoration of contaminated soils. *Environmental Pollution* **2011**, *159(12)*, 3269-3282.

Benavente-García, O.; Castillo, J.; Marin, F.R.; Ortuño, A.; Del Río, J.A. Uses and properties of Citrus flavonoids. *J. Agric. Food. Chem.* **1997**, *45*, 4505-4515.

Berti, S.; Burato, P.; Dionisi-Vici, P.; Allegretti, O.; Orange Wood for Parquet and Engineered Flooring Use. *BioResources* **2018**, *13(1)*, 586-596.

Bond, J.Q.; Alonso, D.M.; Wang, D.; West, R.M.; Dumesic, J.A. Integrated catalytic conversion of γ-valerolactone to liquid alkenes for transportation fuels. *Science* **2010**, *327*, 1110-1114.

Boukroufa, M.; Boutekedjiret, C.; Chemat, F.; Development of a green procedure of citrus fruits waste processing to recover carotenoids. *Resource-Efficient Technologies* **2017**, *3*, 252-262.

Bozym, M.; Florczak, I.; Zdanowska, P.; Wojdalski, J.; Klimkiewicz, M. An analysis of metal concentrations in food wastes for biogas production. *Renew. Energy* **2015**, *77*, 467-472.

Braidy, N.; Behzad, S.; Habtemariam, S.; Ahmed, T.; Daglia, M.; Nabavi, S.M.; Sobarzo-sanchez, E.; Nabavi, S.F. Neuroprotective Effects of Citrus Fruit-Derived Flavonoids. Nobiletin and Tangeretin in Alzheimer's and Parkinson's Disease. *CNS Neurol. Disord. Drug Targets* **2017**, 387-397.

Bueno, A.C.; Brandao, B.B.N.S.; Gusevskaya, E.V. Aromatization of para-menthenic terpenes by aerobic oxidative dehydrogenation catalyzed by p-benzoquinone. *Appl. Catal. A Gen.* **2008**, *351*, 226-230.

Buhl, D.; Roberge, D.M.; Hölderich, W.F. Production of p-cymene from α-limonene over silica supported Pd catalysts. *Appl. Catal. A Gen.* **1999**, *188*, 287-299.

Burguete, P.; Corma, A.; Hitzl, M.; Modrego, R.; Ponce, E.; Renz, M. Fuel and chemicals from wet lignocellulosic biomass waste streams by hydrothermal carbonization. *Green Chem.* **2016**, *18(4)*, 1051-1060.

Bustamante, J.; Stempvoort, S.V.; García-Gallarreta M.; Houghton, J.A.; Briers H.K.; Budarin, V.L.; Matharu A.S.; Clark, J.H. Microwave assisted hydro-distillation of essential oils from wet citrus peel waste. *J. Clean. Prod.* **2016**, *137*, 598-605.

Calabrò, P.; Pontoni, L.; Porqueddu, I.; Greco, R.; Pirozzi, F.; Malpei, F. Effect of the concentration of essential oil on orange peel waste biomethanization: Preliminary batch results. *Waste Manage.* **2016**, *48*, 440-447.

Cannon, J.B.; Cantrell C.L.; Astatkie, T.; Zheljazkov V.D. Modification of yield and composition of essential oils by distillation time. *Ind. Crop. Prod.* **2013**, *41*, 214-220.

Cao, L. Yu, I.K.M; Cho, D.-W.; Wang, D.; Tsang, D.C.W; Zhang, S.; Ding, S.; Wang, L.; Sik Ok, Y. Microwave-assisted low-temperature hydrothermal treatment of red seaweed (Gracilaria lemaneiformis) for production of levulinic acid and algae hydrochar. *Bioresource technology* **2019**, *273*, 251-258.

Catrinescu, C.; Fernandes, C.; Castilho, P.; Breen, C. Influence of exchange cations on the catalytic conversion of limonene over Serra de Dentro (SD) and SAz-1 clays Correlations between acidity and catalytic activity/selectivity. *Appl. Catal. A* **2006**, *311*, 172-184.

Chávez-González, M.L.; López-López, L.I.; Rodríguez-Herrera, R.; Contreras-Esquivel, J.C.; Aguilar, C.N. Enzyme-assisted extraction of citrus essential oil. *Chem. Pap.* **2016**, *70*, 412-417.

Chen, H. Chemical composition and structure of natural lignocellulose. In Biotechnology of Lignocellulose: Theory and Practice Springer Science Business Media B.V: Dordrecht, The Netherlands, 2014; pp. 25-71.

Chen, S.S.; Maneerung, T.; Tsang, D.C.V.; Sik Ok, J.; Wang, C.-H. Valorization of biomass to hydroxymethylfurfural, levulinic acid, and fatty acid methyl

ester by heterogeneous catalysts. *Chemical Engineering Journal* **2017**, *328*, 246-273.

Chen, S.S., Wang, L.; Yu, I.K.M.; Tsang, D.C.W.; Hunt, A.J.; Jérôme, F.; Zhang, S.; Sik Ok, J.; Sun Poon, K. Valorization of lignocellulosic fibres of paper waste into levulinic acid using solid and aqueous Brønsted acid. *Bioresource technology* **2018**, *247*, 387-394.

Chen, X.M.; Tait, A.R.; Kitts, D.D. Flavonoid composition of orange peel and its association with antioxidant and anti-inflammatory activities. *Food Chemistry* **2017**, *218*, 15-21.

Chia, M.; Dumesic, J.A. Liquid-phase catalytic transfer hydrogenation and cyclization of levulinic acid and its esters to γ-valerolactone over metal oxide catalysts. *Chem. Commun.* **2011**, *47*, 12233-12235.

Ciriminna, R.; Fidalgo, A.; Avellone, G.; Danzì, C.; Timpanaro, G.; Locatelli, M.; Carnaroglio, D.; Meneguzzo, F.; Ilharco, L.M.; Pagliaro, M. Integral extraction of Opuntia ficus-indica peel bioproducts via microwave-assisted hydrodiffusion and hydro-distillation. *ACS Sustain. Chem. Eng.* **2019**, 7884-7891.

Ciriminna, R.; Fidalgo, A.; Delisi, R.; Carnaroglio, D.; Grillo, G.; Cravotto, G.; Tamburino, A.; Ilharco, L.M.; Pagliaro, M. High-quality essential oils extracted by an eco-friendly process from different citrus fruits and fruit regions. *ACS Sustain. Chem. Eng.* **2017**, *5*, 5578-5587.

Ciriminna, R.; Lomeli-Rodriguez, M.; Demma Carà, P.; Lopez-Sanchez, J.A.; Pagliaro, M. Limonene: A versatile chemical of the bioeconomy. *Chem. Commun.* **2014**, *50(97)*, 15288.

Ciriminna, R.; Parrino, F.; De Pasquale, C.; Palmisano, L.; Pagliaro, M. Photocatalytic partial oxidation of limonene to 1,2 limonene oxide. *Chem. Commun.* **2018**, *54*, 1008.

Ciriminna, R.; Scurria, A.; Avellone, G.; Pagliaro, M. A Circular Economy Approach to Fish Oil Extraction. *ChemistrySelect* **2019**, *4(17)*, 5106-5109.

Ciriminna, R.; Scurria, A.; Fabiano-Tixier, A.-S.; Lino, C.; Avellone, G.; Chemat, F.; Pagliaro, M. Omega 3 Extraction from Anchovy Fillet Leftovers with Limonene: Chemical, Economic, and Technical Aspects. *ACS Omega* **2019**, *4*, 15359-15363.

Cook, N.C.; Samman, S. Flavonoids-Chemistry, metabolism, cardioprotective effects, and dietary sources. *J. Nutr. Biochem.* **1996**, *7*, 66-76.

Corma, A.; De la Torre, O.; Renz, M.; Villandier. N. Production of High-Quality Diesel from Biomass Waste Products. *A journal of the German Chemical Society* **2011**, *50*, 2375-2378.

Corma, A.; Iborra, S.; Velty, A. Chemical Routes for the Transformation of Biomass into Chemicals. *Chem. Rev.* **2007**, *107*, 2411-2502.

Cui, H.; Zhang, J.; Luo, Z.; Zhao, C. Mechanisms into dehydroaromatization of bio-derived limonene to p-cymene over Pd/HZSM-5 in the presence and absence of H_2. *RSC Adv.* **2016**, *6*, 66695-66704.

De, S.; Saha, B.; Luque, R. Hydrodeoxygenation processes: Advances on catalytic transformations of biomass-derived platform chemicals into hydrocarbon fuels. *Bioresour. Technol.* **2015**, *178*, 108-118.

De María, P.D. (**2016**). *Industrial Biorenewables: A Practical Viewpoint*. Hoboken, NJ, USA: Wiley.

Delidovich, K.; Leonhard, R. Palkovits Cellulose and hemicellulose valorisation: an integrated challenge of catalysis and reaction engineering. *Energy Environ. Sci.* **2014**, *7*, 2803-2830.

Demirbaş A. Biomass resource facilities and biomass conversion processing for fuels and chemicals. *Energy Convers. Manag.* **2001**, *42*, 1357-78.

Deuss, P.J.; Barta, K. From models to lignin: transition metal catalysis for selective bond cleavage reactions Coord. *Chem. Rev.* **2016**, *306*, 510-532.

Diaz, D.; Espinosa, S.; Brignole, E.A.; Citrus peel oil deterpenation with supercritical fluids: optimal process and solvent cycle design. *J. Supercrit. Fluids* **2005**, *35*, 49-61.

Dugo, G.; Di Giacomo, A. (**2002**). *Citrus*. London: CRC Press.

Dutta, S.; Yu, I.K.M.; Tsang, D.C.W.; Ng, Y.H.; Ok, Y.S.; Sherwood, I.; Clark., J.H. Green synthesis of gamma-valerolactone (GVL) through hydrogenation of biomass-derived levulinic acid using non-noble metal catalysts: A critical review. *Chem. Eng. J.* **2019**, *372*, 992-1006.

Eggersdorfer, M. (**2012**). Terpenes. In *Ullmann's Encyclopedia of Industrial Chemistry*. Weinheim, Germany: Wiley-VCH. Volume 36, 29-45.

Erasto, P.; Viljoen, A.M. Limonene- A Review: Biosynthetic, Ecological and Pharmacological Relevance. *Nat. Prod. Commun.* **2008**, *3*, 1193-1202.

Epstein, E. (**2017**). *The Science of Composting*. CRC Press LLC.

Espachs-Barroso, A.; Soliva-Fortuny, R.C.; Martín-Belloso, O. A Natural clouding agent from orange peels obtained using polygalacturonase and cellulase, *Food Chem*. **2005**, *92*, 55-61.

Espitia, P.J.P.; Du, W.X.; Avena-Bustillos, R.de J.; Soares, N. de F.F.; McHugh, T.H. Edible films from pectin: Physical-mechanical and antimicrobial properties–A review. *Food Hydrocoll*. **2014**, *35*, 287-296.

Espro, C.; Gumina, B.; Szumelda, T; Paone, E; Mauriello, F. Catalytic transfer hydrogenolysis as an effective tool for the reductive upgrading of cellulose, hemicellulose, lignin, and their derived molecules. *Catalysts* **2018**, *8*, 313.

Fakayode, O.A.; Abobi, K.E. Optimization of oil and pectin extraction from orange (Citrus sinensis) peels: a response surface approach. *J. Anal. Sci. Technol.* **2018**, *9*, 20.

Fang, J.; Zhan, L.; Ok, Y.S.; Gao, B. Minireview of potential applications of hydrochar derived from hydrothermal carbonization of biomass. *J. Ind. Eng. Chem.* **2018**, *57*, 15-21.

FAO, **2014**. FaoStat Database. Available from: http://www.fao.org/faostat.

FAO, **2017**. FaoStat Database. Available from: http://www.fao.org/faostat.

FAO, **2018**. FaoStat Database. Available from: http://www.fao.org/faostat.

FAO, **2020**. FaoStat Database. Available from: http://www.fao.org/faostat.

Fasolini, A.; Cucciniello, R.; Paone, E.; Mauriello, F.; Tabanelli, T. Short Overview on the Hydrogen Production Via Aqueous Phase Reforming (APR) of Cellulose, C6-C5 Sugars and Polyols. *Catalysts* **2019**, *9*, 917.

Ferhat, M.A.; Boukhatem, M.N.; Hazzit, M.; Meklati, B.Y.; Farid, C. Cold Pressing, Hydrodistillation and Microwave Dry Distillation of Citrus Essential Oil from Algeria: A Comparative Study. *Electron. J. Biol.* **2016**, *S1*, 30-41.

Ferhat, M.A.; Meklati, B.Y.; Chemat, F. Comparison of different isolation methods of essential oil from Citrus fruits: cold pressing, hydrodistillation and microwave 'dry' distillation. *Flavour Fragrance J.* **2007**, *22*, 494-504.

Ferguson, U. (**1990**). *Citrus fruits processing*. Horticultural Sciences Department, Florida, 117-118.

Fiege, H. (**2012**). Cresols and xylenols. In *Ullmann's Encyclopedia of Industrial Chemistry*. Weinheim, Germany: Wiley-VCH. Volume 10, 419-460.

Fishman, M.L.; Cooke, P.H. The structure of high-methoxyl sugar acid gels of citrus pectin as determined by AFM. *Carbohydr. Res.* **2009**, *344*, 1792-1797.

Forgács, G. (**2012)**. Biogas production from citrus wastes and chicken feather: pre-treatment and co-digestion. Goteborg, Sweden: Department of Chemical and Biological Engineering, Chalmers University of Technology.

Freitasa, F.A.; Licursi, D.; Lachter, E.R.; Raspolli Galletti, A.M.; Antonetti, C.; Brito, T.C.; Nascimento, R.S.V. Heterogeneous catalysis for the ketalisation of ethyl levulinate with 1,2-dodecanediol: Opening the way to a new class of biodegradable surfactants. *Catalysis Communications* **2016**, *73*, 84-87.

Frigo, S.; Gabbrielli, R.; Seggiani, M.; Vitolo, S.; Puccini, M. Small-scale wood-fuelled CHP plants: A comparative evaluation of the available technologies. *Chemical Engineering Transactions* **2014**, 37.

Funke, A.; Ziegler, F. Hydrothermal carbonization of biomass: a summary and discussion of chemical mechanisms for process engineering. *Biofuels, Bioprod. Biorefining* **2010**, *4*, 160-177.

Gallo, J.M.R.; Alonso, D.M.; Mellmer, M.A.; Dumesic, J.A. Production and upgrading of 5-hydroxymethylfurfural using heterogeneous catalysts and biomass-derived solvents. *Green Chem.* **2013**, *15*, 85-90.

Garves, K. Synthesis of Alkoxymethylfurfurals and Alkyl Levulinates from Cellulose or Lignocelluloses or Starch and Alcohols. Patent DE3621517 **1988**.

Gavahian, M.; Chu, Y.H.; Khaneghah, A.M. Recent advances in orange oil extraction: an opportunity for the valorisation of orange peel waste a review. *International Journal of Food Science and Technology* **2019**, *54*, 925-932.

Ghiaci, M.; Abbaspur, A.; Arshadi, M.; Aghabarari, B. Internal versus external surface active sites in ZSM-5 zeolite: Part 2: Toluene alkylation with methanol and 2-propanol catalyzed by modified and unmodified H_3PO_4/ZSM-5. *Appl. Catal. A: Gen.* **2007**, *316(1)*, 32-46.

Golueke, C.G. Bacteriology of composting. *Biocycle* **2017**, *33*, 55-57.

Gonçalves, D.; Ferreira, P.; Baldwin, E.; Cesar, T. (**2017**). Health benefits of orange juice and citrus flavonoids. In: *Phytochemicals in Citrus: Applications in Functional Foods*. Boca Raton, FL: CRC Press, 299-324.

González-Rivera, J.; Spepi, A.; Ferrari, C.; Duce, C.; Longo, I.; Falconieri, D.; Piras, A.; Tinè, M.R. Novel configurations for a citrus waste based biorefinery: from solventless to simultaneous ultrasound and microwave assisted extraction. *Green Chemistry* **2016**, *18*, 6399-6696.

Grohmann, K.; Baldwin, E.A. Hydrolysis of orange peel with pectinase and cellulase enzymes. *Biotechnol. Lett.* **1992**, *14*, 1169-1174.

Grohmann, K.; Baldwin, E.; Buslig, B.; Ingram, L.N. Fermentation of galacturonic acid and other sugars in orange peel hydrolysates by the ethanologenic strain of Escherichia coli. *Biotechnology Lett.* **1994**, *16(3)*, 281-286.

Guimarães, R., Barros, L., Barreira, J.C.M., Sousa, M.J., Carvalho, A.M. & Ferreira, I.C.F.R. Targeting excessive free radicals with peels and juices of citrus fruits: grapefruit, lemon, lime and orange. *Food and Chemical Toxicology* **2010**, *48*, 99-106.

Gumina, B.; Mauriello, F.; Pietropaolo, R.; Galvagno, S.; Espro, C. Hydrogenolysis of sorbitol into valuable C3-C2 alcohols at low H_2 pressure promoted by the heterogeneous Pd/Fe_3O_4 catalyst. *Mol. Catal.* **2018**, *446*, 152-160.

Gunaseelan, V.N. Biochemical methane potential of fruits and vegetable solid waste feedstocks. *Biomass Bioenergy* **2004**, *26*, 389-399.

Han, Y.; Gholizadeh, M.; Tran, C.C.; Kaliaguine, S.; Li, C.Z.; Olarte, M.; Garcia-Perez, M. Hydrotreatment of pyrolysis bio-oil: A review. *Fuel Process Technol.* **2019**, *195*, 106140.

Hoekman, S.K.; Broch, A.; Robbins, C.; Zielinska, B.; Felix, L. Hydrothermal carbonization (HTC) of selected woody and herbaceous biomass feedstocks. *Biomass Convers. Biorefinery* **2013**, *3*, 113-126.

Ho, S.; Lin, C. Investigation of heat treating conditions for enhancing the anti-inflammatory activity of citrus fruit (Citrus reticulata) peels. *Journal of Agricultural and Food Chemistry* **2008**, *56(17)*, 7976-7982.

Hu, C.; Zawistowski, J.; Ling, W.; Kitts, D.D. Black rice (Oryza sativa L. indica) pigmented fraction suppresses both reactive oxygen species and nitricoxide in chemical and biological model systems. *Journal of Agricultural and Food Chemistry* **2003**, *51(18)*, 5271-5277.

Hu, X.; Gholizadeh, M. Progress of the applications of bio-oil. *Renew. Sustain. Energy Rev.* **2020**, *134*, 110124.

Hu, X.; Jiang, S.; Wu, L.; Wang, S.; Li, C.Z. One-pot conversion of the biomass-derived xylose and furfural into levulinate esters via acid catalysis. *Chem. Commun.* **2017**, *53*, 2938-2941.

Hu, X.; Song, Y.; Wu, L.; Gholizadeh, M.; Li, C.-Z. One-pot synthesis of levulinic acid/ester from C5 carbohydrates in a methanol medium. *ACS Sustainable Chem. Eng.* **2013**, *1*, 1593-1599.

John, I.; Muthukumar, K.; Arunagiri, A.; John, I. A review on the potential of citrus waste for D- Limonene, pectin, and bioethanol production. *Int. J. Green Energy* **2017**, *14*, 599-612.

Jokić, S.; Molnar, M.; Cikoš, A.M.; Jakovljević, M.; Šafranko, S.; Jerković, I. Separation of selected bioactive compounds from orange peel using the sequence of supercritical CO_2 extraction and ultrasound solvent extraction: optimization of limonene and hesperidin content. *Separ. Sci. Tech.* **2020**, *55(15)*, 2799-2811.

Joshi, V.; Attri, D. Solid state fermentation of apple pomace for the production of value added products. *Pollution in Urban Industrial Environment* **2005**, 180.

Kale, P.N.; Adsule, P.G. (**1995)**. Citrus. In *Handbook of Fruit Science and Technology: Production, Composition, Storage, and Processing*. Marcel Dekker, Inc., New York: CRC Press, 39-65.

Kamitsou, M.; Panagiotou, G.D.; Triantafyllidis, K.S.; Bourikas, K.; Lycourghiotis, A.; Kordulis, C. Transformation of α-limonene into p-cymene over oxide catalysts: A green chemistry approach. *Appl. Catal. A Gen.* **2014**, *474*, 224-229.

Karaman, S.; Karasu, S.; Tornuk, F.; Toker, O.S.; Geçgel, Ü.; Sagdic, O.; Ozcan, N.; Gül, O. Recovery potential of cold press byproducts obtained from the edible oil industry: physicochemical, bioactive, and antimicrobial properties. *J. Agric. Food Chem.* **2015**, *63*, 2305-2313.

Khan, M.; Bibi, N.; Zeb, A. Optimization of process conditions for pectin extraction from citrus peel. *Sci. Tech. Dev.* **2015**, *34(1)*, 9-15.

Khandare, R.D.; Tomke, P.D.; Rathod, V.K. Kinetic modeling and process intensification of ultrasound-assisted extraction of d-limonene using citrus industry waste. *Chem. Eng. Process.* **2021**, *159*, 108181.

Khaw, K.Y.; Parat, M.O.; Shaw, P.N.; Falconer, J.R. Solvent Supercritical Fluid Technologies to Extract Bioactive Compounds from Natural Sources: A Review. *Molecules* **2017**, *22*, 1186.

Kimball, D.A., **1999**. *Citrus Processing: a Complete Guide* (2nd ed.). US: Springer.

Kircher, M. Bioeconomy: Markets, Implications, and Investment Opportunities. *Economies* **2019**, *7(3)*, 73.

Kitts, D.D.; Hu, C. Biological and chemical assessment of antioxidant activity of sugar-lysine model Maillard reaction products. *Annals of the New York Academy of Sciences* **2005**, *1043(1)*, 501-512.

Klemm, D. (**1998**). *Comprehensive cellulose chemistry. Volume 1: Fundamentals and analytical methods*. Wiley-VCH Verlag GmbH.

Koppar, A.; Pullammanappallil, P. Anaerobic digestion of peel waste and wastewater for on site energy generation in a citrus processing facility. *Energy* **2013**, *60*, 62-68.

Koutinas, M.; Patsalou, M.; Stavrinou, S.; Vyrides, I. High temperature alcoholic fermentation of orange peel by the newly isolated thermotolerant Pichia kudriavzevii KVMP10. *Lett. Appl. Microbiol.* **2016**, *62*, 75-83.

Kumar, S.P.J.; Prasad, S.R.; Banerjee, R.; Agarwal, D.K.; Kulkarni K.S.; Ramesh, K.V. Green solvents and technologies for oil extraction from oilseeds. *Chemistry Central Journal* **2017**, *11*, 9.

Kumari, P.K.; Rao, B.S.; Padmakar, D.; Pasha, N.; Lingaiah, N. Lewis acidity induced heteropoly tungustate catalysts for the synthesis of 5-ethoxymethyl furfural from fructose and 5-hydroxymethylfurfural. *Mol. Catal.* **2018**, *448*, 108-115.

Kuwahara, Y.; Kaburagi, W.; Fujitani, T. Catalytic conversion of levulinic acid and its esters to γ-valerolactone over silica-supported zirconia catalysts. Bull. *Chem. Soc. Jpn*. **2014**, *87*, 1252-1254.

Kuwahara, Y.; Kango, H.; Yamashita, H. Catalytic Transfer Hydrogenation of Biomass-Derived Levulinic Acid and Its Esters to γ-Valerolactone over Sulfonic Acid-Functionalized UiO-66. *ACS Sustainable Chem. Eng.* **2017**, *5*, 1141-1152.

Lange, J.-P.; Price, R.; Ayoub, P.M.; Louis, J.; Petrus, L.; Clarke, L.; Gosselink, H. Valeric biofuels: A platform of cellulosic transportation fuels. *Angew. Chem. Int. Ed.* **2010**, *49*, 4479-4483.

Lee, C.S.; Binner, E.; Winkworth-Smith, C.; John, R.; Gomes, R.; Robinson, J. Enhancing natural product extraction and mass transfer using selective microwave heating. *Chem. Eng. Sci.* **2016**, *149*, 97-103.

Lefebvre, T.; Destandau, E.; Lesellier, E. Selective extraction of bioactive compounds from plants using recent extraction techniques: A review. *Journal of Chromatography A* **2021**, *1635*, 461770.

Li, X; Jia, P.; Wang, T. Furfural: a promising platform compound for sustainable production of C4 and C5 chemicals. *ACS Catal.* **2016**, *6*, 7621-7640.

Liu, S.X.; Mamidipally, P.K. Quality comparison of rice bran oil extracted with d-limonene and hexane. *Cereal Chem.* **2005**, *82*, 209-215.

Liu, Y.; Shi, J.; Langrish, T.A.G. Water-based extraction of pectin from flavedo and albedo of orange peels. *Chemical Engineering Journal* **2006**, *120(3)*, 203-209.

Liu, Z.; Guo, Y.; Balasubramanian, R.; Hoekman, S.K. Mechanical stability and combustion characteristics of hydrochar/lignite blend pellets. *Fuel* **2016**, *164*, 59-65.

López, J.Á.S; Li, Q.; Thompson, I.P. Biorefinery of waste orange peel. *Critical Reviews in Biotechnology* **2010**, *30(1)*, 63-69.

Lopresto, C.G.; Meluso, A.; Di Sanzo, G.; Chakraborty, S.; Calabrò, V. Process-intensified waste valorization and environmentally friendly d-limonene extraction. *EuroMediterr. J. Environ. Integr.* **2019**, *4*, 31.

Lopresto, C.G.; Petrillo, F.; Casazza, A.A.; Aliakbarian, B.; Perego, P.; Calabrò, V. A non-conventional method to extract D-limonene from waste lemon peels and comparison with traditional Soxhlet extraction. *Sep. Purif. Methods* **2014**, 13-20.

Lohrasbi, M.; Pourbafrani, M.; Niklasson, C.; Taherzadeh, M.J. Process design and economic analysis of a citrus waste biorefinery with biofuels and limonene as products. *Bioresour. Technol.* **2010**, *101*, 7382-7388.

Lycourghiotis, S.; Makarouni, D.; Kordouli, E.; Bourikas, K.; Kordulis, C.; Dourtoglou, V. Activation of natural mordenite by various acids: Characterization and evaluation in the transformation of limonene into p-cymene. *Mol. Catal.* **2018**, *450*, 95-103.

Lynd, L.R.; Van Zyl, W.H.; McBride, J.E.; Laser M. 2005. Consolidated bioprocessing of cellulosic biomass: an update. *Curr. Opin. Biotechnol.* **2005**, *16*, 577-583.

Mahato, N.; Sharma, K.; Koteswararao, R.; Sinha, M.; Baral, E.; Cho, M.H. Citrus essential oils: Extraction, authentication and application in food preservation. *Cri. Rev. Food Sci. Nutr.* **2017**, *59(4)*, 611-625.

Mahato, N.; Sinha, M.; Sharma, K.; Rakoti Koteswararao, R.; Cho, M.H. Modern Extraction and Purification Techniques for Obtaining High Purity Food-Grade Bioactive Compounds and Value-Added Co-Products from Citrus Wastes. *Foods* **2019**, *8*, 523.

Makarouni, D.; Lycourghiotis, S.; Kordouli, E.; Bourikas, K.; Kordulis, C.; Dourtoglou, V. Transformation of limonene into p-cymene over acid activated natural mordenite utilizing atmospheric oxygen as a green oxidant: A novel mechanism. *Appl. Catal. B Environ.* **2018**, *224*, 740-750.

Malara, A.; Paone, E.; Bonaccorsi, L.; Mauriello, F.; Macario, A.; Frontera, P. Pd/Fe_3O_4 Nanofibers for the catalytic conversion of lignin-derived benzyl phenyl ether under transfer hydrogenolysis conditions. *Catalysts* **2020**, *10*, 20.

Mamma, D.; Christakopoulos, P. Biotransformation of Citrus By-Products into Value Added Products. *Waste and Biomass Valorization* **2014**, *5(4)*, 529-549.

Maneffa, A.; Priecel, P.; Lopez-Sanchez, J.A. Biomass-derived renewable aromatics: selective routes and outlook for p-xylene commercialization. *ChemSusChem* **2016**, *9*, 1-14.

Marchese, A.; Arciola, C.R.; Barbieri, R.; Silva, A.S.; Nabavi, S.F.; Tsetegho Sokeng, A.J.; Izadi, M.; Jafari, N.J.; Suntar, I.; Daglia, M.; et al. Update on Monoterpenes as Antimicrobial Agents: A Particular Focus on p-Cymene. *Materials* **2017**, *10*, 947.

360 Market Updates (**2020**). *Global Limonene Market Size, Manufacturers, Supply Chain, Sales Channel and Clients, 2020-2026*; 360 Market Updates: Maharashtra, India.

Martín, M.A.; Fernández, R.; Serrano, A.; Siles, J.A. Semi-continuous anaerobic co-digestion of orange peel waste and residual glycerol derived from biodiesel manufacturing. *Waste Manag.* **2013**, *33*, 1633-1639.

Martin-Luengo, M.A.; Yates, M.; Martinez Domingo, M.J.; Casal, B.; Iglesias, M.; Esteban, M.; Ruiz-Hitzky, E. Synthesis of p-cymene from limonene, a renewable feedstock. *Appl. Catal. B* **2008**, *81*, 218-224.

Martin-Luengo, M.A.; Yates, M.; Rojoa, S.E.; Arribas, D.H.; Aguilar, D.; Hitzkya, R.E. Sustainable p-cymene and hydrogen from limonene. *Appl. Catal. A* **2010**, *387*, 141-146.

Marín, F.R.; Frutos, M.J.; Pérez-Alvarez, J.A.; Martinez-Sánchez, F.; Del Río, J.A. Flavonoids as nutraceuticals: Structural related antioxidant properties and their role on ascorbic acid preservation. *Stud. Nat. Prod. Chem.* **2002**, *26*, 741-778.

Martín, M.A.; Siles, J.A.; Chica, A.F.; Martín, A. Biomethanization of orange peel waste. *Bioresour. Technol.* **2010**, *101*, 8993-8999.

Mauriello, F.; Paone, E.; Pietropaolo, R.; Balu, A.M.; Luque, R. Catalytic transfer hydrogenolysis of lignin-derived aromatic ethers promoted by bimetallic Pd/Ni systems. *ACS Sustain. Chem. Eng.* **2018**, *6*, 9269-9276.

May, C.D. Industrial pectins: sources, production and applications. *Carbohyd. Polym.* **1990**, *12*, 79-99.

M'hiri, N.; Ioannou, I.; Ghoul, M.; Boudhrioua, N.M. Extraction methods of citrus peel phenolic compounds. *Food Reviews International* **2014**, *30(4)*, 265-290.

Mira, B.; Blasco, M.; Berna, A.; Subirats, S. Supercritical CO_2 extraction of essential oil from orange peel. Effect of operation conditions on the extract composition. *J. Supercrit. Fluids* **1999**, *14*, 95-104.

Mirkouei, A.; Haapala, K.R.; Sessions, J.; Murthy, G.S. A review and future directions in techno-economic modeling and optimization of upstream forest biomass to bio-oil supply chains. *Renew. Sustain. Energy Rev.* **2017**, *67*, 15-35.

Mittal, A.; Pilath, H.M.; Johnson, D.K. Direct Conversion of Biomass Carbohydrates to Platform Chemicals: 5-Hydroxymethylfurfural (HMF) and Furfural. *Energy Fuels* **2020**, *34*, 3284-3293.

Mkhabela, M.; Warman, P. The influence of municipal solid waste compost on yield, soil phosphorus availability and uptake by two vegetable crops grown in a Pugwash sandy loam soil in Nova Scotia. *Agriculture Ecosystems & Environment* **2005**, *106(1)*, 57-67.

Mota, T.R.; de Oliveira, D.M.; Marchiosi, R.; Ferrarese-Filho, O.; dos Santos, W.D. Plant cell wall composition and enzymatic deconstruction. *AIMS Bioengineering* **2018**, *5(1)*, 63-77.

Nadar, S.S.; Rao, P.; Rathod, V.K. Enzyme assisted extraction of biomolecules as an approach to novel extraction technology: A review. *Food Res. Int.* **2018**, *108*, 309-330.

Negro, V.; Mancini, G.; Ruggeri, B.; Fino, D. Citrus waste as feedstock for bio-based products recovery: Review on limonene case study and energy valorization. *Bioresour Technol* **2016**, *214*, 806-815.

Nguyen, H. (**2012**). Biogas Production from Solvent Pretreated Orange Peel. M.S. thesis, Department of Chemical and Biological Engineering, Chalmers University of Technology, Goteborg, Sweden.

Nevens, F.; Reheul, D. The application of vegetable, fruit and garden waste (VFG) compost in addition to cattle slurry in a silage maize monoculture: nitrogen availability and use. *European Journal of Agronomy* **2003**, *19(2)*, 189-203.

Nkoa, R. Agricultural benefits and environmental risks of soil fertilization with anaerobic digestates: a review. *Agronomy for Sustainable Development* **2014**, *34(2)*, 473-492.

Ozturk, B.; Winterburn, J.; Gonzalez-Miquel, M. Orange peel waste valorisation through limonene extraction using bio-based solvents. *Biochem. Eng. J.* **2019**, *151*, 107298.

Pagliaro, M.; Pizzone, D.M.; Scurria, A.; Lino, C.; Paone, E.; Mauriello, F.; Ciriminna, R. Sustainably Sourced Olive Polyphenols and Omega-3 Marine Lipids: A Synergy Fostering Public Health. *ACS Food Sci. Technol* **2021**, *1*, *2*, 139-145.

Paini, M.; Casazza, A.A.; Aliakbarian, B.; Perego, P.; Binello, A.; Cravotto, G. Influence of ethanol/water ratio in ultrasound and high-pressure/high-temperature phenolic compound extraction from agri-food waste. *Int. J. Food Sci. Technol.* **2016**, *51*, 349-358.

Pan, M.H.; Lai, C.S.; Ho, C.T. Anti-inflammatory activity of natural dietary flavonoids. *Food Function* **2010**, *1*, 15-31.

Paone, E.; Beneduci, A.; Corrente, G.A.; Malara, A.; Mauriello, F. Hydrogenolysis of aromatic ethers under lignin-first conditions. *Mol. Catal.* **2020**, *497*, 111228.

Paone, E.; Espro, C.; Pietropaolo, R.; Mauriello, F. Selective arene production from transfer hydrogenolysis of benzyl phenyl ether promoted by a co-precipitated Pd/Fe_3O_4 catalyst. *Catal. Sci. Technol.* **2016**, *6*, 7937-7941.

Paone, E.; Tabanelli, T.; Mauriello, F. The rise of lignin biorefinery. *Curr. Opin. Green Sustain. Chem.* **2020**, *24*, 1-6.

Parrino, F.; Fidalgo, A.; Palmisano, L.; Ilharco, L.M.; Pagliaro, M.; Ciriminna, R. Polymers of Limonene Oxide and Carbon Dioxide: Polycarbonates of the Solar Economy. *ACS Omega* **2018**, *3*, 4884-4890.

Patel, M.; Zhang, X.; Kumar, A. Techno-economic and life cycle assessment on lignocellulosic biomass thermochemical conversion technologies: A review. *Renewable and Sustainable Energy Reviews* **2016**, *53*, 1486-1499.

Pauly, M.; Keegstra, K. Cell-wall carbohydrates and their modification as a resource for biofuels *Plant J.* **2008**, *54*, 559-568.

Peterson, A.A.; Vogel, F.; Lachance, R.P.; Fröling, M.; Antal Michael J, J., Tester, J.W. Thermochemical biofuel production in hydrothermal media: a review of sub- and supercritical water technologies. *Energy Environ. Sci.* **2008**, *1*, 32-65.

Peterson, J.; Dwyer, J. Flavonoids: Dietary occurrence and biochemical activity. *Nutr. Res.* **1998**, *18*, 1995-2018.

Pingret, D.; Fabiano-Tixier, A.S.; Chemat, F. An improved ultrasound Clevenger for extraction of essential oils. *Food Anal. Methods* **2014**, *7*, 9-12.

Plöchl, M.; Heiermann, M. Biogas farming in central and northern Europe: a strategy for developing countries? Invited Overview. *Agric. Eng.* **2006**, *Int VIII*, 1-15.

Popp, J; Kovács, S.; Oláh, I.; Divéki, Z.; Balázs, E. Bioeconomy: Biomass and biomass-based energy supply and demand. *New Biotechnology* **2020**, *60*, 76-84.

Proteggente, A.R.; Saija, A.; De Pasquale, A.; Rice-Evans, C.A. The compositional characterisation and antioxidant activity of fresh juices from sicilian sweet orange (Citrus sinensis L. Osbeck) varieties. *Free Radic. Res.* **2003**, *37*, 681-687.

Ptichkina, N.M.; Markina, O.A.; Rumyantseva, G.N. Pectin extraction from pumpkin with the aid of microbial enzymes. *Food Hydrocoll.* **2008**, *22*, 192-195.

Putnik, P.; Kovacevic, D.B.; Jambrak, A.R.; Barba, F.J.; Cravotto, G.; Binello, A.; Lorenzo, J.M.; Shpigelman, A. Innovative "green" and novel strategies for the extraction of bioactive added value compounds from citrus wastes-a review. *Molecules* **2017**, *22*, 1-24.

Rachwalik, R.; Hunger, M.; Sulikowski, B. Transformations of monoterpene hydrocarbons on ferrierite type zeolites. *Appl. Catal. A* **2012**, *427-428*, 98-105.

Ramage, J.; Scurlock, J. (**1996**). Biomass. Energia rinnovabile per un futuro sostenibile. Oxford: Oxford University Press.

Rapisarda, P.; Tomaino, A.; Lo Cascio, R.; Bonina, F.; De Pasquale, A.; Saija, A. Antioxidant effectiveness as influenced by phenolic content of fresh orange juices. *J. Agric. Food Chem.* **1999**, *47*, 4718-4723.

Raspolli Galletti, A.M.; Antonetti, C.; Fulignati, S.; Licursi, D. Direct Alcoholysis of Carbohydrate Precursors and Real Cellulosic Biomasses to Alkyl Levulinates: A Critical Review**.** *Catalysts* **2020**, *10(10)*, 1221.

Rassem, H.H.A; Nour, A.H.; Yunus, R.M. Techniques For Extraction of Essential Oils From Plants: A Review. *Aust. J. Basic & Appl. Sci.* **2016**, *10(16)*, 117-127.

REN21, *Renewables 2018, global status report*, in *Renewable energy policy network for the 21st century* **2019**, 1-324.

Ren, Y.; Liu, S.; Jin, G.; Yang, X.; Zhou, Y.J. Microbial production of limonene and its derivatives: Achievements and perspectives. *Biotechnol. Adv.* **2020**, *44*, 107628.

Retajczyk, M.; Wróblewska, A.A. Isomerization and Dehydroaromatization of R-(+)-Limonene Over the Ti-MCM-41 Catalyst: Effect of Temperature, Reaction Time and Catalyst Content on Product Yield. *Catalysts* **2019**, *9*, 508.

Rezzadori, K.; Benedetti, S.; Amante, E. R. Proposals for the residues recovery: Orange waste as raw material for new products. *Food and Bioproducts Processing* **2012**, *90(4),* 606-614.

Reverchon, E. Supercritical desorption of limonene and linalool from silica gel: experiments and modelling. *Chem. Eng. Sci.* **1997**, *52*, 1019-1027.

Rivas, B.; Torrado, A.; Torre, P.; Converti, A.; Domínguez, J.M. Submerged citric acid fermentation on orange peel autohydrolysate. *J. Agric. Food Chem.* **2008**, *56*, 2380-2387.

Roberge, D.M.; Buhl, D.; Niederer, J.P.M.; Hölderich, W.F. Catalytic aspects in the transformation of pinenes to p-cymene. *Appl. Catal. A Gen.* **2001**, *215*, 111-124.

Robinson, A.M.; Hensley, J.E.; Medlin, J.W. Bifunctional catalysts for upgrading of biomass-derived oxygenates: a review. *ACS Catal.* **2016**, *6*, 5026-5043.

Rouse, A.H.; Crandall, P.C. Nitric acid extraction of pectin from citrus peel. *Proc. Fla. State Hort. Soc* .**1976**, *89*, 166-76.

Rubulotta, G.; Luska, K.L.; Urbina-Blanco, C.A.; Eifert, T.; Palkovits, R.; Quadrelli, E.A.; Thieuleux, C.; Leitner, W. Highly Selective Hydrogenation of R-(+)-Limonene to (+)-p-1-Menthene in Batch and Continuous Flow Reactors. *ACS Sustain. Chem. Eng.* **2017**, *5(5)*, 3762-3767.

Ruiz, B.; de Benito, A.; Rivera, J.D.; Flotats, X. Assessment of different pre-treatment methods for the removal of limonene in citrus waste and their effect on methane potential and methane production rate. *Waste Manag. Res.* **2016**, *34(12)*, 1249-1257.

Ruiz, B; Flotats, X.; Citrus essential oils and their influence on the anaerobic digestion process: an overview. *Waste Manag.* **2014**, *34*, 2063-2079.

Ruiz, B.; Flotats, X. Effect of limonene on batch anaerobic digestion of citrus peel waste. *Biochemical Engineering Journal* **2016**, *109*, 9-18.

Ruppert, A.M.; Weinberg, K.; Palkovits, R. Hydrogenolysis goes bio: From carbohydrates and sugar alcohols to platform chemicals. *Angew. Chem. Int. Ed.* **2012**, *51*, 2564-2601.

Salunkhe, D.K.; Kadam, S.S. (**1995**). *Handbook of fruit science and technology Production, composition, storage and processing*. Boca Raton, FL: CRC Press.

Sánchez-Segado, S.; Lozano, L.J.; de los Ríos, A.P.; Hernández-Fernández, F.J.; Godínez, C.; Juan, D. Process design and economic analysis of a hypothetical bioethanol production plant using carob pod as feedstock. *Bioresour. Technol.* **2012,** *104*, 324-328.

Santiago, B.; Moreira, M.T.; Feijoo, G.; González-García, S. Identification of environmental aspects of citrus waste valorization into D-limonene from a biorefinery approach. *Biomass Bioenergy* **2020**, *143*, 105844.

Satari, B.; Karimi, K. Citrus processing wastes: Environmental impacts, recent advances, and future perspectives in total valorization. *Resour. Conserv. Recycl.* **2018**, *129*, 153-167.

Scheller, H.V.; Ulvskov, P. Hemicelluloses. *Annu. Rev. Plant Biol.* **2010**, *61*, 263-289.

Seggiani, M.; Prati, M.V.; Costagliola, M.A.; Puccini, M.; Vitolo, S. Bioethanol-gasoline fuel blends: Exhaust emissions and morphological characterization of particulate from a moped engine. *Journal of the Air and Waste Management Association* **2012**, *62(8)*, 888-897.

Sergeev, A.G.; Hartwig, J.F. Selective, nickel-catalyzed hydrogenolysis of aryl ethers. *Science* **2011**, *332*, 439-443.

Sharma, K.; Mahato, N.; Cho, M.H. Converting citrus wastes into value-added products: Economic and environmentally friendly approaches. *Nutrition* **2017**, *34*, 29-46.

Sharma, K.; Mahato, N.; Lee, Y.R. Extraction, characterization and biological activity of citrus flavonoids. *Rev. Chem. Eng.* **2019**, *35(2)*, 265-284.

Sheldon, R.A. Catalysis: The key to waste minimization. *J. Chem. Tech. Biotechnol.* **1997**, *68*, 381-388.

Sheldon, R.A. Green chemistry and resource efficiency: towards a green economy. *Green Chem.* **2016**, *18*, 3180-3183.

Shivhare, A.; Kumar, A.; Srivastava, R. An Account of the Catalytic Transfer Hydrogenation and Hydrogenolysis of Carbohydrate-Derived Renewable Platform Chemicals over Non-Precious Heterogeneous Metal Catalysts. *ChemCatChem* **2020**, *13(1*).

Shokouhimehr, M. Magnetically separable and sustainable nanostructured catalysts for heterogeneous reduction of nitroaromatics. *Catalysts* **2015**, *5*, 534-560.

Shrikhandea, S.; Bhaskar Babub, G.U.; Ahmad, Z.; Patl, D.S. Intensification and analysis of ethyl levulinate production process having a reactive distillation through vapor recompression and bottom flash techniques. *Chemical Engineering and Processing - Process Intensification* **2020**, *156*, 108081.

Siles, J.; Vargas, F.; Gutiérrez, M.; Chica, A.; Martín, M. Integral valorisation of waste orange peel using combustion, biomethanisation and co-composting technologies. *Bioresource Technology* **2016**, *211*, 173-182.

Silva, J.F.L.; Grekin, R.; Mariano, A.P.; Filho, R.M. Making Levulinic Acid and Ethyl Levulinate Economically Viable: A Worldwide Technoeconomic and Environmental Assessment of Possible Routes. *Energy Technology* **2018**, *6*, 613-639.

Somerville, C.; Youngs, H.; Taylor, C.; Davis, S.C.; Long, S.P. Feedstocks for lignocellulosic biofuels. *Science* **2010**, *329*, 790-792.

Sood, N.; de Vries, H.; Gutierrez, I.; Lakdawalla, D.N.; Goldman, D.P. The effect of regulation on pharmaceutical revenues: experience in nineteen countries. *Health Aff.* **2009**, *28*, 125-137.

Strezov, V.; Patterson, M.; Zymla, V.; Fisher, K.; Evans, T.J.; Nelson, P.F. Fundamental aspects of biomass carbonization. *J. Anal. Appl. Pyrolysis* **2007**, *79*, 91-100.

Sustainable Development Goals, United Nations, **2019**. Available from: https://sustainabledevelopment.un.org/sdgs.

Swift, K.A.D. Catalytic transformations of the major terpene feedstocks. *Topics Catal.* **2004**, *27*, 1-4.

Taarning, E.; Osmundsen, C.M.; Yang, X.; Voss, B.; Andersen, S.I.; Christensen, C.H. Zeolite-catalyzed biomass conversion to fuels and chemicals. *Energy Environ. Sci.* **2011**, *4*, 793-804.

Tabanelli, T.; Paone, E.; Blair Vásquez, P.; Pietropaolo, R.; Cavani, F.; Mauriello, F. Transfer Hydrogenation of Methyl and Ethyl Levulinate Promoted by a ZrO_2 Catalyst: Comparison of Batch vs Continuous Gas-Flow Conditions. *ACS Sustain. Chem. Eng.* **2019**, *7*, 9937-9947.

Tavera Ruiz, C.P.; Gauthier-Maradei, P.; Capron, M.; Pirez, C.; Gardoll, O.; Katryniok, B.; Dumeignil, F. Transformation of DL Limonene into Aromatic Compounds Using Supported Heteropolyacid Catalysts. *Catal. Lett.* **2019**, *149*, 328-337.

Teigiserova, D.A.; Ligia Tiruta-Barna, L.; Ahmadi, A.; Hamelin, L.; Thomsen, M. A step closer to circular bioeconomy for citrus peel waste: A review of yields and technologies for sustainable management of essential oils. *J. Environ. Manage.* **2021**, *280*, 111832.

Terao, J. Dietary flavonoids as plasma antioxidants on lipid peroxidation: significance of metabolic conversion. *Antioxid. Food Suppl. Hum. Heal* **1999**, 255-268.

Tiong, Y.W.; Yap, L.; Gan, S.; Yap, W.S.P. Conversion of biomass and its derivatives to levulinic acid and levulinate esters via ionic liquids. *Industrial & Engineering Chemistry Research* **2018**, *57(14)*, 4749-4766.

Tripoli, E.; Guardia, M.La.; Giammanco, S.; Majo, D.Di; Giammanco, M. Citrus flavonoids: Molecular structure, biological activity and nutritional properties: A review. *Food Chem.* **2007**, *104*, 466-479.

Tuck, C.O.; Perez, E.; Horvath, I.T.; Sheldon, R.A.; Poliakoff, M. Valorization of biomass: deriving more value from waste. *Science* **2012**, *337*, 697-699.

Tütem, E.; Başkan, K.S; Ersoy, Ş.K.; Apak, R. (**2020**). *Nutritional Composition and Antioxidant Properties of Fruits and Vegetables*, Academic Press.

Ueno, H.; Tanaka, M.; Hosino, M.; Sasaki, M.; Goto, M. Extraction of valuable compounds from the flavedo of Citrus junos using subcritical water. *Sep. Purif. Technol.* **2008**, *62*, 513-516.

Uwidia, I.E.; Owolabi, B.J.; Okafor, R.C. Extraction, Derivatization, Characterization and Antifungal Investigation of Limonene from Citrus sinensis Peels. *Tanz. J. Sci.* **2020**, *46(2)*, 419-429.

Van Heerden, I.; Cronjé, C.; Swart, S.H.; Kotzé, J.M. Microbial, chemical and physical aspects of citrus waste composting. *Bioresour. Technol.* **2002**, *81*, 71-76.

Veillet, S.; Tomato, V.; Ruiz, K.; Chemat, F. Green procedure using limonene in the Dean-Stark apparatus for moisture determination in food products. *Anal. Chim. Acta* **2010**, *674(1)*, 49-52.

Velez, D.C.P.; Magalhaes, W.L.E.; Capobianco, G. Carbon fiber from fast pyrolysis bio-oil. *Sci. Technol. Mater.* **2018**, *30*, 16-22.

Villas-Bôas, S. G.; Esposito, E.; de Mendonca, M.M. Bioconversion of apple pomace into a nutritionally enriched substrate by Candida utilis and Pleurotus ostreatus. *World Journal of Microbiology and Biotechnology* **2003**, *19(5)*, 461-467.

Xu, G.; Ye, X.; Chen, J.; Liu, D. Effect of heat treatment on the phenolic compounds and antioxidant capacity of citrus peel extract. *Journal of Agricultural and Food Chemistry*, **2007**, *55*, 330-335.

Yao, Q.; Lu, Z.; Wang, Y.; Chen, X.; Feng, G. Synergetic catalysis of non-noble bimetallic CueCo nanoparticles embedded in SiO_2 nanospheres in hydrolytic dehydrogenation of ammonia borane. *J. Phys. Chem. C* **2015**, *119*, 14167-14174.

Yan, K.; Yang, Y.; Chai, J.; Lu, Y. Catalytic reactions of gamma-valerolactone: A platform to fuels and value-added chemicals. Appl. Catal. B: Environmental **2015**, *179*, 292-304.

Yang, J.; Park, J.; Son, J.; Kim, B.; Lee, J.W. Enhanced ethyl levulinate production from citrus peels through an in-situ hydrothermal reaction. *Bioresource Technology Reports* **2018**, *2*, 84-87.

Yılmazoğlu, E.; Akgün, M. p-Cymene production from orange peel oil using some metal catalyst in supercritical alcohols. *J. Supercrit. Fluids* **2018**, *131*, 37-46.

Wadhwa, M.; Bakshi, M. Utilization of fruit and vegetable wastes as livestock feed and as substrates for generation of other value-added products. *Rap. Publication* **2013**, *4*, 30.

Wang, Y.T.; Zhao, D.Y.; Rodriguez-Padron, D.; Len, C. Recent Advances in Catalytic Hydrogenation of Furfural. *Catalysts* **2019**, *9*, 796, 1-33.

Wei, Y.; Li, J.; Shi, D.; Liu, G.; Zhao, Y.; Shimaoka, T. Environmental challenges impeding the composting of biodegradable municipal solid waste: A critical review. *Resour. Conserv. Recycl*. **2017**, *122*, 51-65.

Weldekidan, H.; Strezov, V.; Town, G. Review of solar energy for biofuel extraction. *Renew Sustain. Energy Rev.* **2018**, 88, 184-192.

Werpy, T.; Petersen, G. (**2004**). *Top Value Added Chemicals from Biomass: Volume I. Results of Screening for Potential Candidates from Sugars and Synthesis Gas*. United States: National Renewable Energy Laboratory (NREL).

Wheatley, A. Anaerobic Digestion: A Waste Treatment Technology. *Applied Science* **1990**.

Wilkins, M.R.; Suryawati, L.; Maness, N.O. Chrz, D. Ethanol production by Saccharomyces cerevisiae and Kluyveromyces marxianus in the presence of orange-peel oil. *World J. Microbiol. Biotechnol.* **2007**, *23(8)*, 1161-1168.

Wilkins, M.R.; Widmer, W.W.; Grohmann, K. Simultaneous saccharification and fermentation of citrus peel waste by Saccharomyces cerevisiae to produce ethanol. *Process Biochem.* **2007**, *42*, 1614-1619.

Wright, W.R.H.; Palkovits, R. Development of heterogeneous catalysts for the conversion of levulinic acid to γ-valerolactone. *Chemsuschem* **2012**, *5*, 1657-1667.

Xu, C.; Arancon, R.A.D.; Labidi, J.; Luque, R. Lignin depolymerisation strategies: towards valuable chemicals and fuels. *Chem. Soc. Rev.* **2014**, *43*, 7485-7500.

Xu, C.; Paone, E.; Rodrìguez-Padrón, D.; Luque, R.; Mauriello, F. Reductive catalytic routes towards sustainable production of hydrogen, fuels and chemicals from biomass derived polyols. *Renew. Sustain. Energy Rev.* **2020**, *127*, 109852.

Xu, C.; Paone, E.; Rodríguez-Padrón, D.; Luque, R.; Mauriello, F. Recent catalytic routes for the preparation and the upgrading of biomass derived furfural and 5-hydroxymethylfurfural. *Chem. Soc. Rev.* **2020**, *49*, 4273-4306.

Yan, K.; Yang, Y.; Chai, J.; Lu, Y. Catalytic reactions of gamma-valerolactone: a platform to fuels and value-added chemicals. *Appl. Catal. B: Environ.* **2015**, *179*, 292-304.

Zema, D.A.; Calabrò, P.S.; Folino, A.; Tamburino, V.; Zappia, G.; Zimbone, S.M. Valorisation of citrus processing waste: A review. *Waste Management* **2018**, *80*, 252-273.

Zema, D.A.; Fòlino, A.; Zappia, G.; Calabrò, P.S.; Tamburino, V.; Marcello, S. Anaerobic digestion of orange peel in a semi-continuous pilot plant: An environmentally sound way of citrus waste management in agro-ecosystems. *Sci. Total Environ.* **2018**, *630*, 401-408.

Zhang, B.; Heidari, M.; Regmi, B.; Salaudeen, S.; Arku, P.; Thimmannagari, M.; Dutta, A. Hydrothermal Carbonization of Fruit Wastes: A Promising Technique for Generating Hydrochar. *Energies* **2018**, *11*, 2022.

Zhang, J.; Zhao, C. A new approach for bio-jet fuel generation from palm oil and limonene in the absence of hydrogen. *Chem. Commun.* **2015**, *51*, 17249-17252.

Zhang, J.; Zhao, C. Development of a Bimetallic Pd-Ni/HZSM-5 Catalyst for the Tandem Limonene Dehydrogenation and Fatty Acid Deoxygenation to Alkanes and Arenes for Use as Biojet Fuel. *ACS Catal.* **2016**, *6*, 4512-4525.

Zhang, L.; Ye, X.; Ding, T.; Sun, X.; Xu, Y.; Liu, D. Ultrasound effects on the degradation kinetics, structure and rheological properties of apple pectin. *Ultrason. Sonochem.* **2013**, *20*, 222-231.

Zhou, C.H.; Xia, X.; Lin, C.X.; Tong, D.S.; Beltramini, J. Catalytic conversion of lignocellulosic biomass to fine chemicals and fuels. *Chem. Soc. Rev.* **2011**, *40*, 5588-5617.

Zhou, L.; Gao, D.; Yang, J.; Yang, X. Su, Y.; T. Lu, T. Conversion of recalcitrant cellulose to alkyl levulinates and levulinic acid via oxidation pretreatment combined with alcoholysis over $Al_2(SO_4)_3$. *Cellulose* **2020**, *27*, 1451-1463.

Zoghlami, A.; Paës, G. Lignocellulosic biomass: understanding recalcitrance and predicting hydrolysis. *Frontiers in Chemistry* **2019**, *7*, 874.

Chapter 2

Hydrothermal Carbonization Process for the Complete Upgrading of OPW into Value-Added Chemicals and Bio-Carbon Materials

2.1 Introduction

The hydrothermal carbonization (HTC) is a simply thermochemical conversion process, carried out in water medium under autogeneous pressure at a relative mild temperature (180-300 °C), and represents a promising treatment technique for the wet lignocellulosic biomass waste since it permits to overcome the drawbacks of conventional thermochemical processes that require the use of dry feedstocks [Burguete et al., 2016].

Hydrothermal methods are largely used in petroleum-based refineries and are getting more and more attentions from both scientific and industrial researchers since their process parameters can be easily translated into modern biorefineries aimed to the upgrading of lignocellulosic residues and wastes [Satira et al., 2021]. With respect to other (bio)refinery processes, HT protocols

present several advantages in terms of sustainability since they generally adopt mild reaction conditions (e.g. temperature and pressure) without any homogeneous or heterogeneous catalysts and in the presence of water as green reaction solvent (used as such or in combination with simple aliphatic alcohols) [Satira et al., 2021].

The carbonaceous residue obtained by the HTC of the citrus processing waste is rich in oxygenated functional groups, making it a promising material in a wide range of applications, including pollutants adsorption [Xiao et al., 2020], soil amendment [Kalderis et al., 2019], as fuel in energy application [Burguete et al., 2016] and as low-cost material for capacitor and sensing applications [Pistone and Espro, 2020; Gou et al., 2019; Bressi et al., 2021; Espro et al., 2021].

At the same time, the liquid phase obtained via the hydrothermal carbonization of the orange peel ensures the production of several platform molecules. Among the considerable range of chemical building blocks that can be obtainable from citrus wastes, furfural (FU), 5-hydroxymethylfurfural (HMF), levulinic acid and its derivatives have shown a great potential in replacing fossil derived molecules in the synthesis of valuable chemicals – including levulinate derivatives – and pharmaceuticals [Xu et al., 2020].

Thus, the optimization of the process operating parameters of the HTC, to obtain simultaneously and in a single step biocarbon materials and value-added products, could represent a valid approach aimed at minimizing the environmental and economic impact caused by the management of the agro-industrial waste.

In this chapter, the effect of process variables on the hydrothermal carbonization (HTC) of the orange peel as industrial processing waste, has been investigated for both hydrochar and furan derivative (FU and 5-HMF) in the bio-oil liquid fraction, in order to optimize the yields to solid and liquid

fractions. The exploration of the single-step hydrothermal treatment represents a promising example of the wet organic waste valorization to produce value-added products with high yields and, at the same time, to avoid potential and serious environmental issues arising from the citrus processing waste management and disposal. A particular attention was given to the peculiar chemical composition of the liquid fraction obtained from HT process that is rich in components of absolute strategic interest for the chemical and pharmaceutical industry.

2.2 Materials and methods

2.2.1 Raw materials

The orange peels (OPW), obtained from an industry located in Sicily (Italy), were grounded to a particle size smaller than 2 mm and stored in a sealed plastic bag at -20 °C (in order to decrease the rate of degradation and the loss of volatile matter) and defrosted before their use in the experimental tests. Acetic acid (CH_3COOH) ≥ 99.8 w/w% and sulfuric acid (H_2SO_4) 95.0-97.0 w/w% as well as other chemicals were purchased from Merk Life Science S.r.l.

2.2.2 HTC Experimental procedure

In a typical run, a mixture of wet OPW and deionized water at the desired biomass: water ratio was ultrasonically agitated for 15 min at room temperature (20 °C) and then transferred into a 300 ml stainless steel autoclave (series 4540 Parr Instrument Company, IL, USA) for HTC. Since the water:solid ratio has a significant effect on the reaction products, a series of experiments setting the L:S ration to 4:1, 6:1, 12:1 and 24:1 (w/w), were performed. For all the experiments, a fixed amount of water was used. Prior to reaction, residual air was removed from the sealed reactor by repeatedly

pressurizing with nitrogen and venting to atmosphere. In a typical HTC test, the reaction mixture was heated under autogenous pressure up to the reaction temperature (150-300 °C), at a heating rate of 5 °C min^{-1} continuously monitored through a thermocouple placed into the autoclave and connected to the reactor controller within the whole. The residence time, after reaching the reaction temperature, was set at 30 min, 60 min, 180 min and 300 min, at a stirring speed of 600 rpm. After the HTC reaction, the autoclave was rapidly cooled at room temperature. Then, the HTC solid and liquid products were separated by vacuum filtration, with a Buchner funnel and filter paper. Afterwards, 40 ml of the so-obtained liquid aqueous product was extracted by 40 ml of diethyl ether in a separation funnel for carrying out the GC-MS analysis. A rotary evaporator was used for removing diethyl ether at 40 °C. Each extraction was performed twice (150 ml of diethyl ether). The remaining liquid was defined as light bio-oil in this study. Anhydrous sodium sulfate was used as drying agent of the light bio-oil after the extraction. The so obtained light bio-oil samples were hereafter named as L-HC T-t, where T denotes the reaction temperature (°C) and t represents the time (min) of the HTC experiments. The product yield was calculated using the following equation:

$$\text{product yield (\%)} = \frac{\text{mass of desired product (g)}}{\text{mass of initial wet OPW (g)}} \times 100 \qquad (1)$$

The solid hydrochar was sequentially washed with warm distilled water and finally dried overnight under vacuum at 100 °C. The so obtained hydrochar samples are hereafter named as S-HC T-t, where T denotes the reaction temperature (°C) and t represents the time (min) of the HTC experiments.

The hydrochar samples, obtained in the experiments performed at different initial pH value at 180 °C and 60 min, were designated as SA-HC1, SA-HC2, AA-HC1, AA-HC2 and AA-HC3, where the number represents the pH value theoretically calculated, and the prefixes SA and AA refer respectively to

sulfuric acid and acetic acid used as acidifying agents. The mass yield of HC (MY) was calculated using the following equation:

$$\text{mass yield, wt \%} = \frac{M_{Hydrochar,g(db)}}{M_{Feedstock,g(db)}} \text{ x } 100 \qquad (2)$$

It's well known that the relationship between temperature and time, defined and quantified by Overend and Chornet using the severity coefficient (R0), based on the assumptions of first-order kinetics and Arrhenius temperature since the behavior of the aqueous pre-hydrolysis of Kraft pulping, greatly influences the physicochemical properties of the lignocellulosic substrates during subcritical and supercritical water treatments [Overend and Chornet, 1987]. Therefore, the role of time and temperature on the HTC of OP was interpreted in terms of the (R_0) parameter, expressed as:

$$\log_{10} R_0 = \log_{10}[t \times \exp(\frac{T-T_0}{14,75})] \qquad (3)$$

where t is the time (min), T is the temperature (°C), T0 is the reference temperature generally set at 100 °C. Assuming the overall reaction following first-order kinetics and Arrhenius relation of temperature, the empirical parameter ω, is the fitted parameter which in this and most other studies has assigned the value of 14.75 and equates to a reaction that doubles its reaction rate for every 10°C increase at the temperature. The ω value in Equation 4 was shown to be inversely proportional to the activation energy, as expressed below (4):

$$\varpi = \frac{Tf^2 R}{Ea} \qquad (4)$$

where Tf is the temperature in the middle of the range of experimental conditions (floor temperature); R is the universal gas constant; Ea is the apparent activation energy.

2.2.3. Characterization of the bio-oil fraction

Products of the aqueous liquid phase as obtained after the separation of the solid carbonaceous fraction, were quantified by using an off-line Shimadzu HPLC equipped with an Aminex HPX-87-H column, using the following parameters: mobile phase 5 mM H_2SO_4 at a speed flow of 0,6 ml min^{-1} and the oven heated at 70 °C. Every measurement was performed in 30-60 min time [Gumina et al., 2019].

The chemical content of the extracted light bio-oil was analyzed by using a GCMS-QP2010 system (Shimadzu, Japan) equipped with a split–splitless injector. A HP-5 weak polar capillary column, 30 m × 0.25 mm i.d. x 0.32 µm film thickness, was used for each GC analysis. The carrier gas was helium at a constant flow rate of 24.3 ml/min. For the set-up of each system, 0.5 µL of the GC sample was injected in split mode, with a split ratio of 1:10 for the sample injection into the column. The oven temperature started at 40 °C (held for 1 min) and then was increased to 300 °C (maintained for 5 min), with a heating speed of 3 °C/min. The mass spectrometer operated, in electron ionization mode, at 70 eV, and mass spectra were obtained in a molecular mass range (m/z) of 40-660. The temperature of the transfer line was 250 °C. Compounds identification was performed by a comparison with spectra obtained from the US National Institute of Standards and Tecnology (NIST) mass spectral library (ver. 11).

2.2.4 Characterization of the hydrochar fraction

Fourier transform infrared (FTIR) spectra were registered using a Perkin Elmer Spectrum 100 spectrometer, furnished with a common ATR sampling accessory. Spectra were recorded, at room temperature, from 4000 to 600 cm-1 and with a resolution of 4.0 cm^{-1}, without any earliest handling. The morphology of hydrochar samples was investigated using a Zeiss 1540XB FE SEM (Zeiss, Germany) instrument operating at 10 kV [Malara et al, 2020]. The

crystalline structure of synthesized materials was investigated using the X-ray powder diffraction (XRD) by means of a Bruker D8 Advance A 25 X-ray diffractometer operating at 40 kV and in the range 20-80° (2-theta), with an increasing rate of 0.01°/s and the recorded diffractograms were deconvolved via an OriginPro 2018 software. B.E.T. surface area and porosity of samples were evaluated by nitrogen adsorption and desorption isotherms carried out at 77 K by a Quantachrome® ASiQwin™ instrument (Anton Paar Companies, Graz, Austria). The thermal stability in air of investigated hydrochar samples was evaluated by thermogravimetry (TGA) carried out with TA Instruments SDTQ 600 (balance sensitivity: 0.1 mg). Samples (~15 mg) were heated at 20 °C/min from 100 °C up to 1000 °C using a constant air flow rate (100 ml/min), after a preliminary sample stabilization for 30 min at 100 °C to remove the eventually adsorbed water [Malara et al., 2018]. The weight loss (%) was calculated.

2.3 Results and discussion

2.3.1 Hydrochar yields and chemical-structural characteristics

In order to analyse separately the effect of reaction temperature and time on hydrochar yields, a series of experiments, at fixed solid:water ratio, have been carried out [Zhuang et al., 2019]. After 60 min of reaction, the hydrochar yield rises with the reaction temperature from 18.8% at 180 °C up to a maximum of 30.4% at 300 °C (Figure 2.1). The reaction time provided the decomposition of biomass less than the temperature. It can be assumed that for relatively short reaction times, 60 min, and for low reaction temperatures, the conversion of the initial biomass is still at a germinal stage, as evidenced also by SEM analysis reported in Figure 2.3. On the other hand, after only 60 min of reaction, as the temperature increases, the conversion process becomes significant, favoring the increase in hydrochar yield.

After 180 min of reaction, the yield increases with the temperature from 45.4% at 180 °C up to the highest value of 54.1% at 210 °C. Such behaviour is in line with the generally accepted reaction mechanism of the HTC process of lignocellulosic materials where the cellulose degradation starts at a reaction temperature higher than 200 °C while, for a higher reaction temperature, a clear decrease in hydrochar yield is observed as a consequence of gas phase products formation. Accordingly, due to the more relevant volatilization processes under drastic conditions, a notable yield decrease is evident at longer reaction times (300 min) already at 180 °C. Such findings, taking into account also data obtained by other authors [Zhuang et al., 2019], confirm that process parameters (the reaction time and the reaction temperature) play a fundamental role on the hydrochar yields and cannot be analyzed separately. The reported results differ from those reported by Erdogan et al [Erdogan et al., 2015] where a correlation between the reaction time and the hydrochar yield, in the HTC of the orange pomace, in the T range 175-260 °C, was not found. This substantial difference is probably due to the distinctive content of cellulose and hemicellulose and their weight ratio, in the orange peel and in the pomace [Rivas-Cantu et al., 2013], that probably affects the global carbonization process with a consequent different amount of solid obtained over time, making the results between the two materials difficult to compare.

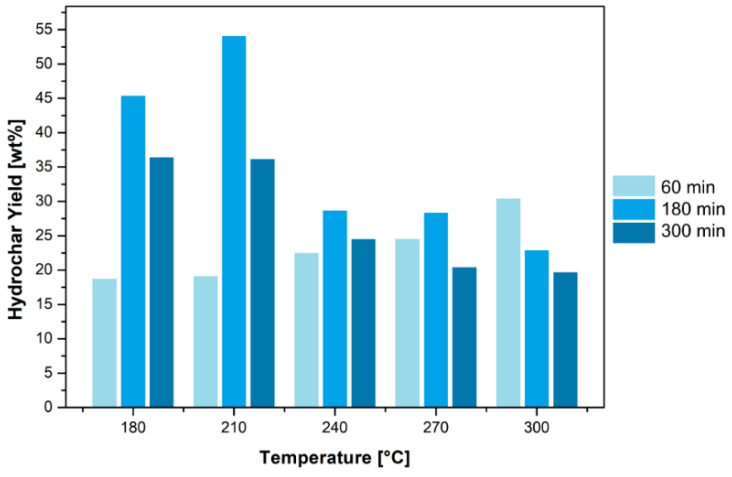

Figure 2.1. Hydrochar yield as a function of reaction temperature at a fixed reaction time.

The simultaneous effect of temperature and reaction time, expressed in terms of $logR_0$, on hydrochar yields is reported in Table 2.1. A substantial difference was observed in hydrochar yield produced at different $logR_0$. Experimental data, also summarized in Table 2.1, indicate that a rise in the $logR_0$ exerts a comparable promoting effect on the hydrochar production, resulting in a peculiar increasing trend with the severity coefficient, attaining a plateau of ca. 54.05 wt% at log R_0 equal to 5.49 (210 °C at 180 min). A further increase of the $logR_0$ causes a hydrochar yield decrease with the lowest value of 19.69% found at the highest severity of 8.36 (300 °C at 300 min).

Table 2.1. Hydrochar yields as function of $logR_0$.

Sample	$LogR_0$	HC yields (wt%)
$S\text{-}HC_{150\text{-}60}$	3.25	13.27
$S\text{-}HC_{180\text{-}60}$	4.13	18.74
$S\text{-}HC_{180\text{-}180}$	4.61	35.37
$S\text{-}HC_{180\text{-}300}$	4.83	36.40
$S\text{-}HC_{210\text{-}60}$	5.01	49.10
$S\text{-}HC_{210\text{-}180}$	5.49	54.05
$S\text{-}HC_{210\text{-}300}$	5.71	36.13
$S\text{-}HC_{240\text{-}60}$	5.90	29.45
$S\text{-}HC_{240\text{-}180}$	6.37	28.66
$S\text{-}HC_{240\text{-}300}$	6.59	24.48
$S\text{-}HC_{270\text{-}60}$	6.78	24.53
$S\text{-}HC_{270\text{-}180}$	7.26	22.34
$S\text{-}HC_{270\text{-}300}$	7.48	20.39
$S\text{-}HC_{300\text{-}60}$	7.66	20.40
$S\text{-}HC_{300\text{-}180}$	8.14	20.87
$S\text{-}HC_{300\text{-}300}$	8.36	19.69

A similar trend in the simultaneous effect of temperature and reaction time upon energy densification and mass yield have been reported by other researchers, using different biomass raw materials [Reza et al, 2016; Yan et al., 2017; Yao et al., 2016], evidencing that higher temperature and reaction time lead to an enrichment in fixed carbon and a consequent higher heat production but lower solids recovery, probably due to a higher conversion of cellulose, hemicellulose and lignin, allowing a series of deoxygenating processes (e.g

dehydration, decarboxylation) resulting in the formation of organic matter and a decrease in oxygen and hydrogen content [Cai et al., 2016].

Termogravimetric (TGA) and energy-dispersive spectroscopy (EDS) analysis (shown in Figure 2.2 and Figure 2.3) of the different hydrochar samples, obtained under different hydrothermal temperatures at a fixed residence time of 180 min, confirm the noticeable role of reaction temperature in the yield and elemental composition of hydrochar. Apart the S-$HC_{180\text{-}180}$ sample, the breakdown of all samples in air atmosphere takes place in three stages. Until 200 °C the weight loss (stage I) is very low (less than 2%), probably due to the hydrophobic nature of the hydrochars, which hinders the absorption of a large water quantity inside their structures. On increasing the temperature a large weight loss (stage II) starts, centered at around 300 °C and associated with the release of organic volatile matters due to the decomposition of hemicellulose and cellulose. The successive stage (III) is related to surface and bulk hydrochar oxidation and suggests that the progressive loosing of the organic constituents, originary present in the orange peels, and the surface groups of hydrochar are formed at different hydrothermal temperatures, leading to samples production characterized by a different chemical composition.

Furthermore, EDS spectra of S-$HC_{210\text{-}60}$ reveal that at lower temperatures of reaction, many residual oxygenated groups still remain on the surface, evidenced by a high content of oxygen (about 20 wt%) and a lower content of carbon (ca. 78 wt%). On the contrary, an increasing of the reaction temperature up to 300 °C causes a decrease of the oxygen content (12.1%), ascribed to dehydration processes from cellulose to hydrochar [Cai et al., 2016] and a consequent enhancement of the carbon content (ca. 88 wt%).

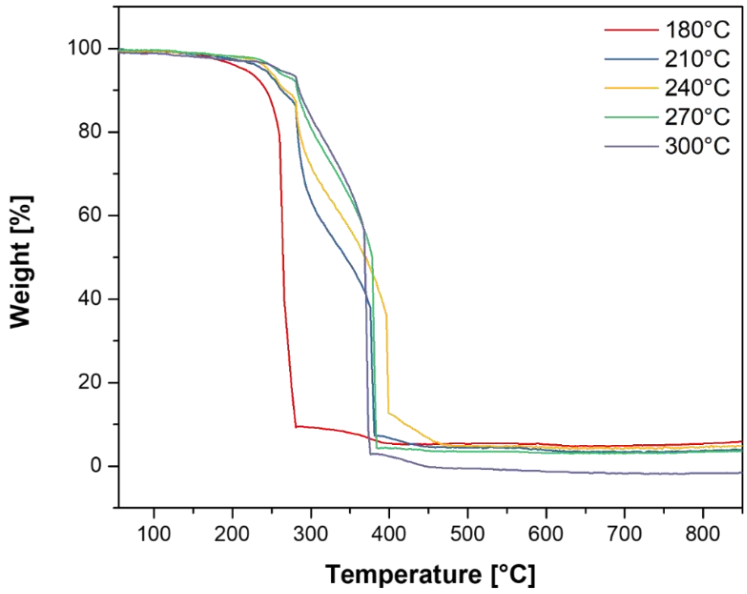

Figure 2.2. TGA curve in air of the hydrochar samples.

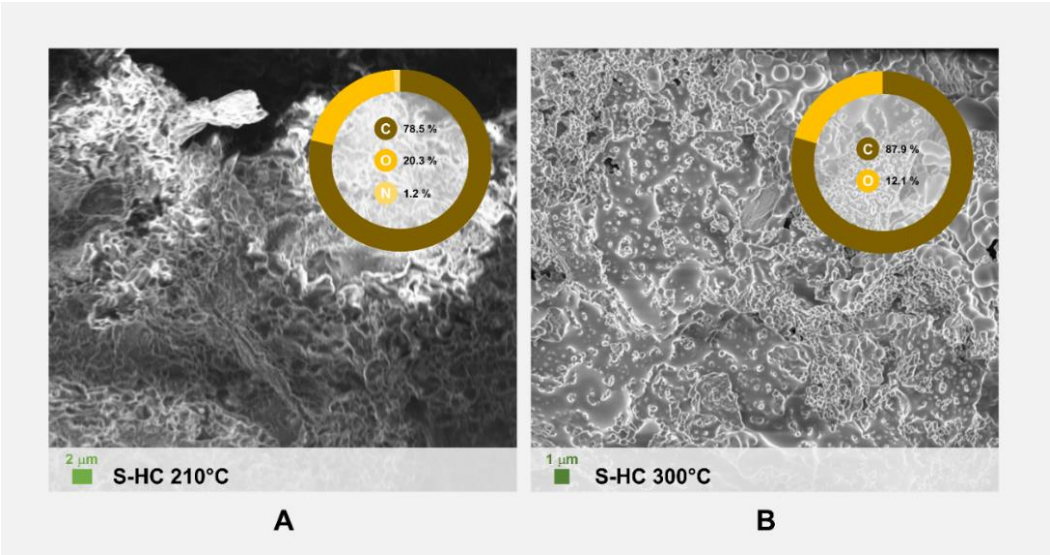

Figure 2.3. SEM-EDS analyses of a) S-HC$_{210\text{-}60}$ and b) S-HC$_{300\text{-}60}$. The inset shows the elemental analysis of these samples.

As above mentioned, the reaction temperature influences not only the yields of the obtained hydrochar samples, but also their morphology and composition, as revealed by SEM experiments.

The morphology of samples, prepared at lower hydrothermal temperature (Figure 2.4a), is not very dissimilar than that of the pectine and lignocellulose (the main components of the orange peels raw material) [Rivas-Cantu et al., 2013]. On the other hand, at 300 °C, the material produced shows the presence of the characteristic hydrochar microspheres (Figure 2.4b).

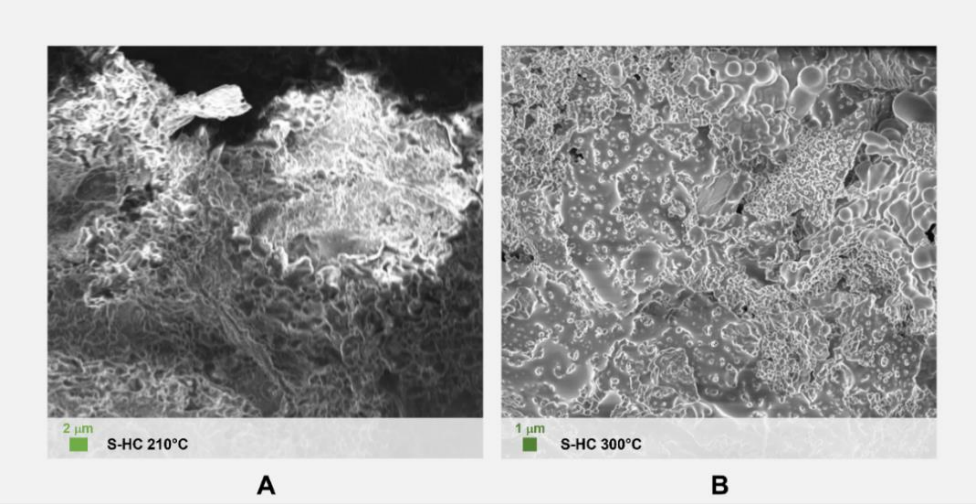

Figure 2.4. SEM analysis of (a) S-$HC_{210\text{-}60}$ and (b) S-$HC_{300\text{-}60}$.

XRD analysis was used for the determination of crystalline structures in the hydrochar samples (Figure 2.5). The reflections of crystalline cellulose at 16 and 22.6 theta are noticeably evidenced in hydrochars obtained at the lowest temperature. As the temperature of the hydrochar preparation increases, a gradual shift from orderly crystallites to transition crystallites can be noticed in XRD spectra. Upon further increasing the hydrothermal temperature, these peaks disappear, whereas new broad peaks, at around 25 and 40 2-theta (*), related to turbostratic structure of disordered carbon coming from the (100) plane of graphite, appear and gradually grow in intensity. Further increasing of temperature to 300 °C leads to complete conversion of the "crystalline stage" to the "amorphous stage" as diffraction peaks at 300 °C suffer from broad shape, low intensities and low signal to noise ratio. As

evidenced in Figure 2.6, the reaction time is irrelevant on the crystalline structure of the samples obtained at different reaction temperatures.

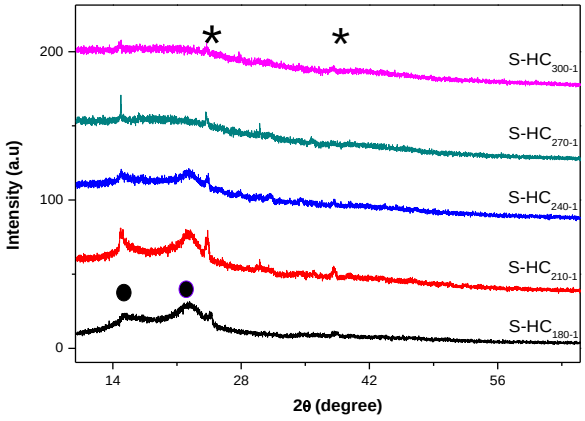

Figure 2.5. X-ray diffrattograms of the hydrochar obtained at different temperature after 60 min of reaction time.

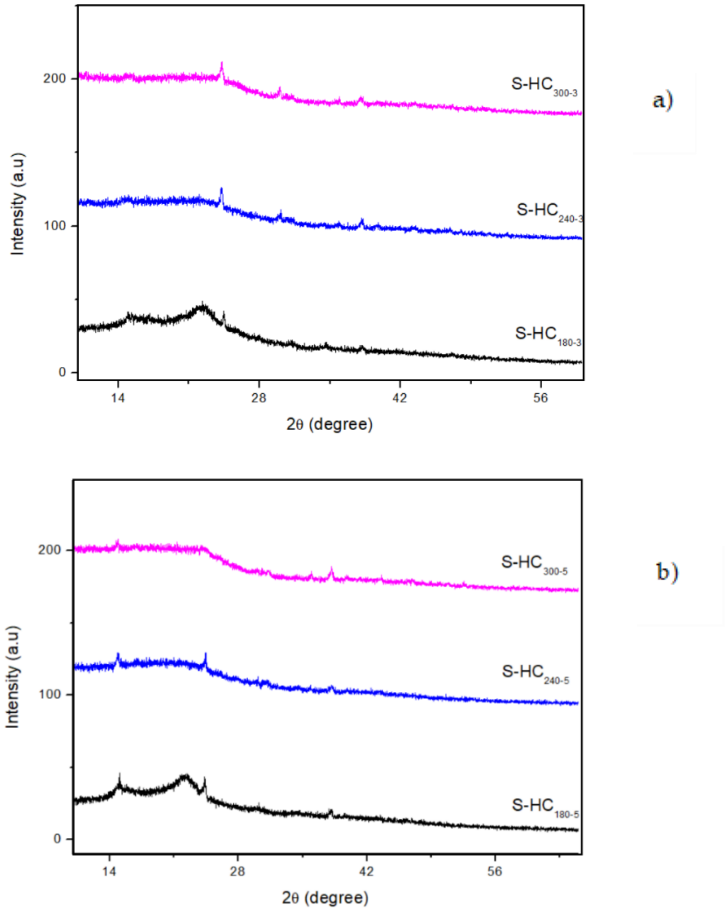

Figure 2.6. X-ray diffrattograms of the hydrochar obtained at different temperature after a) 180 min of reaction time and b) 300 min of reaction time.

This phenomenon can be explained considering that the crystalline structure of cellulose in the lignocellulosic biomass has well-packed long chains characterized by strong hydrogen bonding networks, which well-maintain the sugar ring assembly promoted by the hydrolysis reaction occurring during the hydrothermal carbonization process [Wang et al., 2017].

The FTIR spectra at different reaction temperature and reaction time are reported in Figure 2.7. As it can be seen, the reaction time does not affect the structural properties of the samples obtained at different reaction temperatures, therefore, as an example a summary of the structural properties and N_2 adsorption-desorption isotherms, obtained at various temperatures, and at a fixed reaction time of 60 min, is reported in Table 2.2. Adsorption bands at 1608 cm^{-1} and 1701cm^{-1} correspond to C=C vibrations and C=O band respectively displaying the asymmetric stretch of aromatic rings, carbonyl, quinone, ester or carboxylic groups probably with a small quantity of amide, revealing the decarboxylation reaction and the aromatization of the orange peel waste during the hydrothermal process. The peaks at 1026 cm^{-1} can be attributed to the C–O stretching vibrations of carboxylic acids and esters or carbohydrates, while the band at about 3300 cm^{-1} suggests the O-H stretching of hydroxylic or caboxylic functionalities.

Aliphatic C–H bands are found at 3000–2800 cm^{-1}. The spectrum of S-HC_{180-60} reveals a peak at 1120–1050 cm^{-1}, possibly related to a C-O band of the lignocellulose component of the orange peels still present. According to XRD data, this peak decreases in intensity on increasing the treatment temperature. The presence of a peak at 1527 cm^{-1} strongly suggests the presence of a nitro-compound characterized by the N–O asymmetric stretching. The peak at 1431 cm^{-1} may also correspond to the asymmetric and symmetric stretching of the carboxylate (COO-) group.

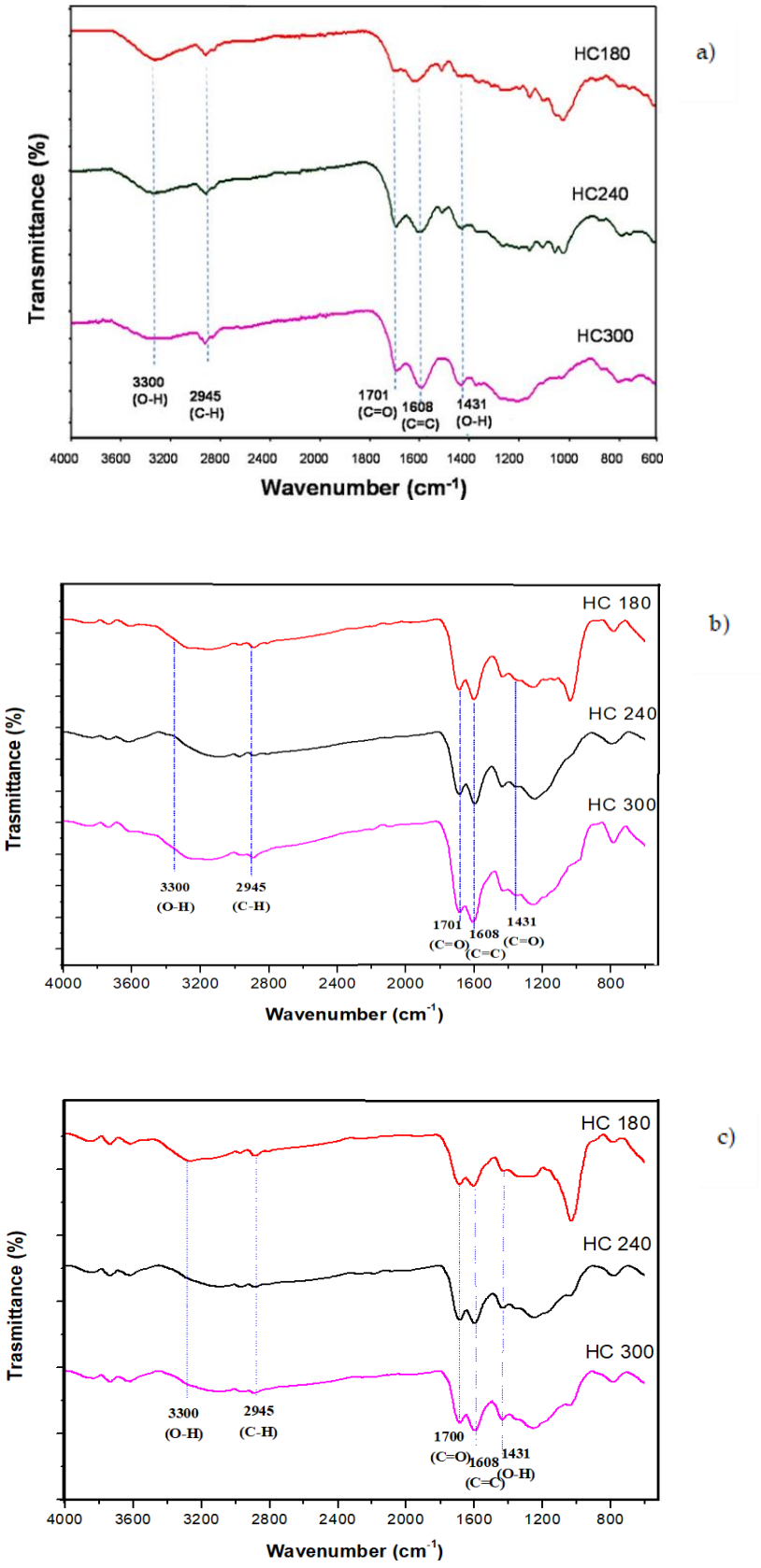

Figure 2.7. FT-IR analysis of the hydrochar samples at a) 60 min of reaction time; b) 180 min of reaction time; c) 300 min of reaction time.

Fragments values become stronger and broader when experiments are carried out at higher temperatures, in agreement with TGA and EDS analyses confirming that, during the HTC process, a series of dehydratation, decarboxylation and aromatization reactions occur, with a consequent decrease in the hydrochar yield as well as an enrichment in the C content.

Moreover, the presence of an absorptions peak at 1026 cm^{-1} in the S-$HC_{180\text{-}60}$ sample, related to the C–O stretching vibration, can be again related to the presence of a small amount of crystalline cellulose. As expected, upon increasing the reaction temperature, the absence of such peak is indicative of the full conversion of OPW into biochar and bio-oil.

Values of BET surface area and pore volume, reported in Table 2.2, relative to S-HC samples, at various temperatures, and at the fixed reaction time of 60 min, in accord with other hydrochar prepared in similar experimental conditions [Sevilla et al., 2009], show that both parameters increase of about 3-4 time by increasing the reaction temperature going from 180 to 300 °C.

Table 2.2. FT-IR assignments and structural properties of the hydrochar samples at different reaction temperature and fixed reaction time of 60 min.

Observed peaks intensity	Possible Functional groups	Sample	B.E.T. S.A. (m^2/g)	Pore volume (cc/g)	Pore radius Dv(r) (Å)
3300 cm^{-1}	O–H (alcohols, phenols, carboxylic acid)	S-$HC_{180\text{-}60}$	4.9	0.009	17.9
3000 cm^{-1}	C-H (aliphatic methyl)	S-$HC_{210\text{-}60}$	5.5	0.008	20.4
1701 cm^{-1}	C=O (ketone, aldehydes, amides)	S-$HC_{240\text{-}60}$	7.7	0.010	17.6
1608 cm^{-1}	C=C (aromatic rings, carbonyl, quinone, ester or carboxyl groups)	S-$HC_{270\text{-}60}$	9.1	0.011	17.8
1527 cm^{-1}	N-O (nitro)	S-$HC_{300\text{-}60}$	18.4	0.029	22.4
1431 cm^{-1}	COO- (carboxylate)				
1120 cm^{-1}	C-O of lignocellulose				
1026 cm^{-1}	C–O (carboxylic acid, esters)				

2.3.2 Effect of initial pH and solid: water ratio

Although the more relevant literature results identify reaction temperature and residence time as the main process parameters, affecting the amount and chemical composition of the hydrochar produced, it is worth mentioning that both the solid: water ratio and the initial pH, could play an important role, given that one of the goals of the HTC process is to break down the unbending structure of the starting biomass material into small and lower molecular weight chains. In fact, it is well known that addition of sulfuric acid or acetic acid in the reaction mixture can positively influence the HTC process by catalyzing hydrolysis reactions of cellulose and hemicellulose, formed in the experimental conditions usually adopted. Regarding the effect of the initial pH, results reported in Table 2.3 show that the initial pH impacts the hydrochar yield increasing as the higher acid concentration increase, with the highest yield of 30.12 wt%, attained SA-HC1, almost 50% higher than that observed in the reference experiment (180 °C, 60 min), but changes slightly as the acetic acid concentration increases. Incidentally we observe that CH_3COOH is a weak acid whereas H_2SO_4 is a strong acid for what the first dissociation constant is concerned. Results suggest also that rather than the pH itself, it is the type of the additive used that affects the yield. Indeed, the change in hydrochar yields could be explained considering that during the sulfuric acid catalysed hydrolysis, insoluble humins indistinguishable from HC products are formed, with a subsequent enhancement of the amount of solid products obtained.

On the contrary, the acetic acid is a natural by-product of HTC of lignocellulosic feedstocks due to the hydrolysis and dehydratation of cellulose and hemicellulose in the presence of subcritical water [Reza et al., 2014; Reza et al., 2015]. Therefore, a further addition of acetic acid in the reaction media, favoring the degradation of biomass components, leads to a higher heat production and a lower hydrochar yield.

Results obtained in this study (see Table 2.4) also indicate that the role of the biomass/water ratio on the hydrochar yield is insignificant for all values investigated. This finding is in agreement with the results reported by A. Toptas Tag et al. [Tag et al., 2018] for the HTC of sunflower stalk as agricultural waste, poultry litter as animal waste, and algal biomass, by Sabio et al. [Sabio, E. et al., 2018], but disagree with data reported by other authors [Volpe et al., 2017; Borrero-López et al., 2017]. In any case, in the literature there is no unanimous opinion on the role played by the different water/biomass ratio, and generally a fixed biomass: water ratio has been used by many authors. However, all results, obtained as a function of the reaction temperature, reaction time, biomass/water ratio and pH, confirm that it is not always easy to make a direct comparison between the hydrochar yields reported in the literature and those reported in this study, since there are many parameters that can affect the process, such as the experimental setup, the type of feedstock, the total solid and water amount, and then the final amount of the hydrochar produced.

Table 2.3. Hydrochar Yields as function of initial pH.

Sample	pH[1]	pH[2]	Hydrochar Yield (wt%)
S-$H_{180\text{-}60}$	-	3.60	18.74
SA-HC1	1	1.61	30.62
SA-HC2	2	1.89	27.36
AA-HC1	1	1.20	21.51
AA-HC2	2	1.80	19.39
AA-HC3	3	2.40	15.24

Table 2.4. Hydrochar yield as function of L:S ratio.

Sample	L:S ratio	HC yield (wt%)
$S\text{-}HC_{180\text{-}60}$	4:1	16.25
$S\text{-}HC_{180\text{-}60}$	6:1	18.74
$S\text{-}HC_{180\text{-}180}$	12:1	18.21
$S\text{-}HC_{180\text{-}300}$	24:1	16.54
$S\text{-}HC_{210\text{-}60}$	48:1	17.23

2.3.3 Composition of hydrothermal bio-oil liquid fraction

The general chemical composition of the light bio-oil obtained at different reaction temperatures and at a fixed residence time of 60 min, was analyzed by GC-MS (Table 2.5). The reaction mechanism, involved in the formation of bio-oil during the HTC of various lignocellulosic biomasses, has been described by several authors [Reza et al, 2014; Wu et al., 2017] consisting of a series of consecutive and parallel reactions starting with acid hydrolysis of polysaccharides to form monosaccharides. Glucose and fructose can be dehydrated by acids into 5-hydroxymethylfurfural and furfural. Furans and other reaction intermediates can undergo further transformation processes (e.g. isomerization, condensation, rehydration, hydrations) or they can be degraded into humins [Chheda et al., 2007].

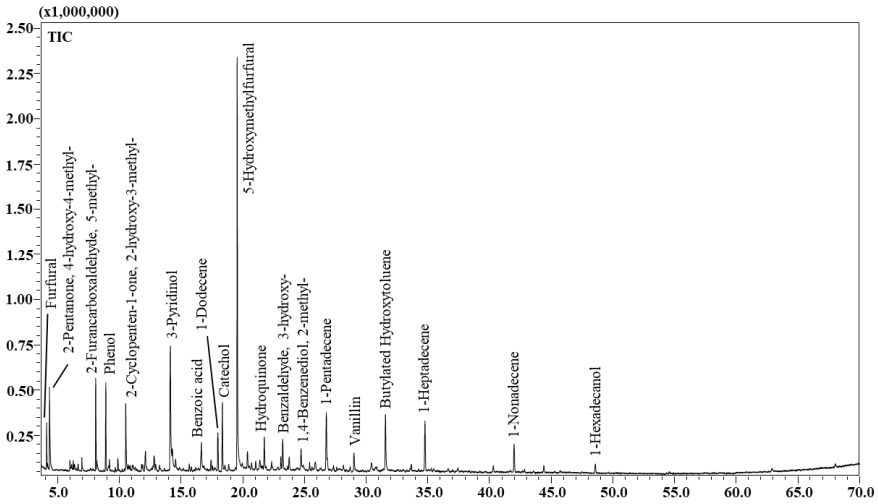

Figure 2.8. The chromatogram of the light bio-oil refers to an experiment carried out at 240 °C - 60 min by GC-MS. Main peaks are labeled.

As illustrated in Table 2.5, the light bio-oil is mainly divided into seven categories: furans, phenols, acids, ketones, aldehydes, alcohols and alkenes (Figure 2.8). At lower HT temperatures, the main compounds at 200 °C were furan derivatives. On increasing the temperature, the composition of the light bio-oil becomes more complex showing a higher concentration of acids phenolic compounds as a consequence of humins formation.

Table 2.5. Major chemical components of the light bio-oil determined by GC-MS analysis.

	Compounds Name	Sample			
		L-HC$_{150\text{-}60}$	**L-HC$_{180\text{-}60}$**	**L-HC$_{240\text{-}60}$**	**L-HC$_{300\text{-}60}$**
		Peak area%			
Furans	Furfural	18.94	16.69	1.63	-
	2-Furancarboxaldehyde, 5-methyl	14.86	7.88	5.05	-
	5-Hydroxymethylfurfural	41.97	61.82	28.61	-
Phenols	Phenol	0.57	0.10	4.72	9.62
	Catechol	0.60	0.29	4.52	8.64
	1,2-Benzenediol, 3-methyl	-	0.11	0.78	1.04
	Hydroquinone	-	-	1.91	7.26
	p-Cresol	-	-	0.79	2.17
	Phenol, 2-methyl	-	-	0.27	0.69
Acids	Benzoic acid	2.27	0.61	2.67	6.21
	2-Pentenoic acid	-	-	0.32	-
Ketones	2-Pentanone, 4-hydroxy-4-methyl	0.40	0.68	3.87	1.20
	Ethanone, 1-(2-furanyl)	0.69	0.46	0.40	1.86
	1,2-Cyclopentanedione, 3-methyl	0.63	0.81	-	-
	2-Cyclopenten-1-one, 2-hydroxy-3-methyl	-	-	4.37	0.99
	2-Cyclopenten-1-one, 2-methyl	-	-	0.61	5.83
	2-Cyclopenten-1-one, 3-methyl	-	-	0.61	7.41
Aldehydes	1H-Pyrrole-2-carboxaldehyde	0.86	0.41	0.66	-
	Benzaldehyde, 3-hydroxy	-	0.17	0.83	-
	Vanillin, acetate	-	-	1.07	-
Alcohols	α-Terpineol	0.91	0.24	-	1.01
	Benzyl alcohol	-	-	0.29	-
	3-Pyridinol	-	-	10.14	4.63
Alkenes	1-Nonadecene	0.24	0.33	1.65	-
	1-Pentadecene	-	0.59	3.51	-
	1-Heptadecene	-	-	3.64	-

2.3.4 Production of furan derivatives and levulinates from hydrothermal upgrading of orange peel waste

In order to investigate the best reaction conditions that maximize the production of furan and levulinate derivatives, a systematic study on the effect of (i) time; (ii) temperature; (iii) initial acid concentration and (iv) co-solvent was carried out. Reaction temperature is surely a crucial parameter for investigating the overall productivity of furan derivatives starting from OPW. The yield profiles of FU, 5-HMF and levulinic acid are reported in Figure 2.9. Under neutral conditions, FU and 5-HMF yields gradually increase reaching the highest value at 180 °C. The observed decrease in the production of furans at higher reaction temperatures is in line with other reports [Puccini et al., 2016] and can be related to the formation of humin type by-products. Indeed, dark-brown insoluble products were formed in experiments carried out at 240 °C and 300 °C.

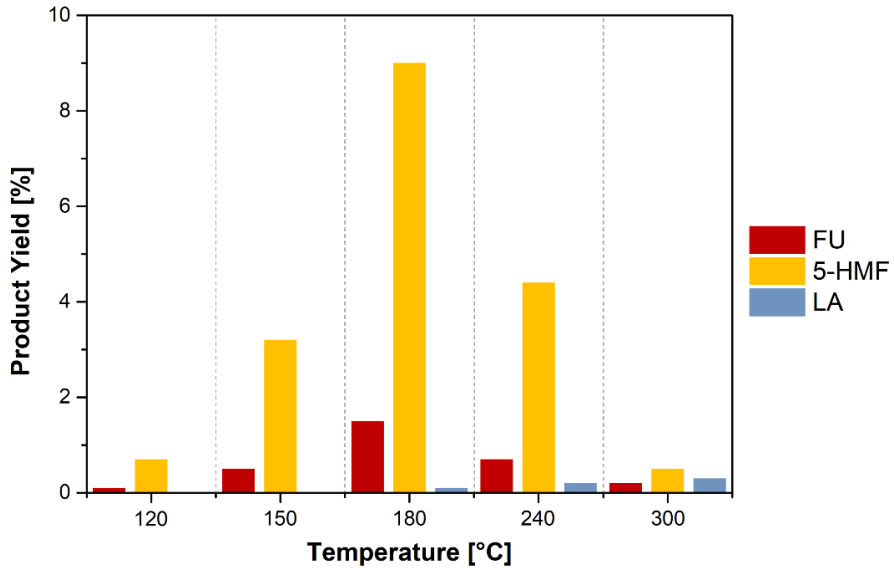

Figure 2.9. Effect of HTC reaction temperature on the production of furfural (FU), 5-hydroxymethylfurfural (5-HMF) and levulinic acid (LA) from OPW under neutral conditions (Reaction conditions: 20 g of OPW; 20 ml of H_2O; time: 60 min; autogenous pressure; stirring: 600 rpm).

As expected, under the reaction conditions adopted, very low concentrations of levulinic acid (LA) were registered at all investigated reaction temperatures. A noticeable amount of LA can be noticed at 300 °C due to the higher concentration of protons deriving from the dissociation, promoted by high reaction temperature.

Having found 180 °C as the best reaction temperature that maximizes FU derivatives, the conversion of OPW was also investigated at different reaction times (15, 30, 60, 180 and 300 min) (Figure 2.10). The highest 5-HMF and FU yields were already gained after only 30 min. A slight decrease in the production of furans is registered after 300 min and may be related both to the thermal degradation of furan derivatives as well as to the fact that a prolonged hydrolysis time increases formation of humins [Silva et al., 2021].

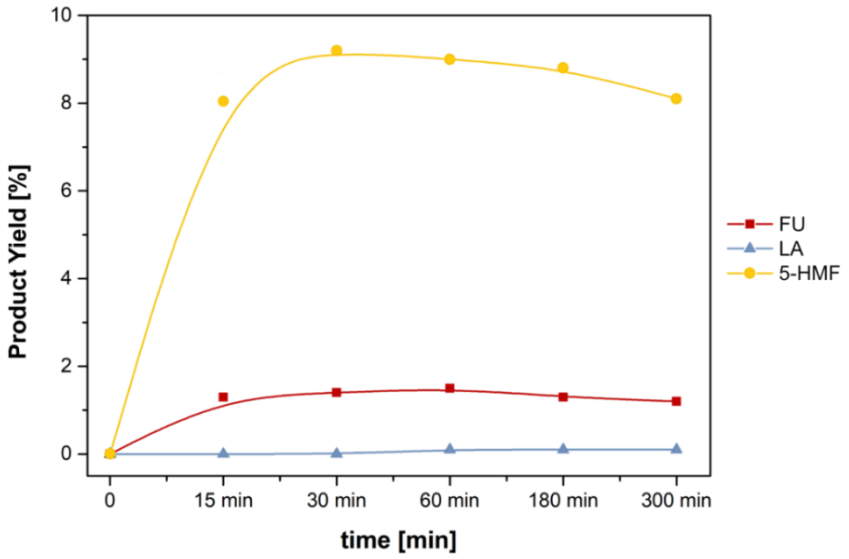

Figure 2.10. Effect of HTC reaction time on the production of furfural (FU), 5-hydroxymethylfurfural (5-HMF) and levulinic from (LA) OPW under neutral conditions (Reaction conditions: 20 g of OPW; 20 ml of H_2O; temperature: 180 °C; autogenous pressure; stirring: 600 rpm).

On the other hand, by changing the conditions by using as reaction media a sulfuric acid solution, a decrease in the production of furans together with a higher production of levulinic acid is observed as a consequence of the

acid hydrolysis (Figure 2.11). Upon increasing the H_2SO_4 content (from 0,2 to 1,0 M), a slight decrease in the overall LA can be noticed.

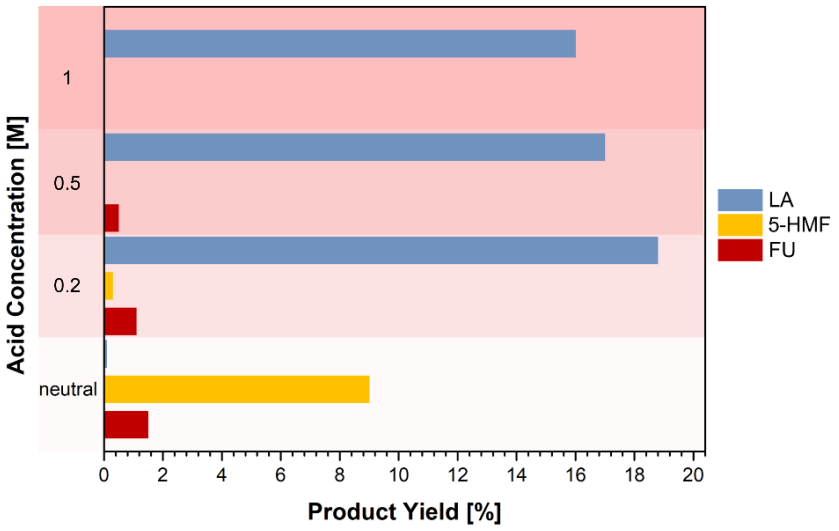

Figure 2.11. Effect of acid conditions on the production of furfural (FU), 5-hydroxymethylfurfural (5-HMF) and levulinic acid (LA) (Reaction conditions: 20 g of OPW; 20 ml solution of H_2SO_4 (from 0,1 to 1,0 M) in H_2O; temperature: 180 °C; time: 60 min; autogenous pressure; stirring: 600 rpm).

Analogous results are registered in the presence of simple alcohols as co-solvents, such as methanol and ethanol, that permit the direct formation of alkyl levulinates (Figure 2.12), used as flavoring/fragrance agents or as fuel bio-additives [Sen et al, 2012; Bond et al., 2010]. Moreover, methyl- and ethyl-levulinate now represent valid starting bio-based feedstocks for the preparation of γ-valerolactone [Tabanelli et al., 2019; Vaśquez et al., 2019] and find many applications ranging from flavoring agent to green solvent or intermediate in the synthesis of bio-based chemicals and polymers [Wright et al., 2012; Omoruyi et al, 2016].

Indeed, the best results in terms of alkyl-levulinate production were obtained when using a 0,2 M sulphuric acid solution with higher yields obtained from the methanol esterification that, being characterized by a

shorter carbon chain, is definitely a better entering group than ethanol (Table 2.6).

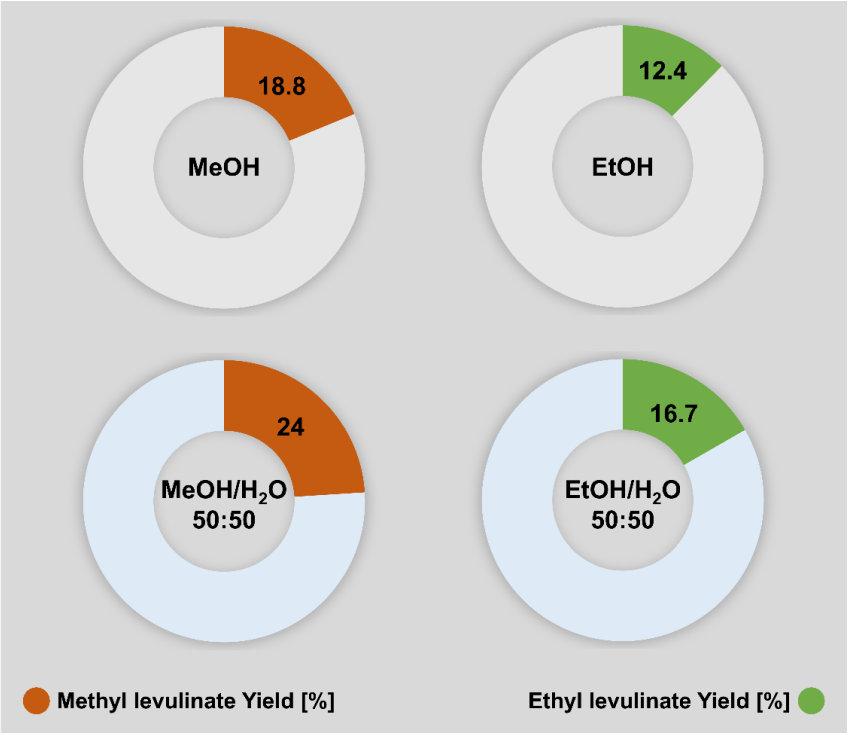

Figure 2.12. Co-solvent effect of HTC reaction temperature on the production of alkyl levulinates (Reaction conditions: 20 g of OPW; temperature: 180 °C; time: 60 min; autogenous pressure; stirring: 600 rpm).

Table 2.6. Effect of acid conditions on the preparation of methyl-levulinate and ethyl-levulinate starting from OPW by using HTC process (Reaction conditions: 20 g of OPW; temperature: 180 °C; time: 60 min; autogenous pressure; stirring: 600 rpm).

Product	**Solvent (wt: wt)**	**[0.1 M H_2SO_4]**	**[0.1 M H_2SO_4]**	**[0.1 M H_2SO_4]**
Methyl levulinate	water: methanol (50:50)	7.1 (% yield)	24.0 (% yield)	14.2 (% yield)
Ethyl levulinate	water: ethanol (50:50)	4.9 (% yield)	16.7 (% yield)	7.5 (% yield)

2.4 Conclusions

In this chapter we demonstrate that the hydrothermal carbonization process can be successfully adopted for the complete upgrading of the orange peel waste into hydrochar and value-added chemicals. The main processing variables, reaction temperature, initial pH and residence time, affect the mass yield (MY), while the solid:liquid ratio was found insignificant for all L/S investigated. Indeed, there is a strong correlation between temperature and residence time, suggesting that the role of these two variables cannot be analyzed independently. The highest yield of hydrochar is obtained at a 210°C reaction temperature, 180 min residence time, 6/1 w/w orange peel waste to water ratio and a 3.6 initial pH. The results suggest that the conversion of the citrus waste occurs during the hydrothermal carbonization process, due to a series of reactions such as decarboxylation, and dehydration, leading to an improvement of the chemical, structural and morphological characteristics of the optimized hydrochar, making it a carbonaceous material suitable for a wide range of applications, both in the chemical and energy fields.

The bio-products distribution strongly depends on the applied reaction conditions. Overall, 180 °C was found to be the best reaction temperature that maximizes the production of furfural and 5-HMF in the presence of pure water as reaction medium. On the other hand, by using a sulfuric acid solution as reaction medium, levulinic acid can be easily obtained as main product. Accordingly, a good production in methyl levulinate and ethyl levulinate can be achieved in the presence of methanol or ethanol, respectively, with the best yield obtained with methanol in the esterification reaction.

References

Bond, J.Q.; Martin Alonso, D.; Wang, D.; West, R.M.; Dumesic, J.A. Integrated catalytic conversion of gamma-valerolactone to liquid alkenes for transportation fuels. *Science* **2010**, *327*, 1110-1114.

Borrero-López, A.M.; Fierro, V.; Jeder, A.; Ouederni, A.; Masson, E.; Celzard, A. High added-value products from the hydrothermal carbonization of olive stones. *Environ. Sci. Pollut. Res.* **2017**, *24*, 9859-9869.

Bressi, V.; Ferlazzo, A.; Iannazzo, D.; Espro, C. Graphene Quantum Dots by Eco-Friendly Green Synthesis for Electrochemical Sensing: Recent Advances and Future Perspectives. *Nanomaterials* **2021**, *11*, 1120-1146.

Burguete, P.; Corma, A.; Hitzl, M.; Modrego, R.; Ponceb, E.; Renz, M. Fuel and chemicals from wet lignocellulosic biomass waste streams by hydrothermal carbonization. *Green Chem.* **2016**, *18*, 1051-1060.

Cai, J.; Li, B.; Wang, J.; Zhao, M.; Zhang, K. Hydrothermal carbonization of tobacco stalk for fuel application. *Bioresource Technology* **2016**, *220*, 305-311.

Chheda, J.N.; Román-Leshkov, Y.; Dumesic, J.A. Production of 5-hydroxymethylfurfural and furfural by dehydration of biomass-derived mono- and polysaccharides. *Green Chem.* **2007**, *9*, 342-350.

Erdogan, E.; Atila, B.; Mumme, J.; Reza, M.T.; Toptas, A.; Elibol, M.; Yanik, J. Characterization of products from hydrothermal carbonization of orange pomace including anaerobic digestibility of process liquor. *Bioresource Technology* **2015**, *196*, 35-42.

Espro C., Satira, A.; Mauriello, Anajafi, Moulaee K., Iannazzo D., Neri G. Orange peels-derived hydrochar for chemical sensing applications. *Sensors & Actuators B: Chemical* **2021**, *341*, 130016-130027.

Gou, H.; He, J.; Zhao, G.; Zhang, Li.; Yang, C.; Rao, H. Porous nitrogen-doped carbon networks derived from orange peel for high-performance supercapacitors. *Ionics* **2019**, *25*, 4371-4380.

Gumina, B.; Espro, C.; Galvagno, S.; Pietropaolo, R.; Mauriello, F. Bioethanol Production from Unpretreated Cellulose under Neutral Selfsustainable Hydrolysis/Hydrogenolysis Conditions Promoted by the Heterogeneous Pd/Fe_3O_4 Catalyst. *ACS Omega* **2019**, *4*, 352-357.

Kalderis, D.; Papameletiou, G.; Kayan, B. Assessment of Orange Peel Hydrochar as a Soil Amendment: Impact on Clay Soil Physical Properties and Potential Phytotoxicity. *Waste Biomass* **2019**, *10*, 3471-3484.

Malara, A.; Paone, E.; Bonaccorsi, L.; Mauriello, F.; Macario, A.; Frontera, P. Pd/Fe3O4 Nanofibers for the Catalytic Conversion of Lignin-Derived Benzyl Phenyl Ether under Transfer Hydrogenolysis Conditions. *Catalysts* **2020**, *10*, 20.

Malara, A.; Paone, E.; Frontera, P.; Bonaccorsi, L.; Panzera, G.; Mauriello, F. Sustainable Exploitation of Coffee Silverskin in Water Remediation. *Sustainability* **2018**, *10*, 3547.

Omoruyi, U.; Page, S.; Hallett, J.; Miller, P.W. Homogeneous Catalyzed Reactions of Levulinic Acid: To γ-Valerolactone and beyond. *ChemSusChem* **2016**, *9(16)*, 2037-2047.

Overend, R.P.; Chornet, E. Fractionation of lignocellulosics by steam-aqueous pretreatments. *Philos. Trans. R. Soc. Lond. Ser. A Math. Phys. Sci.* **1987**, *321*, 523-536.

Pistone A., Espro C. Current trends on turning biomass wastes into carbon materials for electrochemical sensing and rechargeable battery applications. *Curr. Opin. Green Sustain. Chem.* **2020**, *26*, 100374-100381.

Puccini M.; Licursi D.; Stefanelli E.; Vitolo S.; Raspolli Galletti A.M.; Heeres H.J. Hydrothermal treatment of orange peel waste for the integrated production of furfural, levulinic acid and reactive hydrochar: towards the application of the biorefinery concept. *Chemical Engineering Transactions* **2016**, *50*, 223-228.

Reza, M.T.; Yang, X.; Coronella, C.J.; Lin, H.; Hathwaik, U.; Shintani, D.; Neupane, B.P.; Miller, G.C. Hydrothermal Carbonization (HTC) and Pelletization of Two Arid Land Plants Bagasse for Energy Densification. *ACS Sustainable Chem. Eng.* **2016**, *4(3)*, 1106-1114.

Reza; M.T.; Rottler E.; Herklotz, L.; Wirth, B. Hydrothermal carbonization (HTC) of wheat straw: Influence of feedwater pH prepared by acetic acid and potassium hydroxide. *Bioresource Technology* **2015**, *182*, 336-344.

Reza, M.T.; Uddin, M.H.; Lynam, J.G.; Hoekman S.K.; Coronella, C.J. Hydrothermal carbonization of loblolly pine: reaction chemistry and water balance. *Biomass Conv. Bioref.* **2014**, *4*, 311-321.

Rivas-Cantu, R.C.; Jones, K.D., Mills, P. L. A citrus waste-based biorefinery as a source of renewable energy: technical advances and analysis of engineering challenges. *Waste Manag. Res.* **2013**, *31*, 413-420.

Satira, A.; Espro, C.; Paone, E.; Calabrò, P.S.; Pagliaro, M; Ciriminna, R.; Mauriello, F. The Limonene Biorefinery: From Extractive Technologies to Its Catalytic Upgrading into p-Cymene. *Catalysts* **2021**, *11*, 00387.

Sen, M.S.; Gürbüz, E. I.; Wettstein, S. G.; Martin Alonso, D.; Dumesic, J. A.; Maravelias, C. T. Production of butene oligomers as transportation fuels using butene for esterification of levulinic acid from lignocellulosic biomass: process synthesis and technoeconomic evaluation. *Green Chem.* **2012**, *14*, 3289-3294.

Sevilla, M.; Fuertes, A.B. Chemical and structural properties of carbonaceous products obtained by hydrothermal carbonization of saccharides. *Chem. Eur. J.* **2009**, *15*, 4195-4203.

Silva, J.F.L; Pinto Mariano, A.; Filho, R.M. Less severe reaction conditions to produce levulinic acid with reduced humins formation at the expense of lower biomass conversion: Is it economically feasible? *Fuel Communications* **2021**, *9*, 100029.

Tabanelli, T.; Paone, E.; Blair Vásquez, P.; Pietropaolo, R.; Cavani, F.; Mauriello, F. Transfer Hydrogenation of Methyl and Ethyl Levulinate Promoted by a ZrO2 Catalyst: Comparison of Batch vs Continuous Gas-Flow Conditions. *ACS Sustainable Chem. Eng.* **2019**, *7*, 9937-9947.

Tag, A.T.; Duman, G.; Yanik, J. Influences of feedstock type and process variables on hydrochar properties. *Bioresource Technology* **2018**, *250*, 337-344.

Vaśquez, P.B.; Tabanelli, T.; Monti, E.; Albonetti, S.; Dimitratos, N.; Cavani, F. Gas-phase catalytic transfer hydrogenation of alkyl levulinates with ethanol over ZrO_2. *ACS Sustain. Chem. Eng.* **2019**, *7*, 8317.

Volpe, M.; Fiori, L. From olive waste to solid biofuel through hydrothermal carbonization: the role of temperature and solid load on secondary char formation and hydrochar energy properties. J. Anal. *Appl. Pyrolysis* **2017**, *124*, 63-72.

Wang, S.; Dai, G.; Yang, H.; Luo, Z. Lignocellulosic biomass pyrolysis mechanism: a state-of-the-art review. *Progress in Energy and Combustion Science* **2017**, *62*, 33-86.

Wright, W.R.H.; Palkovits, R. Development of Heterogeneous Catalysts for the Conversion of Levulinic Acid to γ-Valerolactone. *ChemSusChem* **2012**, *5(9)*, 1657-1667.

Wu, K.; Gao, Y.; Zhu, G.; Zhu, J.; Yuan, Q.; Chen, J.; Cai, M.; Feng, L. Characterization of dairy manure hydrochar and aqueous phase products generated by hydrothermal carbonization at different temperatures. *Journal of Analytical and Applied Pyrolysis* **2017**, *127*, 335-342.

Xiao, K.; Liu, H.; Li, Y.; Yang, G.; Wang, Y.; Yao, H. Excellent performance of porous carbon from urea-assisted hydrochar of orange peel for toluene and iodine adsorption. *Chemi. Eng. J.* **2020**, *382*, 122997.

Xu, C.; Paone, E.; Rodríguez-Padrón, D.; Luque, R.; Mauriello, F.; Recent catalytic routes for the preparation and the upgrading of biomass derived furfural and 5-hydroxymethylfurfural. *Chem. Soc. Rev.* **2020**, *49*, 4273-4306.

Yan, W.; Perez, S.; Sheng, K. Upgrading fuel quality of moso bamboo via low temperature thermochemical treatments: dry torrefaction and hydrothermal carbonization. *Fuel* **2017**, *196*, 473-480.

Yao, Z.; Ma, X.; Lin, Y. Effects of hydrothermal treatment temperature and residence time on characteristics and combustion behaviors of green waste. *Appl. Therm. Eng*. **2016**, *104*, 678-686.

Zhuang, X.; Zhan, H.; Songa, Y.; He, C.; Huang, Y.; Yin, X.; Wu, C. Insights into the evolution of chemical structures in lignocellulose and non-lignocellulose bio-wastes during hydrothermal carbonization (HTC). *Fuel* **2019**, *236*, 960-974.

Chapter 3

Orange peels-derived hydrochar for chemical sensing application

3.1 Introduction

Carbon-based materials, including active charcoal, carbon nanotubes, and graphene, quite comprise the excellent properties of all the materials on the earth such as lightweight, high porosity, high-temperature resistance, acid and alkali resistance, good structural stability, easy conductivity, easy heat transfer, and easy processing. They were extensively studied for their practical applications in numerous fields such as gas adsorption, electrocatalysts, gas sensors, electrochemical sensors and energy production [Gopinath et al., 2020; Elhaes et al, 2016; Asadian et al., 2019; Calabrò et al., 2019]. At present, our society faces the identical tasks of dwindling supply oil resource depletion and waste accumulation, leading to quickly rising of raw material's costs and more and more expensive and pre-emptive waste disposal legislation, focusing the

attention on the possible way to obtain building blocks, for chemicals and biofuels, from renewable lignocellulosic biomass wastes [Gumina et al, 2018; Calabrò et al., 2018]. On this account, great efforts are devoted currently to the preparation of novel carbon materials with enhanced characteristics from low-cost and reproducible natural sources.

Biomass-derived carbon materials can be obtained by easy and suitable physical and chemical procedures and can be extensively used as functional materials, as long as a valid strategy for the effective utilization of biomass wastes [Xiao et al., 2018]. In this respect, various organic wastes have been used as precursors to produce carbon-based materials through hydrothermal carbonization, HTC [Pistone and Espro, 2020; Zhang et al., 2021]. HTC is a type of thermochemical conversion technique, through which biomass can be converted into hydrochar. This process carried out in a water medium under autogenous pressure at a quite low temperature (typically 150-300 °C), represents a promising bio-waste treatment technique [Fang et al., 2018]. The final product, hydrochar, is a carbon solid form, rich in oxygenated functional groups, and shows attractive features attracting considerable attention for potential applications in substitution of carbon materials like carbon nanotubes, graphene, and others [Xiao et al, 2018; Pistone and Espro, 2020; Zhang et al., 2021; Fang et al., 2018].

Despite the numerous properties and applications of biomass-derived carbon materials that have been thoroughly studied, chances for their use in higher- value technologies not yet broadly explored, e.g., such as their use in the fields of electrochemical sensors still remain. Here, we report an investigation on the preparation of hydrochar obtained from orange peels waste (OPW). Orange is among the most worldwide cultivated fruit. The global orange production is estimated over 55 million metric tons for 2020, and the processing industry yearly generates huge amounts of agricultural waste (peel, pulp, etc.). OPW alone accounts for almost the 50% of the wet fruit mass.

The direct disposal of this secondary product, without previous proper processing, therefore causes serious environmental issues and economic loss for the citrus industry [Fazzino et al., 2021].

The hydrochar product is mainly used as an adsorbent, in catalysis, etc [Yaah et al., 2021; Babeker and Chen, 2021; Zhang et al., 2019]. Our aim was instead focused on the evaluation of their electrical and electrochemical performance, with the main objective to develop high performances chemical sensors. Many types of research cover the applications of these carbon nanostructures in the field of chemical sensing actuated through conductometric or electrochemical devices [Bezzon et al., 2019]. The interaction between a gaseous species and the carbon surface in their unidimensional (carbon nanotube), bidimensional (graphene), or 3D (carbon black) structure, has been largely recognized for proposing conductometric sensors able to detect many gases such as H_2, NO_2, NH_3, etc [Liang et al., 2020; Han et al., 2020; Lee et al., 2018]. Besides, the carbon surface can be easily functionalized/additivated by modifying the surface reactivity, to address the sensitivity towards the target gas and consequently to modulate the selectivity [Hung et al., 2020]. Carbon nanostructures also possess unique electro-chemical properties which make them the primary choice as electrode materials for the electroanalytical determination of a variety of analytes, such as organic pollutants, heavy metals, pesticides, pharmaceuticals, etc [Babeker and Chen, 2021; Torrinha et al., 2020]. However, despite the growing production of hydrochars from different waste sources and the promising applications in various fields [Fang et al., 2018; Maniscalco et al., 2020] very few studies involving their use in chemical sensing have been so far reported [Jagdale et al., 2019; Randviir et al., 2019].

In this chapter, it was demonstrated how to utilize the produced hydrochar in some advanced sensing applications, i. e. the conductometric detection of NO_2 in the air at ppb (part per billion) levels and the

electrochemical determination of dopamine at nanomolar concentration. Both these two applications are of high importance, having industrial, environmental and health implications. NO_2 is a toxic gas found in the ambient air of a polluted city. Indeed, NO_2 is mainly produced by motor vehicles and is harmful to the environment and people [Lee et al., 2018]. Thus, the monitoring of NO_2 at ppb levels is a highly demanding issue [Giampiccolo et al., 2019]. Dopamine (DA), a catecholamine neurotransmitter molecule, plays an important role in the central nervous system in our body. Dopamine has a significant effect since we feel pleasure, whereas an abnormal secretion of DA leads to Parkinson disease, bipolar disorder, agitation, mania, drugs, and alcohol abuse [Murray, 2019]. The detection of DA by electrochemical techniques is searched for its good response and reliability [Cernat et al., 2020; Lavanya et al., 2018]. Thereby, the new NO_2 and dopamine sensors based on hydrochar are surely of high technological value and may add more value to orange peels waste.

3.2 Experimental

3.2.1 Hydrochar preparation

The general preparation procedure of hydrochar via hydrothermal carbonization of orange peels here followed is illustrated in Scheme 3.1.

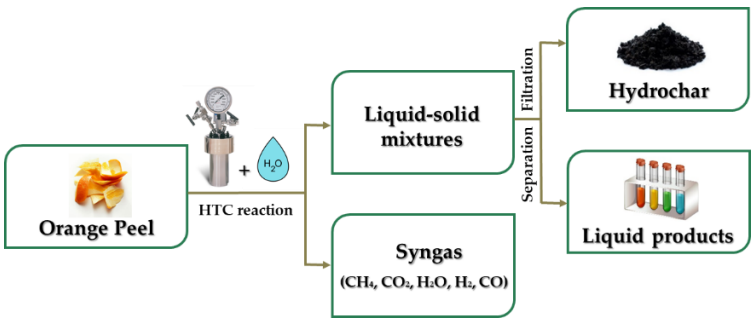

Scheme 3.1. Schematic representation of preparation of hydrochar via hydrothermal carbonization (HTC) of orange peels waste.

HTC tests were performed in a 300 ml stainless steel autoclave (series 4540 Parr Instrument Company, IL, USA), under autogenous pressure and air atmosphere. The vessel was charged with 20 g of OPW, then deionized water was added to achieve a solid-liquid mass ratio of 1:2.5, and finally, the reactor was heated at the reaction temperature (180-300 °C), continuously monitored through a thermocouple fixed into the autoclave and connected to the reactor controller, within the duration of the test. The residence time, after reaching the reaction temperature, was set at 60 min at a stirring speed of 600 rpm. Then, the HTC solid and liquid products were separated by vacuum filtration, with a Buchner funnel and filter paper. The solid hydrochar was sequentially washed with warm distilled water and finally dried overnight at 100 °C. The so obtained hydrochar samples are hereafter named HC180, HC210, HC240, HC270, and HC300.

3.2.2 Characterization

Fourier transform infrared (FTIR) spectra were registered using a Perkin Elmer Spectrum 100 spectrometer, equipped with an universal ATR sampling accessory. Spectra were recorded at room temperature from 4000 to 600 cm^{-1} and with a resolution of 4.0 cm^{-1}, without any preliminary treatment. The morphology of hydrochar samples was investigated using a Zeiss 1540XB FE SEM (Zeiss, Germany) instrument operating at 10 kV. The crystalline structure of synthesized materials was investigated using X-ray powder diffraction (XRD) employing a Bruker D8 Advance A 25 X-ray diffractometer operating at 40 kV and in the range 20–80°(2-theta), with an increasing rate of 0.01°/s. BET surface area and porosity of the samples were evaluated by nitrogen adsorption and desorption isotherms carried out at 77 K by a Quantachrome® ASiQwin™ instrument (Anton Paar Companies, Graz, Austria). Thermal stability in the air of investigated hydrochar samples was evaluated by thermogravimetry (TGA) conducted with TA Instruments SDTQ 600 (balance sensitivity: 0.1 mg). Samples (~15 mg) were heated at 20 °C/min from 100 °C

up to 1000 °C using a constant airflow rate (100 mL/min), after preliminary sample stabilization for 30 min at 100 °C to remove the eventually adsorbed water. Weight loss (%) was calculated.

3.2.3 Gas sensing tests

Sensor devices were fabricated by mixing hydrochar with water to obtain a paste and then printing it on alumina substrates (3 mm x 6 mm) supplied with interdigitated Pt electrodes and heater. Electrical measurements were carried out at the working temperature range from room temperature to 400 °C. Sensing tests were performed in a lab apparatus allowing to operate at a controlled temperature and to perform resistance measurements while varying the NO_2 concentration in the carrier stream. Measurements were performed under a dry synthetic air with a total stream of 100 sccm, collecting the sensors resistance data in the four-point mode using an Agilent 34970A multimeter. The reproducibility of data was confirmed by repeating the experiments at least three times. The gas response is defined as the ratio $S= R_0/R$, where R_0 represents the electrical resistance of the sensor in dry air and R its electrical resistance at different NO_2 concentrations. Dynamic characteristics, such as response time, τ_{res}, defined as the time required for the sensor resistance to reach 90% of the equilibrium value after the target gas is injected, and recovery time, τ_{rec}, taken as the time necessary for the sensor resistance to reach 90% of the baseline value in air, were also evaluated.

3.2.4 Electrochemical measurements

Screen-printed carbon electrodes (SPCEs) were purchased from DropSens, Spain. The platform used was DRP-100 (named SPCE), constituted of a 4-mm diameter carbon working electrode, a silver pseudo-reference electrode, and a carbon auxiliary electrode. In order to modify the bare SPCE, the hydrochar paste was directly printed onto the surface of the working electrode and left at room temperature to dry until any further use.

Electrochemical experiments were performed with a DropSens μStat 400 potentiostat/galvanostat. The electrochemical behavior of the prepared sensor was investigated by cyclic voltammetry (CV) in a 0.1 M Phosphate Buffered Saline (PBS) solution at pH 7, in presence and absence of dopamine (DA), in the 0.1 to 0.9 V potential region and at a scan rate of 50 mVs^{-1}. The reproducibility of the data was confirmed by repeating the experiments at least three times. Analyses, using the same concentration in any single run and three separate runs three times, were achieved to examine the intra-day and inter-day precisions, respectively.

The limit of detection (LOD) was obtained from the S/N= 3 and confirmed by the formula: LOD $3S_b/q$ where S_b is the standard deviation of the blank solution and q is the slope of the calibration plot.

3.3 Results and discussion

3.3.1 Morphological and microstructural characterization

Hydrochar samples prepared from OPW and water under autogenous pressure and air atmosphere at different reaction temperatures have been characterized in detail by different complementary techniques. Figure 3.1 shows the TGA analysis of the different hydrochar samples obtained under different hydrothermal temperatures.

Apart the HC180 sample, the decomposition of all samples in the air atmosphere takes place in 3 main different steps. Until 200 °C the weight loss (step I) is very low (less than 2%), likely due to the hydrophobic nature of the hydrochars, which hinders the absorption of large water quantity inside their structures. On increasing the temperature, a large weight loss (step II) starts, centered around 300 °C, and associated with the release of organic volatile

matters due to the decomposition of hemicellulose and cellulose. The successive step III is related to surface and bulk hydrochar oxidation.

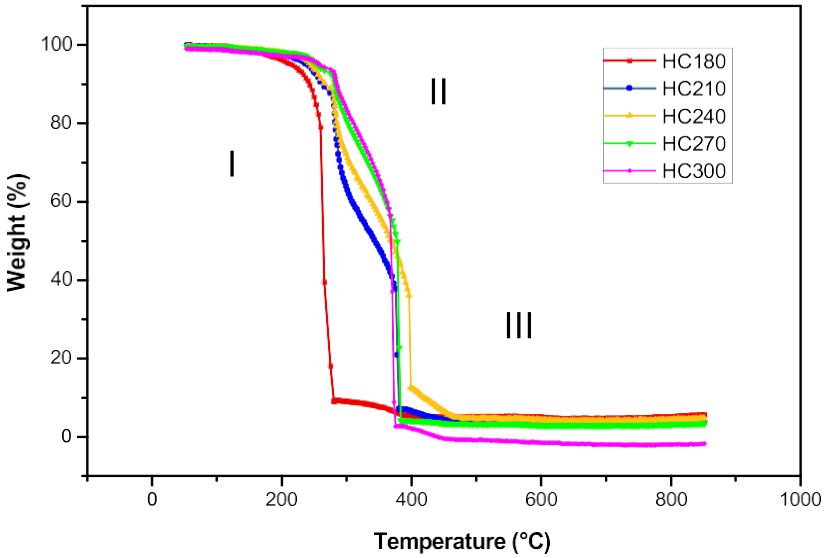

Figure 3.1. TGA curve in air of the hydrochar samples.

The different temperature ranges observed for steps II and III, suggest that hydrochar samples have a different composition, due to progressive loosing the organic components originally present in the orange peels and the surface groups of hydrochar formed at the different hydrothermal temperatures. Above 550 °C, a very small amount of residue (less than 3 %) was found.

The morphology of the hydrochar samples was investigated by using the SEM technique. The typical morphology observed for the HC210 (Figure 3.2a) and the HC300 (Figure 3.2b) is here shown. The morphology of samples prepared at lower hydrothermal temperature (180-210 °C) is not very dissimilar then that of the pectine-lignocellulose which constitutes the orange peels raw material [Rivas-Cantu et al., 2013]. On the other hand, at 300 °C, the material produced shows the presence of the characteristic hydrochar microspheres.

The elemental composition of hydrochar was evaluated by energy-dispersive spectroscopy (EDS) (Figure 3.2 c, d).

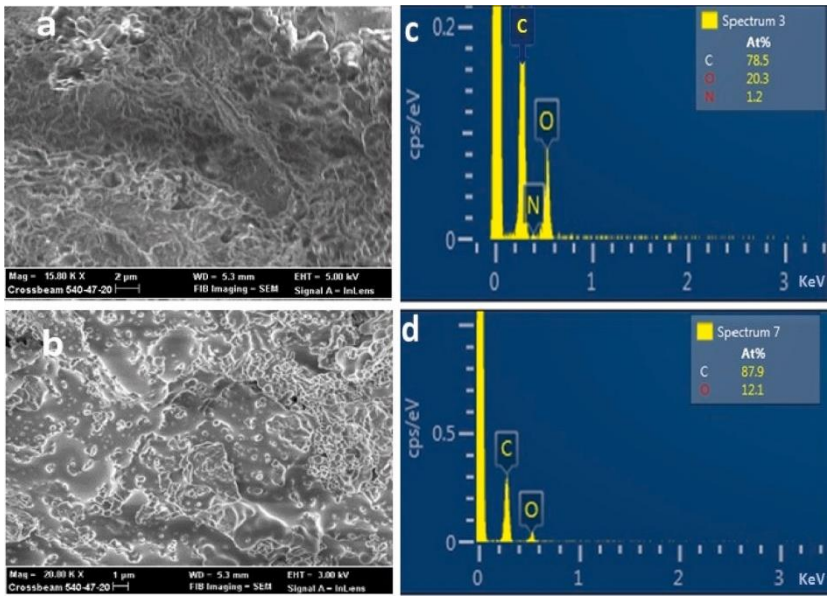

Figure 3.2. SEM of a) HC 210 and b) HC300; c) and d) EDS analyses. The inset shows the elemental analysis of these samples.

EDS spectra of HC210 reveals a high content of O (about 20%) because, at the lower temperature of the hydrothermal carbonization, many residual oxygenated groups remain on the surface. On increasing the hydrothermal temperature up to 300 °C a decrease of the oxygen content (12.1%), ascribed to the dehydration process from cellulose to hydrochar [Sevilla and Fuertes, 2009], was observed.

TGA and SEM-EDX indicate that the composition of hydrochars changes remarkably with the hydrothermal treatment temperature. In order to acquire deeper pieces of information also on the surface functional groups and their evolution with the hydrothermal treatment temperature, HC samples were investigated by XRD and FT-IR (see Figures 3.3 and 3.4).

The XRD evidences that hydrochars obtained at the lowest amorphous temperature have a combination of crystalline and (semi-crystalline)

structures (Figure 3.3). The reflections of crystalline cellulose at 16 and 22.6 are noted. Upon increasing the hydrothermal temperature, these peaks disappear, whereas new broad peaks, at around 22 and 44 2-theta, related to the turbostratic structure of the disordered carbon and coming from the (100) plane of graphite, appear and gradually increase in intensity.

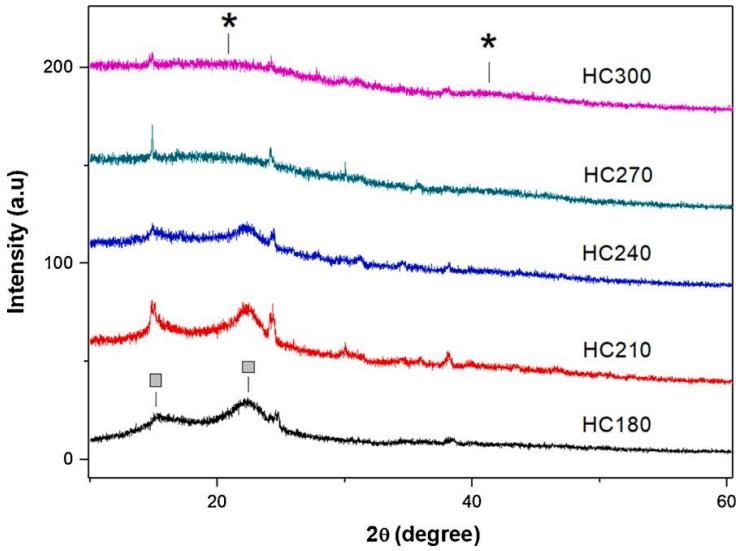

Figure 3.3. XRD of the prepared hydrochars.

The FT-IR gives helpful information about the surface groups present in the hydrochar samples (Figure 3.4). The characteristic bands of C=O at 1701 cm^{-1}, and C=C at 1608 cm^{-1}, reveal the presence of abundant aromatic rings, carbonyl, quinone, ester or carboxyl groups. The peak at 1431 cm^{-1} and the broadband at around 3300 cm^{-1} are attributable to the O–H bending of carboxylic acids and the O–H stretching of hydroxylic functionalities, respectively.

Aliphatic C–H bands are found at 3000–2800 cm^{-1}. The spectrum of HC180 reveals a peak at 1120-1050 cm^{-1}, possibly related to C-O band of the lignocellulose component of the orange peels still present. According to XRD data, this peak decreases in intensity on increasing the treatment temperature.

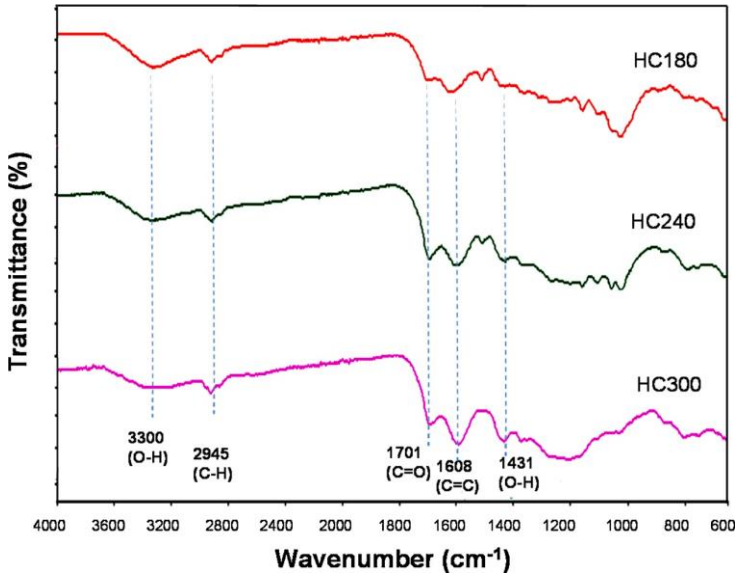

Figure 3.4. FT-IR of the prepared hydrochars.

The structural characteristics of hydrochar samples have been evaluated performing N_2 adsorption-desorption measurements. A typical adsorption isotherm, collected for the sample HC210, is reported, as an example, in Figure 3.5.

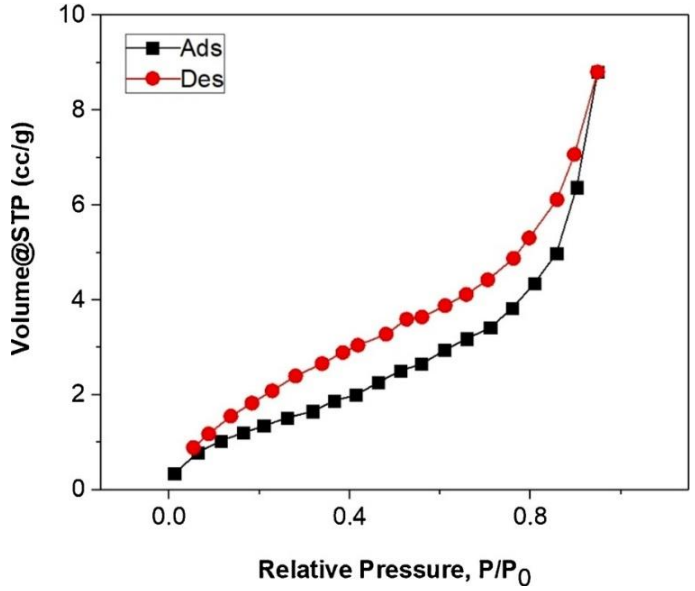

Figure 3.5. N_2 adsorption-desorption isotherm for the HC210 sample.

A hysteresis loop is clearly seen that, according to the current IUPAC classification, is classified within the IV category type [Rouquerol et al., 1994].

A summary of the structural properties of the hydrochar samples derived by N_2 adsorption-desorption isotherms such as BET surface area, pore volume, and radius are reported in Table 3.1. Values obtained for HC samples are in fair agreement with other hydrochars prepared in similar experimental conditions [Sevilla and Suertes, 2009b]. The HC performed at various treatment temperatures show that both the BET surface area and pore volume increase (about 3–4 four-time) on going from 180 to 300 °C.

Table 3.1. Structural properties of the hydrochar samples.

Sample	B.E.T. S.A (m^2/g)	Pore volume (cc/g)	Pore radius Dv(r) (Å)
HC 180	4.9	0.009	17.9
HC 210	5.5	0.008	20.4
HC 240	7.7	0.010	17.6
HC 270	9.1	0.011	17.8
HC 300	18.4	0.029	22.4

3.3.2 Electrical and electrochemical characterization

Hydrochar samples were then characterized in order to evaluate their electrical and electrochemical characteristics, performing the experiments with the same conductometric and electrochemical platforms used for the successive sensing experiments. These have been described in the experimental section, whereas further details can be found in previous papers [Neri et al., 2008; Ansjafi et al., 2019].

First of all the electrical properties of hydrochar samples have been evaluated. HC obtained at lower hydrothermal temperature (i.e. HC180, HC210, HC240, and HC270) display a high resistance, undetectable by our instrumentation. Only for the HC300 sample, we have obtained acceptable

resistance values, compatible with the practical use. Figure 3.6a shows the electrical resistance of the HC300 sample in nitrogen at different temperatures. As expected for a semiconductor, the electrical resistance decreases on increasing the temperature, in the range of 50–250 °C. The resistance in air, measured at 100 °C, is in the range of Giga ohm, near the upper limit of the measurement of our instrumentation.

Lower temperatures were not practicable because of the very high resistance, while at a higher temperature the baseline resistance was found not stable exciting a continuous drift deriving from modification/ oxidation of the hydrochar surface. This means, practically, that the optimal temperature range for sensing operation of HC300-based conductometric platforms is around 100 °C. As the electrochemical properties regard, one of the most important characteristics to evaluate is the electron transfer rate at the interface between the analyte and the working electrode surface of the electrochemical platform. This has been evaluated by carrying out cyclic voltammetry (CV) tests with modified hydrochar screen-printed carbon electrodes (HC/SPCE) in presence of 10 mM of dopamine in a 0.1 M PBS (see Figure 3.6b). On the bare screen - printed carbon electrode (SPCE) a pair of weak redox peaks with a peak-to-peak separation (ΔEp) of 0.476 V was observed, indicating the sluggish electron transfer rate at the interface. On the modified hydrochar/SPCE, the redox peak currents of dopamine increases while the peak-to-peak separation decreases, suggesting that the hydrochar modification of the working electrode accelerates the electron transfer of DA on the electrode surface. In particular, HC300/SPCE shows the most significant increase in both current and decrease in peak-to-peak separation (ΔEp= 0.269 V).

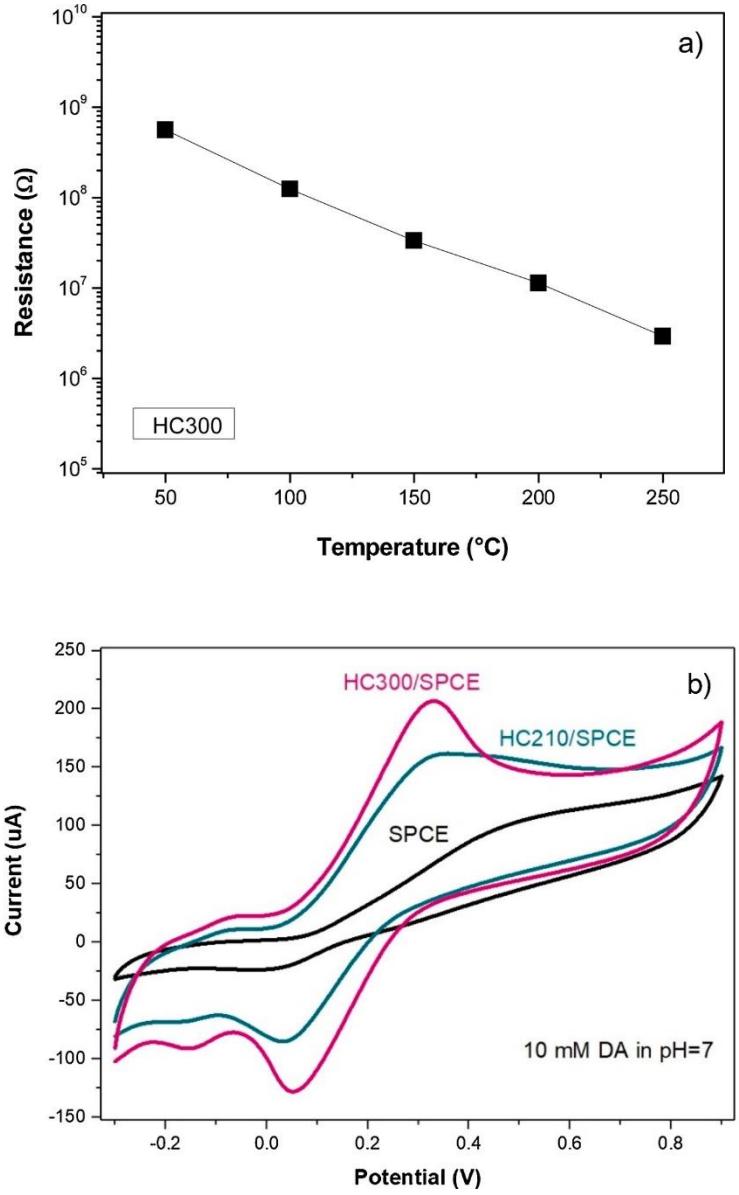

Figure 3.6. a) Electrical resistance of the HC300 sample in nitrogen as a function of temperature. b) CV of bare SPCE and hydrochars modified-SPCE.

3.3.3 Hydrochar for NO_2 sensing

Hydrochars-based conductometric sensors have been tested for the sensing of low concentration of NO_2 in the air as target gas. Conductometric sensors are used for the detection of toxic environmental pollutants, for the prevention of hazardous gas leaks, and so forth, attracting intense researches and marketing interest [Neri, 2015; Dey, 2018;

Korotcenkov and Cho, 2017]. The use of carbon nanostructures (CNTs, graphene) as a sensing layer has been one of the most important and rapidly growing topics in this field [Mao et al., 2014]. Currently, the search for new, alternative and facile strategies to achieve novel carbon structures for the fast and accurate detection of toxic gases, is ongoing.

As above described, for the HC300 sample, the electrical resistance is within the range of the measurement of our instrumentation. Thus, we could carry out sensing tests with the HC300 based conductometric sensor. Sensing tests were carried out at the mild temperature of 100 °C, where a stable baseline was observed. Even though TGA analyses (Figure 3.1) suggest good bulk stability for HC up to 250 °C in air, preliminary electrical tests show that baseline resistance drift starts just above 100 °C, due to surface oxidation. Figure 3.7 shows the dynamics characteristics of the sensor exposed to 2.8 ppm of NO_2 in the air at the temperature of 100 °C. The response and recovery times are in the order of 120 s and 450 s, respectively. In the presence of nitrogen dioxide, a decrease of the baseline resistance was observed. This behavior is typically ascribed to a semiconducting material with a p-type behavior, i.e. where the major electrical carriers are holes.

A remarkable variation of the baseline resistance was observed when pulses of NO_2 at different concentrations (from 2800 to 140 ppb) were passed over the sensor (Figure 3.8a). The resistance variation is reversible and its magnitude depends on the NO_2 concentration, making this hydrochar highly promising as a sensing element for gas sensors.

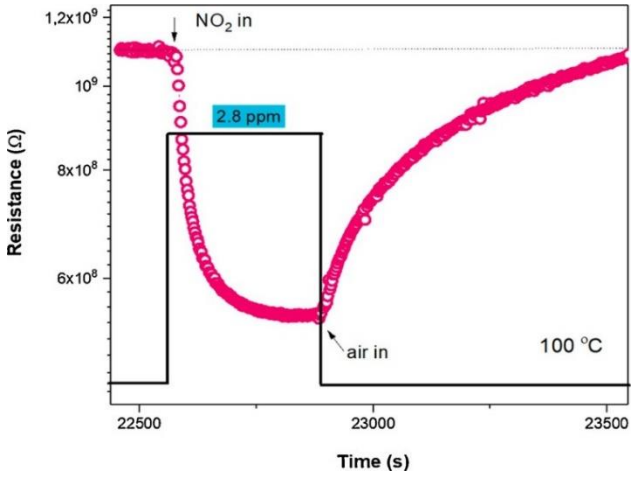

Figure 3.7. Response of the HC300-based conductometric sensor, at the operating temperature of 100 °C, to a pulse of 2.8 ppm of NO_2 in air.

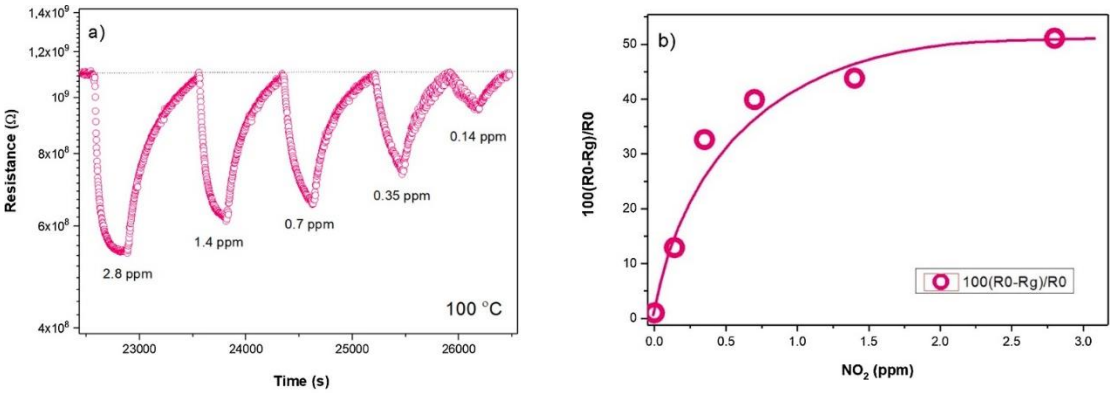

Figure 3.8. a) Transient response towards different concentrations of NO_2 for the HC300 sensor; b) calibration curve.

This behavior can be understood considering that the sensing mechanism of conductometric sensors is primarily governed by the chemical surface properties of the sensing material and its interaction with the target gas [Ji et al., 2019]. Many structural defects and functional groups on the carbon sensing layer can serve as adsorption sites [Travlou et al., 2015]. Gas adsorption modulates the energy band structure of the sensing layer leading to the variation of the energy band-gap and changes the density of states (DOS). However, a quantitative discussion on the

band structure modulation under gas adsorption regarding carbon-based gas sensors has been made only for the most simple and ordered carbon structures, i.e CNT and graphene [Hosseingholipourasl et al., 2020]. For the HC-based sensor, the surface oxygenate groups detected by FT-IR to be present on the hydrochar surface, are electron-withdrawing and promote holes in the valence band. This also explains the high baseline resistance in the air. Then, the interaction with NO_2, which is an oxidizing gas, would cause the depletion of holes from the valence band and hence the decrease of the material resistance [Hosseingholipourasl et al., 2020; Yamazoe and Shimanoe, 2008]. The calibration curve reported in Figure 3.8b highlights the high sensitivity of the sensor in the ppb range.

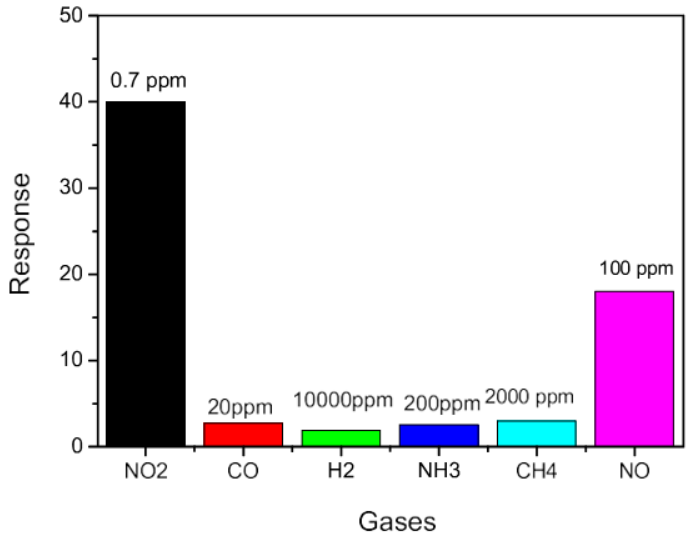

Figure 3.9. Response of the sensor to selected environmental pollutant gases.

In order to evaluate the selectivity of the sensor, the response to NO_2 was compared with the response obtained by testing other environmental pollutant gases (e.g., CO, NH_3, CH_4, H_2, and NO). As shown in Figure 3.9, the response of the sensor to 0.7 ppm of NO_2 is much higher than for the other gases investigated, except NO. demonstrating the good selectivity for these nitrogen oxide gases.

This aspect is very important for possible practical applications since NO_2 is a very toxic and hazardous environmental pollutant, present in the urban outdoor and indoor atmosphere in mixture with other potential interfering gases [Neri et al., 2013; Kumar et al., 2020].

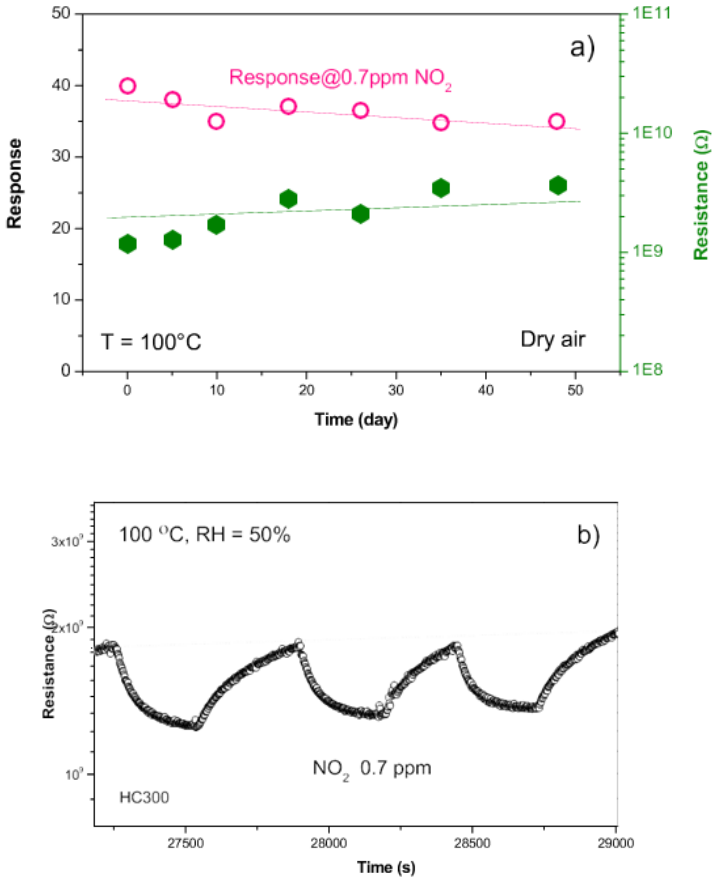

Figure 3.10. a) Sensor response evaluated for a long period; b) Response of the sensor to consecutive pulses of 0.7 ppm of NO_2.

Besides the selectivity, other characteristics are important for the gas sensor applicability, such as reproducibility, repeatability, stability, and negligible humidity interference. The sensor response was evaluated for more than 1 month (Figure 3.10a) and we found no significant change, suggesting that the stability of the sensors is good and suitable for a practical application.

The signal reproducibility was investigated by exposing the sensor to repeated consecutive pulses of 0.7 ppm of NO_2. The measurement reported in Figure 3.10b indicates that the response reproducibility of the fabricated hydrochar-based sensor is good.

In order to study the repeatability of the fabricated sensor, different sensors were fabricated and tested under identical conditions. The value of RSD associated with measurements with these sensors was found to be less than 10 %, a good result considering that no efforts have been made to optimize/standardize any step of the sensor fabrication.

The response of the sensor toward 0.7 ppm of NO_2 in dry and 50% relative humidity conditions was investigated at 100 ◦C and the results are presented in Figure 3.11. Only a slight increase of the resistance baseline (1.1 MΩ vs. 1.8 MΩ) is observed while the little change in the response to NO_2 (40 vs. 33) was observed in the opposite direction (a decrease).

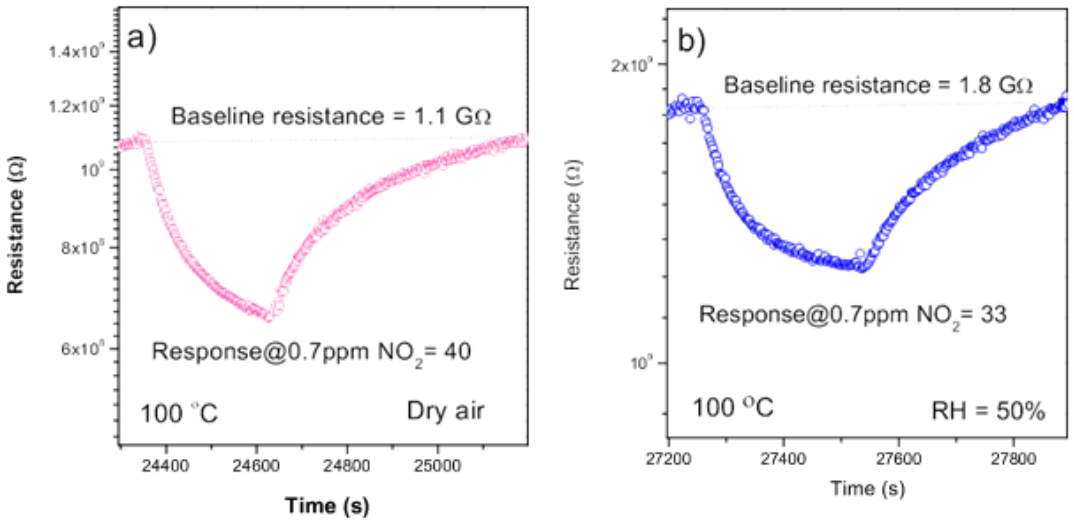

Figure 3.11. a) Response of the sensor toward 0.7 ppm of NO_2 in a) dry and b) 50 % relative humidity conditions.

From this result we infer, then, that humidity does not influence remarkably the response of the sensors towards NO_2. Tentatively it is possible

to explain this issue considering that in the sample calcined at 300 °C the amount of oxygen-containing functional groups decreases while the carbon aromaticity structure increases, thereby rendering the sensing layer of the HC300 sensor highly hydrophobic and repelling water [Liu et al., 2013]. It is noteworthy to mention that, to our knowledge, the developed device represents the first example of a conductometric gas sensor based on the use of hydrochar obtained for the agro-industrial biomass waste, with performances comparable or also better than the previous state of the art NO_2 sensors based on other carbon materials (see Table 3.2).

3.3.4 Hydrochar as an electrochemical sensor for DA

Carbon materials are also widely used for the design of electrodes in electroanalytical chemistry because of their relatively wide potential windows in aqueous media, low cost, low background current, and relative chemical inertness in most electrolyte solutions resulting in very appreciate for biomolecules sensing [Ramachandran et al., 2019; Lounasvuori et al., 2018; Elsworth and Roth, 2009; Ou et al., 2019]. Dopamine is one of the most important catecholamines, a class of biomolecules that are significant neurotransmitters and play a vital role in the central nervous system [Huang at al., 2020]. Severe neurological diseases such as Parkinson's and schizophrenia are often caused by low levels of DA. Therefore, it is important to determine the concentration of this neurochemical sub- stance in the clinic laboratory [Huang at al., 2020; Zhao et al., 2005; Yue et al., 2012; Kim et al., 2017]. The electroanalytical quantification of dopamine was carried out with HC300/SPCE, through the Linear Sweep Voltammetry (LSV) technique (Figure 3.12a).

Table 3.2. Comparison of the NO_2 sensing performances of carbon-based conductometric sensors.

Sensing material	Limit of Detection	Minimum measured conc.	Response[1] at minimum conc.	Operating temperature	Measurement range [ppm]	UV light	Ref.
SWCNTs[2]	0.086 ppm	0.1 ppm	100%	50 °C	0.1-10	no	[Sacco et al., 2020]
Graphene oxide	0.21 ppb	1 ppm	10%	150 °C	1-9	no	[Park et al., 2020]
Aligned SWCNTs	-	0.5 ppm	7%	RT[3]	0.5-10	yes	[Chauhan et al., 2019]
Sulfur doped graphene	-	500 ppt	0.2%	RT	0.5-100	no	[Guo and Li, 2018]
3D rGO[4]	186 ppb	1 ppm	≈ 0.1%	22 °C	1.8	no	[Wu et al., 2015]
rGO	-	5 ppm	37%	RT	5-100	no	[Han et al., 2019]
CVD Graphene	0.04 ppm	1 ppm	3%	RT	1-20	yes	[Yan et al, 2019]
Hydrochar	50 ppb	0.14 ppm	13%	100 °C	0.14-2.8	no	This work

Response (R) is defined as $R= 100*|S_g-S_a|/S_a$, where S_a and S_g are recorded signal in the absence and presence of target gas, respectively.

[2] Single-wall carbon nanotubes; 3Room temperature;4 Reduced Graphene Oxide.

The response to DA in the range of 0–1000 µM is shown in Figure 3.12b. It follows a linear trend, expressed by the linear regression equation: Ip(µA) = 25.40+ 45.14 *(mM)(mM), R^2 = 0.983. The limit of detection (LOD) was obtained from S/N=3 and it is as low as 180 nM, demonstrating that hydrochar contributes to the improved electrochemical detection of DA, likely due to the presence of a high number of electroactive sites (e.g. oxygenate surface groups) on the surface of hydrochar acting as the active sites.

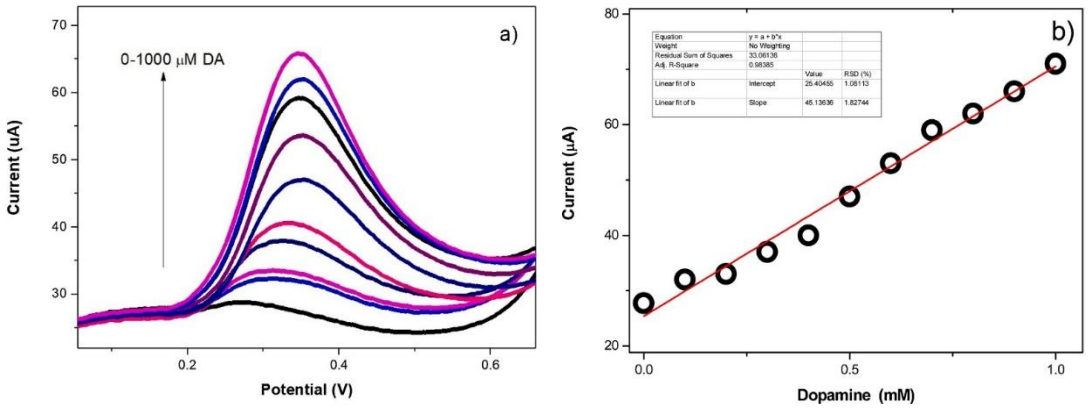

Figure 3.12. Electrochemical tests carried out on modified hydrochar/SPCE. a) LSV on HC300/SPCE electrode with different concentration of DA; b) Calibration curve. Scan rate was 50 mV/s. The inset provide detail on the statistical analysis made.

Therefore, hydrochar may be a strong competitor, with similar or better electrochemical properties, in contrast to other carbon materials (e.g., CNTs graphene), with the advantages deriving by a simple, low-cost and green preparation process (see Table 3.3).

It is also important to mention that although carbon materials, obtained by pyrolysis at high temperatures from biomass or organic wastes (bio-char), have been already reported as electrodes for electrochemical sensing, no studies were so far reported concerning monitoring neurotransmitter compounds such as DA [Ferreira et al., 2018].

Table 3.3. Comparison of performances of carbon-based electrochemical sensors for dopamine sensing.

Electrode	Linear range	Detection limit	Ref.
MWCNT/GC	1-100 µM	0.1 µM	[Zhao et al., 2005]
Mesoporous carbon nanofiber-modified pyrolytic graphite electrode (MCNF/PGE)	0.05-30 µM	0.02 µM	[Yue et al., 2012]
Activated graphene-Nafion modified glassy carbon electrode (AG-NA/GCE)	0.05-35 µM	0.3 µM	[Kim et al.,2017]
Carbon-nanofiber-modified carbon paste electrode (CNF-CPE)	0.04-5.6 µM	0.04 µM	[Liu et al., 2008]
Single-walled carbon nanohorn modified glassy carbon electrode (SWCNH-modified GCE)	0.2-3.8 µM	0.06 µM	[Zhu et al., 2009]
MWCNT /graphene oxide-GCE	0.2-400 µM	0.2 µM	[Cheemalapati et al., 2013]
Au/RGO/GCE	6.8-41 µM	1.4 µM	[Wang et al., 2014]
PANI-GO/GCE	2–18 µM	0.5 µM	[Manivel et al., 2013]
Graphene nano-sheets (GNSs)	4-52 µM	0.6 µM	[Liu et al., 2012]
Graphene nanosheets (GNS)/ carbon paste electrode (CPE)	2-1000 µM	0.8 µM	[Bagherzadeh and Heydari, 2013]
Multilayer graphene nanoflake films (MGNFs)	1-50 mM	0.1 mM	[Shang et al., 2008]
rGO/SPCE	0.2-80.0 µM and 120.0-500 µM	0.4 µM	[Kanyong et al., 2016]
Hydrochar/SPCE	0-1000 µM	0.1 µM	This work

3.4 Conclusion

In this chapter, various hydrochar samples were successfully prepared via a simple hydrothermal method from orange peel waste. Their electrical and electrochemical properties depend on the hydrothermal treatment temperature, as a consequence of the different surface characteristics observed. Hydrochar samples prepared at 300 °C (HC300) exhibit the best electrical properties and therefore are used for fabricating high performance conductometric sensors for the monitoring of NO_2. These results represent the first example of a hydrochar-based conductometric gas sensor that can successfully be utilized for the environmental monitoring of NO_2 pollutants. The electrochemical characteristics of HC300 hydrochar were also exploited for the fabrication of a high-performance screen-printed electrochemical sensor. Experiments have demonstrated that the hydrochar modified-SPCE presents an enhanced dopamine response compared to the SPCE reference one. The improved electroanalytical properties could be beneficial for other electrochemical sensing applications. Obtained results might open up the opportunity to use the low-cost and waste material from the citrus industry for the green production of hydrochars with outstanding electrical and electrochemical properties and its utilization in chemical sensors.

References

Anajafi, Z.; Naseri, M.; Marini, S.; Espro, C.; Iannazzo, D.; Leonardi, S.G.; Neri, G. $NdFeO_3$ as a new electrocatalytic material for the electrochemical monitoring of dopamine. *Anal. Bioanal. Chem.* **2019**, *411*, 7681-7688.

Asadian, E.; Ghalkhani, M.; Shahrokhian, S. Electrochemical sensing based on carbon nanoparticles: a review. *Sens. Actuators B Chem.* **2019**, *293*, 183-209.

Babeker, T.M.A.; Chen, Q. Heavy Metal Removal from Wastewater by Adsorption with Hydrochar Derived from Biomass: Current Applications and Research Trends. *Curr. Pollution. Rep.* **2021**, *7*, 54-71.

Bagherzadeh, M.; Heydari, M. Electrochemical detection of dopamine based on pre-concentration by graphene nanosheets. *Analyst* **2013**, *138(20)*, 6044-6051.

Bezzon, V.D.N.; Montanheiro, T.L.A.; de Menezes, B.R.C.; Ribas, R.G.; Righetti, V.A.N.; Rodrigues, K. F.; Thim, G.P. Carbon nanostructure-based sensors: a brief review on recent advances, *Adv. Mater. Sci. Eng.* **2019**, 4293073.

Calabrò, P.S.; Fazzino, F.; Folino, A.; Paone, E.; Komilis, D. Semi-continuous anaerobic digestion of orange peel waste: effect of activated carbon addition and alkaline pretreatment on the process. *Sustainability* **2019**, *11(12)*, 3386.

Calabrò, P.S.; Paone, E.; Komilis, D. Strategies for the sustainable management of orange peel waste through anaerobic digestion. *J. Environ. Manage.* **2018**, *212*, 462-468.

Cernat, A.; Ştefan, G.; Tertis, M.; Cristea, C.; Simon, I. An overview of the detection of serotonin and dopamine with graphene-based sensors. *Bioelectrochemistry* **2020**, 107620.

Chauhan, S.S.; Kumar, D.; Chaturvedi, P.; Rahman M.R. Highly sensitive and stable NO_2 gas sensors based on SWNTs with exceptional recovery time. *IEEE Sens. J.* **2019**, *19*, 11775-11783.

Cheemalapati, S.; Palanisamy, S.; Mani, V.; Chen, S.M. Simultaneous electrochemical determination of dopamine and paracetamol on multiwalled carbon nanotubes/graphene oxide nanocomposite-modified glassy carbon electrode. *Talanta* **2017**, *117*, 297-304.

Dey, A. Semiconductor metal oxide gas sensors: a review. *Mat. Sci. Eng. B* **2018**, *229*, 206-217.

Elhaes, H.; Fakhry, A.; Ibrahim, M. Carbon nano materials as gas sensors. *Mater. Today Proc.* **2016**, *3(6)*, 2483-2492.

Elsworth, J.D.; Roth, R.H. Encyclopedia of Neuroscience, Academic Press **2009**, 539-547.

Fang, J.; Zhan, L.; Ok, Y.S.; Gao, B. Minireview of potential applications of hydrochar derived from hydrothermal carbonization of biomass, *J. Ind. Eng. Chem.* **2018**, *57*, 15-21.

Fazzino, F.; Mauriello, F.; Paone, E.; Sidari, R.; Calabrò, P.S. Integral valorization of orange peel waste through optimized ensiling: lactic acid and bioethanol production. *Chemosphere* **2021**, *271*, 129602.

Ferreira, P.A.; Backes, R.; Martins, C.A.; de Carvalho, C.T.; da Silva, R.A.B. Biochar: a low-cost electrode modifier forelectrocatalytic, sensitive and selective detection of similar organic compounds. *Electroanalysis* **2018**, *30*, 2233-2236.

Giampiccolo, A.; Tobaldi, D.M.; Leonardi, S.G.; Murdoch, B.J.; Seabra, M.P.; Ansell, M.P.; Neri, G.; Ball, R.J. Sol gel graphene/TiO_2 nanoparticles for the photocatalytic-assisted sensing and abatement of NO_2. *Appl. Catal. B* **2019**, *243*, 183-194.

Gopinath, K.P.; Vo, D.V.N.; Prakash, D.G.; Joseph, A.A.; Viswanathan, S.; Arun, J. Environmental applications of carbon-based materials: a review. *Environ. Chem. Lett.* **2020**, 1-26.

Gumina, B.; Mauriello, F.; Pietropaolo, R.; Galvagno, S.; Espro, C. Hydrogenolysis of sorbitol into valuable C3-C2 alcohols at low H_2 pressure promoted by the heterogeneous Pd/Fe_3O_4 catalyst. *Mol. Catal.* **2018**, *446*, 152-160.

Guo, L.; Li, T. Sub-ppb and ultra-selective nitrogen dioxide sensor based on sulfur doped graphene. *Sens. Actuators B Chem.* **2018**, *255*, 2258-2263.

Han, M.; Kim, J.K.; Lee, J.; An, H.K.; Yun, J.P.; Kang, S.W.; Jung, D. Room-temperature hydrogen-gas sensor based on carbon nanotube yarn. *J. Nanosci. Nanotechnol.* **2020**, *20(7)*, 4011-4014.

Han, T.; Gao, S.; Wang, Z.; Fei, T.; Liu, S.; Zhang, T. Investigation of the effect of oxygen-containing groups on reduced graphene oxide-based room-temperature NO_2 sensor. *J. Alloys Comp.* **2019**, *801*, 142-150.

Hosseingholipourasl, A.; Syed Ariffin, S.H.; Al-Otaibi, Y.D.; Akbari, E.; Hamid, F.K.H.; Koloor, S.S.R.; Petru, M. Analytical approach to study sensing properties of graphene Based Gas Sensor. *Sensors* **2020**, *20*, 1506.

Huang, Q.; Lin, X.; Tong, L.; Tong, Q.-X. Graphene quantum dots/multiwalled carbon nanotubes composite-based electrochemical sensor for detecting dopamine release from living cells. *ACS Sustain. Chem. Eng.* **2020**, *8*, 1644-1650.

Hung, C.M.; Van Duy, N.; Van Quang, V.; Van Toan, N.; Van Hieu, N.; Hoa, N.D. Facile synthesis of ultrafine rGO/WO_3 nanowire nanocomposites for highly sensitive toxic NH_3 gas sensors. *Materials Research Bulletin* **2020**, *125*, 110810.

Jagdale, P.; Ziegler, D.; Rovere, M.; Tulliani, J.M.; Tagliaferro, A. Waste coffee ground biochar: a material for humidity sensors. *Sensors* **2019**, *19*, 801.

Ji, H.; Zeng, W.; Li, Y. Gas sensing mechanisms of metal oxide semiconductors: a focus review. *Nanoscale* **2019**, *11*, 22664-22684.

Kanyong, P.; Rawlinson, S.; Davis, J. A voltammetric sensor based on chemically reduced graphene oxide-modified screen-printed carbon electrode for the simultaneous analysis of uric acid, ascorbic acid and dopamine. *Chemosensors* **2016**, *4*, 25.

Kim, D.; Lee, S.; Piao, Y. Electrochemical determination of dopamine and acetaminophen using activated graphene-Nafion modified glassy carbon electrode. *J. Electroanalytical Chem.* **2017**, *794*, 221-228.

Korotcenkov, G.; Cho, B.K. Metal oxide composites in conductometric gas sensors: achievements and challenges. *Sens. Actuators B Chem.* **2017**, *244*, 182-210.

Kumar, R.; Jenjeti, R.N.; Sampath, S. Two-Dimensional, few-layer $MnPS_3$ for selective NO_2 gas sensing under ambient conditions. *ACS Sens.* **2020**, *5*, 404-411.

Lavanya, N.; Leonardi, S.G.; Sekar, C.; Ficarra, S.; Galtieri, A.; Tellone, E.; Neri, G. Detection of catecholamine neurotransmitters by nanostructured SnO_2-based electrochemical sensors: a review of recent progress. *Mini. Org. Chem.* **2018**, *15*, 382-388.

Lee, S.W.; Lee, W.; Hong, Y.; Lee, G.; Yoon, D.S. Recent advances in carbon material-based NO_2 gas sensors. *Sens. Actuators B Chem.* 2018, *255*, 1788-1804.

Liang, T.; Liu, R.; Lei, C.; Wang, K.; Li, Z.; Li, Y. Preparation and test of NH_3 gas sensor based on single-layer graphene film. *Micromachines* **2020**, *11(11)*, 965.

Liu, S.Q.; Sun, W.H.; Hu, F.T. Graphene nano sheet-fabricated electrochemical sensor for the determination of dopamine in the presence of ascorbic acid using cetyltrimethylammonium bromide as the discriminating agent. *Sens. Actuators B: Chem.* **2012**, *173*, 497-504.

Liu, Y.; Huang, J.; Hou, H.; You, T. Simultaneous determination of dopamine, ascorbic acid and uric acid with electrospun carbon nanofibers modified electrode. *Electrochem. commun.* **2008**, *10(10)*, 1431-1434.

Liu, Z.; Augustine Quek; Hoekman, S.K.; Balasubramanian, R. Production of solid biochar fuel from waste biomass by hydrothermal carbonization. *Fuel* **2013**, *103*, 943-949.

Lounasvuori, M.M.; Kelly, D.; Foord, J.S. Carbon black as low-cost alternative for electrochemical sensing of phenolic compounds. *Carbon* **2018**, *129*, 252-257.

Maniscalco, M.P.; Volpeand, M.; Messineo, A. Hydrothermal carbonization as a valuable tool for energy and environmental applications: a review. *Energies* **2020**, *13*, 4098.

Manivel, P.; Dhakshnamoorthy, M.; Balamurugan, A.; Ponpandian, N.; Mangalaraj, D.; Viswanathan, C. Conducting polyaniline-graphene oxide fibrous nanocomposites: preparation, characterization and simultaneous electrochemical detection of ascorbic acid, dopamine and uric acid. *RSC Adv.* **2013**, *3(34)*, 14428-14437.

Mao, S.; Lu, G.; Chen, J. Nanocarbon-based gas sensors: progress and challenges. *Mater. Chem. A* **2014**, *2*, 5573-5579.

Murray, T.F. Biogenic amine transmitters: acetylcholine, norepinephrine, and dopamine. *Veterinary Psychopharmacology* **2019**, 29-42.

Neri, G.; First fifty years of chemoresistive gas sensors. *Chemosensors* **2015**, *3*, 1-20.

Neri, G.; Bonavita, A.; Micali, G.; Rizzo, G.; Callone, E.; Carturan, G. Resistive CO gas sensors based on In_2O_3 and InSnOx nanopowders synthesized via starch-aided sol-gel process for automotive applications. *Sens. Actuators B: Chem.* **2008**, *132*, 224-233.

Neri, G.; Leonardi, S.G.; Latino, M.; Donato, N.; Baek, S.; Conte, D.E.; Russo, P.A.; Pinna, N. Sensing behavior of SnO_2/reduced graphene oxide nanocomposites toward NO_2. *Sens. Actuators B Chem.* **2013**, *179*, 61-68.

Ou, Y.; Buchanan, A.M.; Witt, C.E.; Hashemi, P. Frontiers in electrochemical sensors for neurotransmitter detection: towards measuring neurotransmitters as chemical diagnostics for brain disorders. *Anal. Methods* 2019, *11*, 2738-2755.

Park, J.; Kim, Y.; Park, S.Y.; Sung, S.J.; Jang, H.W.; Park, C.R. Band gap engineering of graphene oxide for ultrasensitive NO_2 gas sensing. *Carbon* **2020**, *159*, 175-184.

Pistone, A.; Espro, C. Current trends on turning biomass wastes into carbon materials for electrochemical sensing and rechargeable battery applications. *Curr. Opin. Green Sustain. Chem.* **2020**, *26*, 100374.

Ramachandran, R.; Chen, T.-Wei; Chen, S.-Ming; Baskar, T.; Kannan, R.; Elumalai, P.; Raja, P.; Jeyapragasam, T.; Dinakaran, K.; Kumar, G.G. A review of the advanced developments of electrochemical sensors for the detection of toxic and bioactive molecules. *Inorg. Chem. Front.* **2019**, *6*, 3418-3439.

Randviir, E.P.; Kanou, O.; Liauw, C.M.; Miller, J.M.; Andrews, H.G.; Smith, G.C. The physicochemical investigation of hydrothermally reduced textile waste and application within carbon-based electrodes. *RSC Adv.* **2019**, *9*, 11239-11252.

Rivas-Cantu, R.C.; Jones, K.D.; Mills, P.L. A citrus waste-based biorefinery as a source of renewable energy: technical advances and analysis of engineering challenges. *Waste Manag. Res.* **2013**, *31*, 413-420.

Rouquerol, J.; Avnir, D.; Fairbridge, C.W.; Everett, D.H.; Haynes, J.M.; Pernicone, N.; Ramsay, J.D.F.; Sing, K.S.W.; Unger, K.K. Recommendations for the characterization of porous solids, IUPAC commission on colloid and surface chemistry. *Pure Appl. Chem.* **1994**, *66*, 1739-1758.

Sacco, L.; Forel, S.; Florea, I.; Cojocaru, C.-S. Ultra-sensitive NO_2 gas sensors based on single-wall carbon nanotube field effect transistors: monitoring from ppm to ppb level. *Carbon* **2020**, *157*, 631-639.

Sevilla, M.; Fuertes, A.B. The production of carbon materials by hydrothermal carbonization of cellulose. *Carbon* **2009**, *47*, 2281-2289.

Sevilla, M.; Fuertes, A.B. Chemical and structural properties of carbonaceous products obtained by hydrothermal carbonization of saccharides. *Chem. Eur. J.* **2019**, *15*, 4195-4203.

Shang, N.G.; Papakonstantinou, P.; McMullan, M.; Chu, M.; Stamboulis, A.; Potenza, A.; Dhesi, S.S.; Marchetto, H. Catalyst-free efficient growth, orientation and biosensing properties of multilayer graphene nanoflake films with sharp edge planes. *Adv. Funct. Mater.* **2008**, *18*, 3506-3514.

Travlou, N.A.; Seredych, M.; Rodríguez-Castellón, E.; Bandosz, T.J. Activated carbon-based gas sensors: effects of surface features on the sensing mechanism. *J. Mater. Chem. A* **2015**, *3*, 3821-3831.

Torrinha, A.; Oliveira, T.M.; Ribeiro, F.W.; Correia, A.N.; Lima-Neto, P.; Morais, S. Application of nanostructured carbon-based electrochemical (bio) sensors for screening of emerging pharmaceutical pollutants in waters and aquatic species: a review. *Nanomaterials* **2020**, *10(7)*, 1268.

Xiao, K.; Liu, H.; Li, Y.; Yi, L.; Zhang, X.; Hu, H.; Yao, H. Correlations between hydrochar properties and chemical constitution of orange peel waste during hydrothermal carbonization. *Bioresour. Technol.* **2018**, *265*, 432-436.

Yaah, V.B.K.; Zbair, M.; de Oliveira, S.B.; Ojala, S. Hydrochar-derived adsorbent for the removal of diclofenac from aqueous solution. *Nanotechnol. Environ. Eng.* **2021**, *6(1)*, 1-12.

Yamazoe, N.; Shimanoe, K. Theory of power laws for semiconductor gas sensors. *Sens. Actuators B Chem.* **2008**, *128*, 566-573.

Yan, X.; Wu, Y.; Li, R.; Shi, C.; Moro, R.; Ma, Y.; Ma, L. High-performance UV-assisted NO_2 sensor based on chemical vapor deposition graphene at room temperature. *ACS Omega* **2019**, *4*, 14179-14187.

Yue, Y.; Hu, G.; Zheng, M.; Guo, Y.; Cao, J.; Shao, S.; A mesoporous carbon nanofiber-modified pyrolytic graphite electrode used for the simultaneous determination of dopamine, uric acid, and ascorbic acid. *Carbon* **2012**, *50(1)*, 107-114.

Zhang, S.; Sheng, K.; Yan, W.; Liu, J.; Shuang, E.; Yang, M.; Zhang, X. Bamboo derived hydrochar microspheres fabricated by acid-assisted hydrothermal carbonization. *Chemosphere* **2021**, *263*, 128093.

Zhang, X.; Gao, B.; Fang, J.; Zou, W.; Dong, L.; Cao, C.; Zhang, J.; Li, Y.; Wang, H. Chemically activated hydrochar as an effective adsorbent for volatile organic compounds (VOCs), *Chemosphere* **2019**, *218*, 680-686.

Zhao, Y.; Gao, Y.; Zhan, D.; Liu, H.; Zhao, Q.; Kou, Y.; Shao, Y.; Li, M.; Zhuang, Q.; Zhu, Z. Selective detection of dopamine in the presence of ascorbic acid and uric acid by a carbon nanotubes-ionic liquid gel modified electrode. *Talanta* **2005**, *66(1)*, 51-57.

Zhu, S.; Li, H.; Niu, W.; Xu, G. Simultaneous electrochemical determination of uric acid, dopamine, and ascorbic acid at single-walled carbon nanohorn modified glassy carbon electrode. *Biosens. Bioelectron.* **2009**, *25(4)*, 940-943.

Wang, C.; Du, J.; Wang, H.; Zou, C.E.; Jiang, F.; Yang, P.; Du, Y. A facile electrochemical sensor based on reduced graphene oxide and Au nanoplates modified glassy carbon electrode for simultaneous detection of ascorbic acid, dopamine and uric acid. *Sens. Actuators B: Chem.* **2014**, *204*, 302-309.

Wu, J.; Tao, K.; Miao, J.; Norford, L.K. Improved selectivity and sensitivity of gas sensing using a 3D reduced graphene oxide hydrogel with an integrated microheater. *ACS Appl. Mater. Interfaces* **2015**, *7*, 27502-27510.

Chapter 4

Catalytic Upgrading of Orange Peel Waste Derived Molecules

4.1 Introduction

In this chapter we present same results of the catalytic upgrading of levulinates and d-limonene that are building block molecules obtainable from the hydrothermal carbonization of the orange peel waste.

d-Limonene is among the most promising renewable feedstocks for modern biorefineries. In this regard, limonene can be used as a substrate for the sustainable production of p-cymene, a fine chemical intermediate in several industrial chemical processes [Martin-Luengo et al., 2010; Buhl et al., 1999]. The development of new green pathways for p-cymene production from limonene is an excellent alternative to the traditional method of obtaining p-cymene via Friedel-Crafts alkylation of toluene with isopropene. The most recent investigations so far found that supercritical alcohols favoring the

catalytic processes by enriching both the solubility and the diffusivity are the most interesting solvents. In almost all cases, p-cymene, γ-terpinene, α-terpinene and terpinolene are obtained. At the same time, the dehydrogenation process of limonene into p-cymene leads to hydrogen as a co-product that can be used for the reductive upgrading of other bio-based molecules opening new perspectives in its use as renewable H-donor solvent [Tabanelli et al., 2019; Mauriello et al., 2018; Gumina et al., 2018].

However, most of these works are performed in the liquid phase and batch conditions. Catalysis under continuous flow usually offers considerable advantages including (i) a more selective production of a given reaction product; the possibility to afford a catalytic test for a larger time on stream; (ii) fewer wastes production; (iii) minor separation problems and (iv) simpler scaling up processes.

The results obtained show that, under batch conditions, the production of p-cymene increases with increasing reaction temperature from 200 to 300 °C. Reactions conducted under continuous gas-flow conditions were found to be much more efficient showing excellent yields in GVL when EtOH was used as the reducing agent.

Levulinic acid (LA) is surely one of the most promising future building blocks of the bio-based chemical industry [Yan et al., 2015]. One of the most significant chemicals obtained from LA is certainly γ-valerolactone (GVL), commonly used as a flavoring agent in the food industry, as a green solvent, as an intermediate in fine chemicals synthesis, and as a starting material for the production of bio-based polymers and resins [Wright and Palkovits, 2012; Omoruyi et al., 2016]. GVL can be obtained either via the catalytic hydrogenation of LA into 4-hydroxyvaleric acid followed by cyclization or via the acid-catalyzed dehydration of LA to the α-angelica lactone and subsequent hydrogenation.

However, the reduction of LA to GVL under conventional conditions (liquid phase and batch conditions), involves the utilization of molecular hydrogen, working at high operating pressure (in the range 5-100 bar) in the presence of expensive noble metal-based catalysts.

Nevertheless, the use of alkyl levulinates in GVL preparation has attracted great industrial interest thanks to their lower boiling point and free acid characteristics, as compared to LA. Moreover, alcoholic groups are better-leaving groups than OH, facilitating the reaction through a cyclization mechanism.

Given all the promising applications of GVL in the bio-based economy, the time for environmentally friendly and cost-effective GVL production processes has surely arrived. In this regard, one of the most interesting approaches is the catalytic transfer hydrogenation (CTH) [Wang and Astruc, 2015; Gilkey and Bingjun, 2016; Espro et al., 2018]. In CTH reactions, the use of an indirect H-source reduces most of the problems related to the use of high-pressure molecular hydrogen (e.g. purchase, transport, safety hazards, and pricey infrastructure), thus improving the sustainability of industrial processes (at the present time, several H-donor molecules can be obtained from renewable feedstocks).

4.2 Experimental

All chemicals were acquired as analytical grade compounds from commercial sources (Sigma Aldrich, Carlo Erba, and Alfa Aesar), and used without any further purification process. Pd/C (5 wt% of Pd) was purchased from Alfa Aesar.

The ZrO_2 was prepared starting from the nitrate precursor ($ZrO(NO_3)_2{\cdot}2H_2O$) in accordance with the reported synthetic procedure [Chuah et al., 1996]. A solution containing zirconium (IV) nitrate dihydrate

was added dropwise into an aqueous solution of NH_3 (5 M) at room temperature. The heterogeneous mixture was digested at 100°C for 24 h under a reflux system adjusting the pH of the solution to 9, by the dropwise addition of another NH_3 solution (28% w/w). The precipitate was filtered and washed several times, still using an NH_3 (5 M) solution. The precipitate was dried overnight at 120 °C and calcined at 500 °C for 12 hours in flowing air with a heating rate of 2.5 °C/min.

The specific BET surface area of the ZrO_2 catalyst was determined by N_2 adsorption-desorption isotherms at the liquid nitrogen temperature, by using a Sorpty 1750 Fison instrument: before measurement, the sample was outgassed under flowing nitrogen for 1 h at 150 °C.

XRD analyses were recorded with a Bruker Tracer IV-SD Spectrometer (40 keV, 15 µA over 15 s with peak assignment based on the alignment with K-line energy transitions). The XRD pattern of the ZrO_2 catalyst was analyzed by Rietveld refinement [Rietveld, 1969; Young et al., 1982] using TOPAS software [Wragg et al., 2015]. The goodness-of-fit was checked via the GOF value (2.43).

Raman spectroscopy measurements were recorded in the air at room temperature with a diode laser operating at 2.33 eV using a Horiba XploRA spectrometer equipped with a confocal microscope (100x microscope objective lens was used) and Peltier-cooled charge-coupled detector.

NH_3 and CO_2-TPD were analyzed with a POROTEC Chemisorption TPD/R/O 1100 automated system. The fresh catalyst was pretreated in a 10 vol.% O_2 in He (30 ml/min of flow rate) at the chosen calcination temperature (10 °C/min to 500 °C for 1 hour) and then cooled down (40 °C for the CO_2-TPD and 100 °C for the NH_3-TPD analysis). The catalyst surface was saturated with CO_2 or NH_3 for 1 h (a flow rate of 30 ml/min of 10 vol.% of CO_2 or NH_3 in He) and then the physically adsorbed probe molecule was removed by

flushing the sample with He (30 ml/min of He) for 10 min. In order to avoid the contribution of very weak acid sites, NH_3 was adsorbed at 100 °C. TCD and MS methods were used for the temperature-programmed desorption, by increasing the temperature at a constant rate of 10 °C/min from 40/100 °C to 500 °C in He (30 ml/min).

In situ DRIFT spectroscopy was performed using a sample of ZrO_2 loaded and pretreated at 400 °C under a flow of He in order to remove absorbed molecules. Then, using a KBr disc as support, spectra were collected at different temperatures (400, 300, 200, 100, and 50 °C) starting from the highest and progressively cooling down the sample to 50 °C. The pyridine adsorption spectra were recorded by injecting a pulse of base (2 μL) at 1-minute time intervals. Conversely, desorption spectra were acquired by heating the sample at 400 °C with a heating rate of 5 °C/min and then using different temperatures (100, 200, 300, and 400 °C) by using a Bruker Vertex 70 instrument equipped with a Pike DiffusIR cell attachment system. Spectra were collected using a MCT detector after 128 scans with a 4 cm^{-1} resolution in the region 4000-450 cm^{-1}. The equipment used is completed with a mass spectrometer EcoSys-P from the European Spectroscopy 4 Systems.

DRIFT analyses of absorbed ML, α-angelica lactone, and GVL over the fresh ZrO_2 catalyst were carried out following this procedure: ZrO_2 was pre-treated in-situ at 400 °C for 1 hour under a He flow in order to clean the surface from adsorbed species. Afterward, the system was cooled to 200 °C and a pulse of 2 μL of the target molecule was allowed to flow over the IR cell. Spectra were recorded in the temperature range between 200 and 400 °C.

Thermogravimetric/differential thermal analyses (SDT Q600 instrument) were performed using 10 mg of fresh or spent catalysts. A temperature ramp from room temperature up to 700 °C (heating rate of 10 °C/min in air flow - 100 ml/min) was used.

4.2.1 Typical procedure for the catalytic upgrading of levulinates

Batch experiments were performed at 500 rpm in a 160 ml stainless steel autoclave (Parr Instrument - 4560 Mini reactor system). The reactor was loaded with the catalyst (0.3 g), thermally pre-treated at 400 °C for 2 hours under an air flow, suspended in a 10% wt alcoholic solution (MeOH, EtOH, 2-PrOH) containing the chosen substrate. Any trace of air present in the system was eliminated by fluxing N_2 (99.99%) three times. The reactor was subsequently pressurized with 10 bar of N_2 and heated to the final reaction temperature. At the end of the reaction, the system was cooled down to room temperature; the pressure was carefully released and the organic phase was analyzed by using an off-line gas-chromatograph (GC Thermo Focus GC model equipped with an Agilent HP-5 column). For every recycling test, after each run, the catalyst was recovered, thoroughly washed with 2-PrOH, and reused under the same reaction conditions.

Catalytic transfer hydrogenation (CTH) in a continuous gas-phase flow (on a fixed bed reactor) was tested via the vaporization of an alcohol/levulinate ester mixture in a nitrogen stream. A syringe pump (KD Scientific Legacy Syringe-infusion Pump) was used to feed the mixture into a stainless-steel heated line where instant vaporization was obtained. An inlet with the carrier gas (N_2) was also located in this line, making it possible for the reagent to flow across the line toward the connected tubular glass reactor (length 450 mm, inner diameter 19 mm). The reactor was located inside a furnace and its inlet and outlet were constantly heated during the tests with heating tapes equipped with an electrical resistance controlled by thermocouples. In a typical experiment, a mixture of alkyl levulinate and alcohol (molar ratio of 1:10) was fed into the reactor with a flow of 0.5 ml/h in a 30 ml/min N_2 stream, and 1 cm^3 of catalyst was loaded into the reactor. The test residence time was typically 1s and the volumetric percentage of the organic mixture was kept between 9 and 12%. Before each test, the catalyst

was pre-treated inside the reactor for 1 h at 400 °C with 30 ml/min air flow. Temperatures were set to the desired working condition, for both the furnace and heating tapes, and then the catalytic test was performed. The exit stream of the reactor was condensed using a cold trap containing 25 ml of acetonitrile. This solution was taken and analyzed every 50-60 min in order to monitor the reactivity during the time-on-stream process. At the very beginning, blank experiments were also performed by feeding a mixture characterized by alcohol: ML (or EL) molar ratio of 10 into the reactor in a temperature range of 200 to 350 °C. In the absence of any catalyst, a negligible alkyl levulinate conversion was obtained.

4.2.2 Typical procedure for the catalytic upgrading of limonene

Batch experiments for the conversion of limonene were performed in a 160 ml stainless steel autoclave (Parr Instrument - 4560 Mini reactor system) at a stirring speed of 500 rpm. The reactor was loaded with the catalyst (0.25 g), thermally pre-treated at 300 °C for 2 h with 30 ml/min H_2 flow. Any trace of air present in the system was eliminated by fluxing N_2 (99.99%) three times. The reactor was subsequently pressurized with 10 bar of H_2 or N_2 and heated to the final reaction temperature, that was monitored using a thermocouple fixed into the autoclave and connected to the thermo controller. At the end of the reaction, the system was cooled to room temperature, the pressure was carefully released, and the organic phase was analysed. After each run the catalyst was recovered and thoroughly washed with acetone.

The transformation of d-limonene into p-cymene in a continuous gas-phase flow (on a fixed-bed reactor) was tested via the vaporization of an alcohol/limonene mixture in a nitrogen stream. A syringe pump was used to feed the mixture into a stainless-steel heated line, where an instant vaporization was obtained. An inlet with the carrier gas (N_2) was also located in this line, making it possible for the reagent to flow across the line toward the connected tubular reactor (length 450 mm, inner diameter 19 mm). The

reactor was located inside a furnace and its inlet and outlet were constantly heated during the tests with heating tapes equipped with an electrical resistance controlled by thermocouples. In a typical experiment, a mixture of limonene and alcohol (molar ratio of 1:20) was fed into the reactor with a flow of 0.3 ml/min in a 5 ml/min N_2 stream. Into the reactor 1.5 g of catalyst was loaded. Before each test, the catalyst was thermally pre-treated at 300 °C for 2 h with 30 ml/min H_2 flow. Temperatures were set to the desired working conditions, for both the furnace and heating tapes, and then the catalytic test was performed. The exit stream of the reactor was condensed using a cold trap containing 25 ml of acetonitrile. This solution was taken and analyzed every 30-60 min in order to monitor the reactivity during the time-on-stream process.

4.2.3 Liquid fraction analysis

In order to quantify both the reactants and the products, the following procedure was followed: 20 µL of *n*-octane were added (as the external standard) to the 25 ml mixture containing the condensed products in acetonitrile. 0.5 µL of this solution were then analyzed using a gas-chromatograph Thermo Focus GC model equipped with a non-polar capillary column Agilent HP-5 (5% phenyl-95% methyl siloxane) measuring 25 m x 320 µm x 1.05 µm, and a flame ionization detector (FID). The carrier used was N_2 with a flow of 1.0 ml/min. The heating program used was the following: 2 min isotherm at 50 °C, then heating up to 110 °C with a rate of 10 °C/min and later maintained for 2 min; finally, heating up to 280 °C with a heating rate of 20 °C/min and then maintained for 2 min. Each compound was calibrated with respect to *n*-octane in order to find the corresponding response factor in the appropriate range of concentrations.

The conversion, product selectivity (in liquid phase), and product yield were calculated and defined on the basis of the following equations:

$$(1)\ \text{Conversion}\ (\%) = \frac{\text{mol reacted substrate}}{\text{mol of substrated feed}} \times 100$$

(2) $$\text{Liquid phase selectivity (\%)} = \frac{\text{mol of specific product in liquid phase}}{\text{sum of mol of all products in liquid phase}} \times 100$$

(3) $$\text{Product yield (\%)} = \frac{\text{mol of specific product}}{\text{mol substrate in}} \times 100$$

In addition, carbon balance based on the fed alkyl levulinate was calculated as follows:

(4) $$\frac{Y}{C} = \frac{\sum \text{product yields}}{\text{substrate conversion}} \times 100$$

Products were identified by comparison with commercially available samples and by means of a GC-MS equipped with a non-polar column HP-5 (95% dimethylsiloxane and 5% phenyl, 30 m X 320 µm, using the same heating program as stated for the GC-FID analysis), coupled with a mass spectrometer (Agilent Technologies 5973 inert).

4.3 Results and discussion

4.3.1 Catalytic upgrading of limonene under batch conditions

The catalytic conversion of d-limonene into p-cymene can follow three different reaction routes: (i) the isomerization to terpinenes and terpinolenes; (ii) the disproportionation to p-cymene (slow if compared to the isomerization or dehydrogenation, due to the need for two molecule intermediates) followed by dehydrogenation and in some cases polymerization; (iii) the hydrogenation to menthenes and menthanes with further dehydroaromatization to p-cymene [Kamitsou et al., 2014; Catrinescu et al., 2006; Fernandes et al., 2007]. The presence of isomerization compounds (terpinenes and terpinolenes) in the products would support the first mechanism, while the presence of menthenes or menthanes would be indicative of the third mechanism [Scheme 4.1].

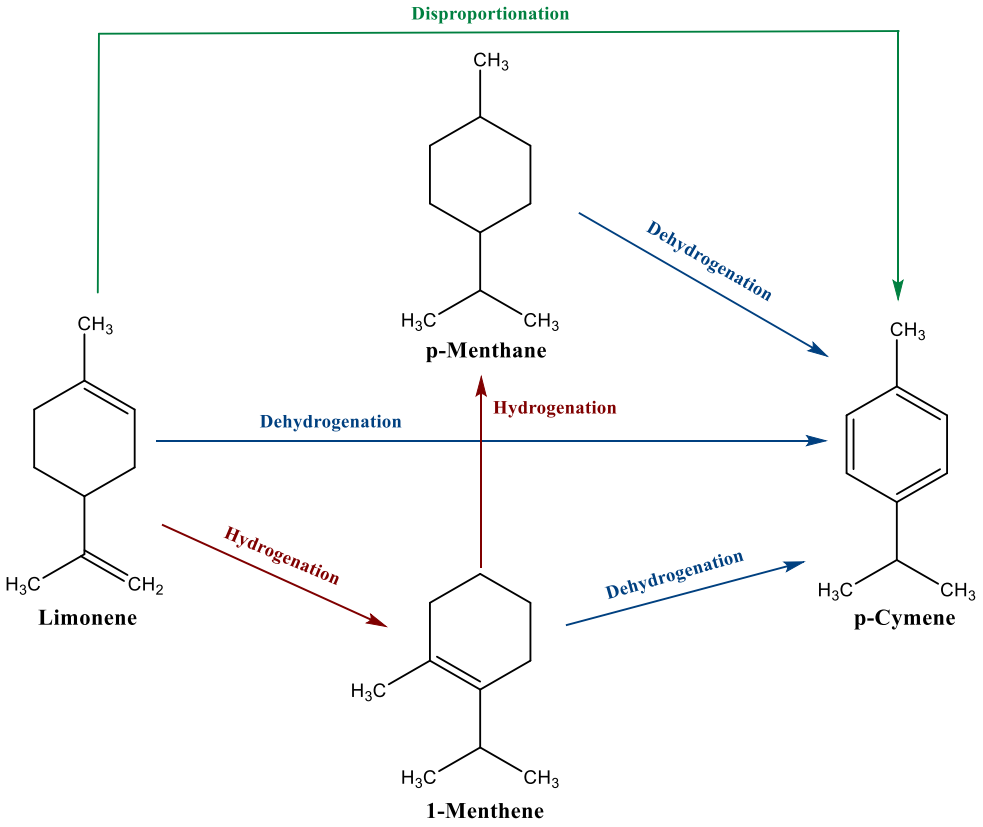

Scheme 4.1. Plausible mechanisms for dehydroaromatization of limonene to p-cymene over Pd/C.

According to the catalytic experiments carried out under batch conditions, Figure 4.1 illustrates the p-cymene selectivity as a function of the temperature, obtained over the Pd/C catalyst under H_2 or N_2 atmosphere. An inspection of this figure shows that the catalytic performance of the Pd/C catalyst is significantly dependent on the kind of atmosphere used (H_2 or N_2). At lower temperatures, on using 10 bar of H_2 pressure (Fig. 4.1a), the fractions of menthanes (cis-p-menthane and trans-p-menthane) compounds is prevalent.

At higher temperatures, the selectivity is progressively oriented towards the formation of p-cymene, in accordance with the formation of this product resulting from an endothermic reaction. In fact, within the 360 min of reaction, the selectivity of these initial products such as p-menthanes decrease and the selectivity to p-cymene, indicating that the C-H bond breaking is the prevalent

way of reaction, increases. From an environmental point of view, it is important to note that the use of N_2 (Fig. 4.1b) allows a complete conversion of limonene without the need of hydrogen and a higher selectivity to p-cymene that falls slightly on increasing of the reaction temperature, is detected. On the contrary, every mole of limonene that produces p-cymene leads to the production of one mole of hydrogen.

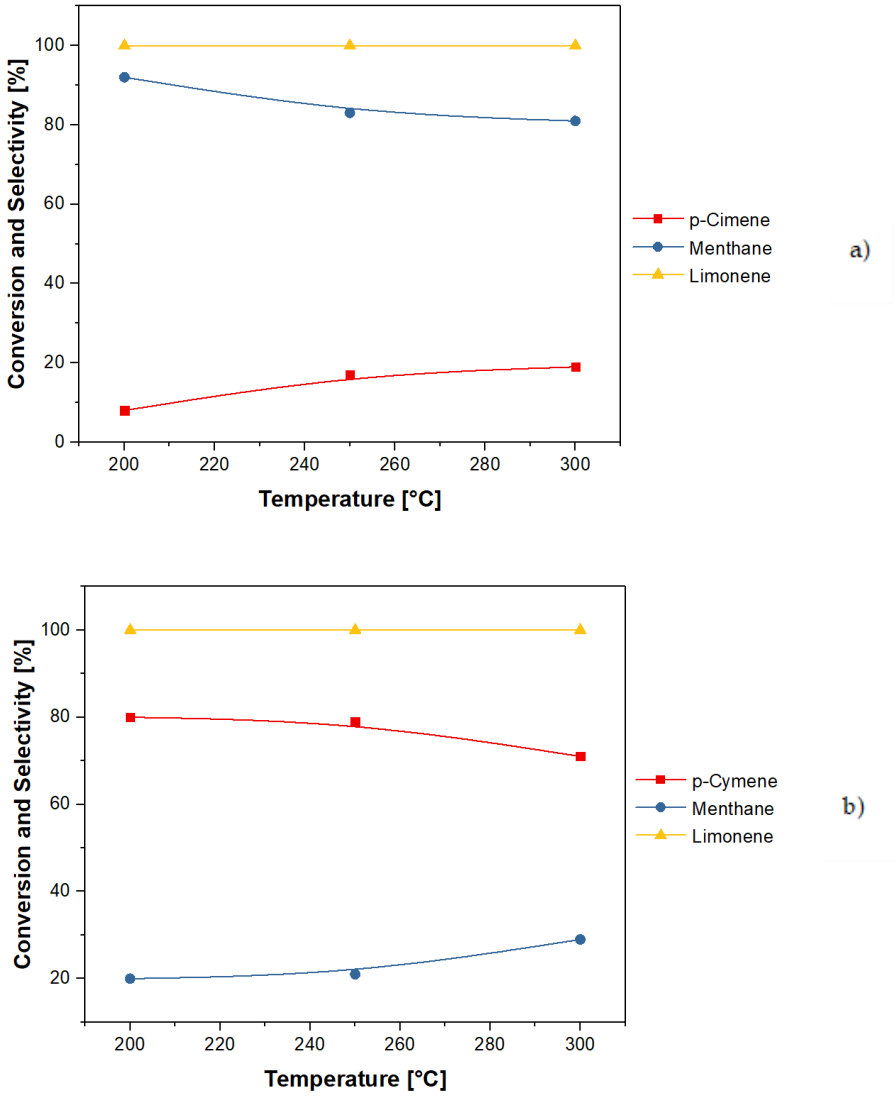

Figure 4.1. Selectivity of p-cymene produced from limonene at reaction temperature range 200-300 °C under H_2 (a) or N_2 (b) atmosphere (Reaction conditions: 0.25 g of Pd/C catalyst (5% wt); 40 ml solution of limonene (4% wt) and EtOH; reaction time: 360 min; H_2 or N_2 pressure: 10 bar; stirring: 500 rpm).

A comparison of the results presented in Figure 4.2 shows that under N_2 atmosphere products distributions, obtained at corresponding reaction temperatures are similar. On the other hand, the conversion of limonene achieved on using 2-PrOH as the reaction medium does not exceed 30% at the lower temperature studied (200 °C), while it increases with the reaction temperature.

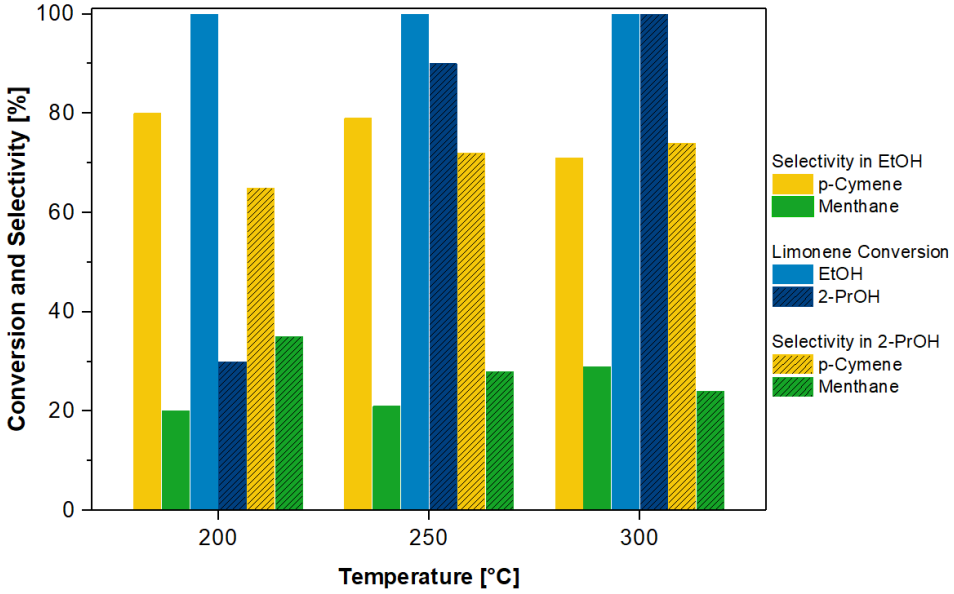

Figure 4.2. Limonene conversion and selectivity of p-cymene obtained using different alcohols over a Pd/C catalyst (Reaction conditions: 0.25 g of Pd/C catalyst (5% wt); 40 ml solution of limonene (4% wt) and EtOH; reaction time: 360 min; H_2 or N_2 pressure: 10 bar; stirring: 500 rpm).

4.3.2 Catalytic upgrading of limonene under continuous gas-flow conditions

The results of experiments conducted by feeding limonene in continuous gas-flow conditions are shown in Figure 4.3. Under the reaction conditions used, Pd/C allows a complete limonene conversion after more than 50 min time-on-stream, promoting the formation of p-cymene with an excellent yield. Moreover, the limonene conversion and the yield to p-cymene remain constant for 360 min time-on-stream, indicating that the Pd/C catalyst is not only a very

active and selective catalyst for limonene transformation to p-cymene, but it is also quite stable.

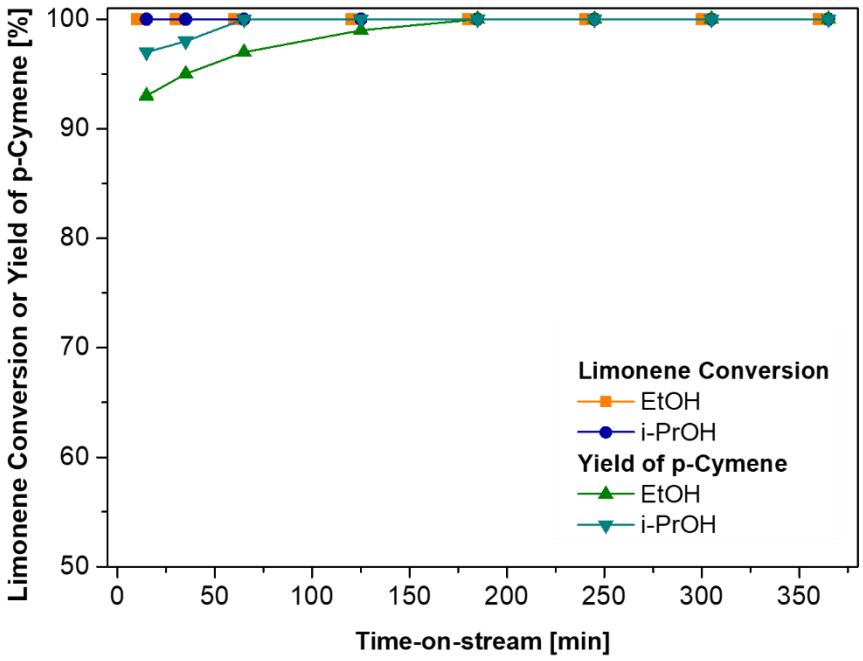

Figure 4.3. Limonene conversion and selectivity of p-cymene obtained over Pd/C catalyst under continuous gas-flow conditions (Reaction conditions: molar ratio limonene (4% wt): alcohol=1:20; reaction temperature: 300 °C; N_2 pressure: 5 bar; resident time: 5 s).

4.3.3 Catalytic upgrading of levulinates under batch conditions

Catalyst synthesis and characterizations

The high-surface-area tetragonal ZrO_2 catalyst was synthesized following the preparation method proposed by Chuah et al. [Chuah et al., 1996]. The main characteristics and structural properties of the ZrO_2 catalyst are shown in Table 4.1. The physical-chemical characteristics of the used ZrO_2 catalyst have been described and discussed in detail in various reports [Chuah et al., 1996; Komanoya et al., 2015], including one by the authors [Vásquez et al., 2019], and may be summarized as follows: (i) a predominance of tetragonal phase as confirmed by XRD analysis (Figure 4.4); high surface area as shown

by BET measurement; the presence of both basic and acidic sites as shown by NH_3 and CO_2-TPD and analyses.

Table 4.1. Main characteristics of high-surface-area tetragonal ZrO_2 catalyst.

Catalyst	S.A. (m^2/g)	Tetragonal phase (%)	Acid density (mmol/g NH_3 desorbed)	Basic density (mmol/g CO_2 desorbed)
ZrO_2	120	61	0.401	0.258

S.A. = Surface area as determined by BET analysis; tetragonal phase (%) = % of tetragonal phase as obtained via Rietveld refinement; Acid Density as determined via NH_3-TPD analysis; Basic density as determined via CO_2-TPD analyses.

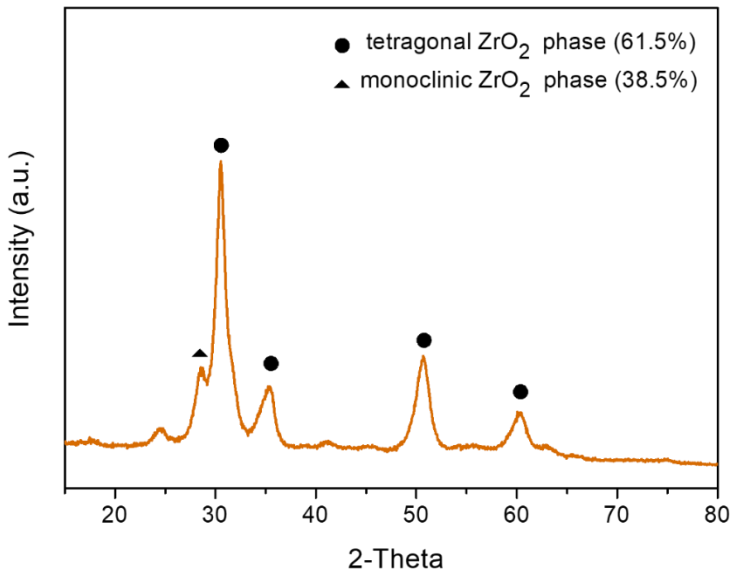

Figure 4.4. XRD patterns of the tetragonal ZrO_2 catalyst.

Moreover, DRIFT analysis shows, after pyridine adsorption/desorption experiments, the presence of bands at 1443 cm^{-1}, 1574 cm^{-1}, and 1604 cm^{-1} all belongings to Lewis acid sites (prerequisites for CTH via the MVP mechanism) [Vásquez et al., 2019].

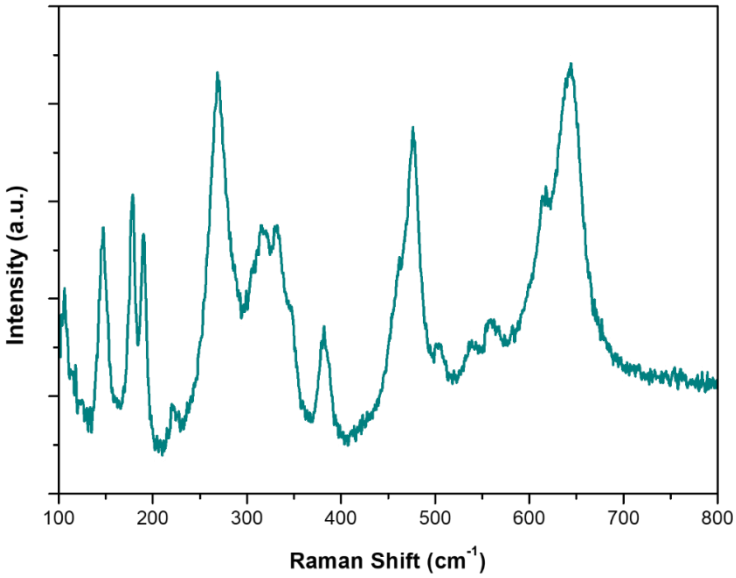

Figure 4.5. Raman spectrum of investigated ZrO_2 catalyst.

Raman spectra of the investigated ZrO_2 catalyst reveals, in agreement with XRD analysis, mainly mixed tetragonal and monoclinic phases with no clear evidence concerning the presence of the characteristic peak for the cubic phase at 625 cm^{-1} (Figure 4.5) [Lopez et al., 2001; Gazzoli et al., 2007].

At the start of our investigations, a set of experiments were planned in order to evaluate both the effect of the alcohol used as a reducing agent (MeOH, EtOH, and 2-PrOH as H-donors) and the effect of the hindrance of the starting alkyl levulinate substrates. Taking into account the results recently obtained [Mauriello et al., 2015], the reaction temperature was set at 250 °C and a reagent mixture characterized by an alcohol-to-alkyl levulinate molar ratio of 10 was used.

In a preliminary laboratory test, almost no conversion (below 1%) in the CTH of ML and EL (250 °C, 8 h, 10 bar N_2) over commercial ZrO_2 - used as benchmark catalyst - and in the presence of 2-PrOH as solvent/H catalyst was registered.

The performances of the synthesized ZrO_2 catalyst in the CTH of ML and EL using MeOH, EtOH, and 2-PrOH as solvents/H-donor molecules under batch conditions are shown in Table 4.2. Reactions occurring in the presence of EtOH and MeOH as solvent/H-donor were found to be inefficient in GVL production. In the presence of MeOH at 250 °C, EL is primarily converted (25%) to methyl-levulinate (selectivity of 79%), while only traces of GVL were detected. In this case, ML may form from EL via a transesterification process promoted by a mass action effect (methoxy ester formation is thermodynamically favored than that of the analogous ethoxy derivative). Conversely, EL conversion was 12%, in the presence of EtOH (which prevents the occurrence of any transesterification reaction), with a good GVL selectivity in the liquid phase.

Table 4.2. Catalytic transfer hydrogenation of methyl levulinate and ethyl levulinate promoted by a ZrO_2 catalyst under batch conditions.

Entry	H-donor	Conversion [%]	Chemoselectivity [%]				GVL Yield [%]
			LEV-R	GVL	GVL-R	O.P.	
EL	2-PrOH	31	9	87	< 2	< 1	27
EL	EtOH	12	-	63	< 3	35	8
EL	MeOH	25	79	< 1	< 1	19	< 1
ML	2-PrOH	21	16	82	< 2	< 1	17
ML	EtOH	22	59	27	< 1	13	6
ML	MeOH	< 5	-	< 5	-	95	< 2

Reaction conditions: 0.30 g of ZrO_2 catalyst, 40 ml solution of methyl levulinate or ethyl levulinate (10% wt), reaction temperature: 250°C; reaction time: 8 hours; N_2 pressure: 10 bar; stirring: 500 rpm; EL: Ethyl Levulinate; ML: Methyl Levulinate; LEV-R: alkyl levulinates (with R = methyl or ethyl or isopropyl) GVL: γ-valerolactone; GVL-R: alkyl-GVL (with R = methyl or ethyl or isopropyl); O.P.: other products

In the presence of MeOH, a very low conversion of ML was obtained, whereas a higher conversion was registered when EtOH was used as the solvent/H-donor, having a low selectivity to GVL as a consequence of the

predominance of the transesterification reaction of ML into EL. Furthermore, a moderate quantity of side products was always registered.

As expected, 2-PrOH is by far the most effective in the production of GVL, in agreement with the well-known greater tendency of secondary alcohols to release hydrogen [Mauriello et al., 2015; Mauriello et al., 2018]. Indeed, by using 2-PrOH as solvent/H-donor, EL and ML were converted, in an appreciable yield, into GVL (27% and 17% respectively) after 8 hours at 250 °C. The higher reactivity of EL can be easily explained considering that, in dealcoholization reactions, a longer alkyl residue is a better leaving group than a short one [Kuwaharaa et al., 2017]. Traces of propyl-GVL were also detected, clearly indicating that, under the conditions adopted, the ZrO_2 catalyst can promote the alkylation of angelica lactones (obtained from intramolecular dealcoholization), behaving as reaction intermediates. At the same time, a significant amount of isopropyl levulinate was also obtained. In principle, it may be produced via two potential reaction pathways: (i) a direct transesterification reaction with 2-PrOH, or (ii) alcoholysis of α- and β-angelica lactones, with the latter being the most likely to occur since the transesterification reaction should be less probable as a consequence of the higher steric hindrance of 2-PrOH with respect to ethoxy and methoxy groups. In order to confirm this hypothesis, the β-angelica lactone was allowed to react in the presence of the ZrO_2 catalyst under the same reaction conditions as that adopted for CTH reactions (0.30 g of ZrO_2 catalyst, 40 ml solution of β-angelica lactone 10% wt, reaction time: 8 hours; N_2 pressure: 10 bar; stirring: 500 rpm). A 30% conversion was obtained and isopropyl levulinate was found to be the main reaction product (60% selectivity) together with GVL (14%), isopropyl-GVL (10%), and other side reaction products (16%).

The product distribution obtained in the conversion of β-angelica lactone over the ZrO_2 catalyst also means that, when 2-PrOH is used as the H-donor/solvent under batch reaction conditions, GVL production from ethyl

levulinate occurs mainly from the transfer hydrogenation to the carbonyl group in the 4th position to produce 4-hydroxypentanoic acid esters (4-HPE) and its further dealcoholization to form GVL. This result is in agreement with a recent report in which 4-HPE is formed through the direct transfer of the hydrogen of 2-PrOH to alkyl levulinates mediated by the catalytic surface via the MVP mechanism [Kuwaharaa et al., 2017].

The yield in GVL can increase on increasing the reaction temperature (Figure 4.6). After 8 hours, the CTH of EL with iPrOH over the ZrO_2 catalyst at 300 °C gives a GVL yield of 56% (72% conversion), while a modest yield of 5% (6% conversion) was observed at 200 °C.

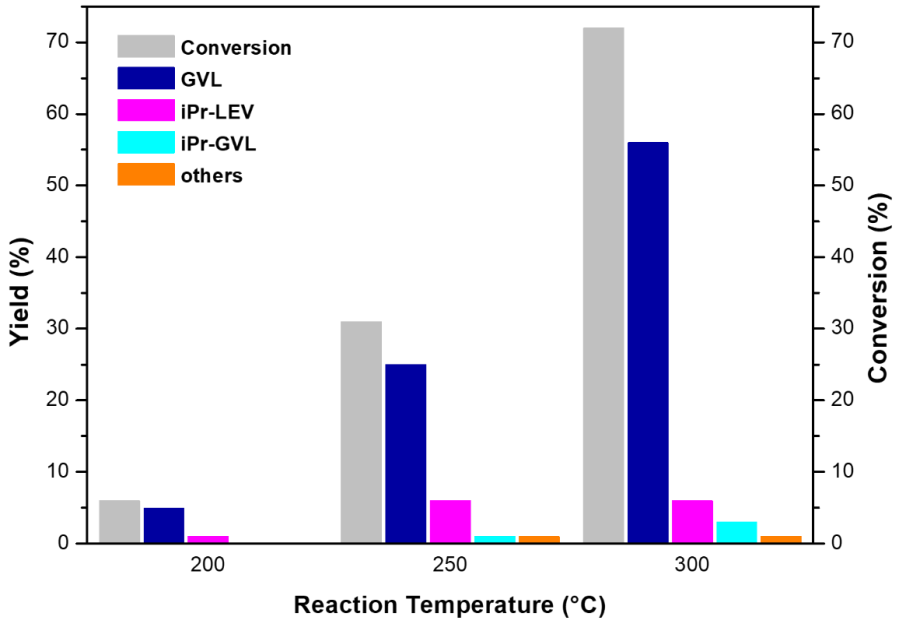

Figure 4.6. Temperature effect in the CTH of EL under batch conditions.

Furthermore, the reaction time effect at 250 °C was investigated. GVL yield progressively increases on increasing of the reaction time, reaching the highest value of 64% after 24 hours (Figure 4.7).

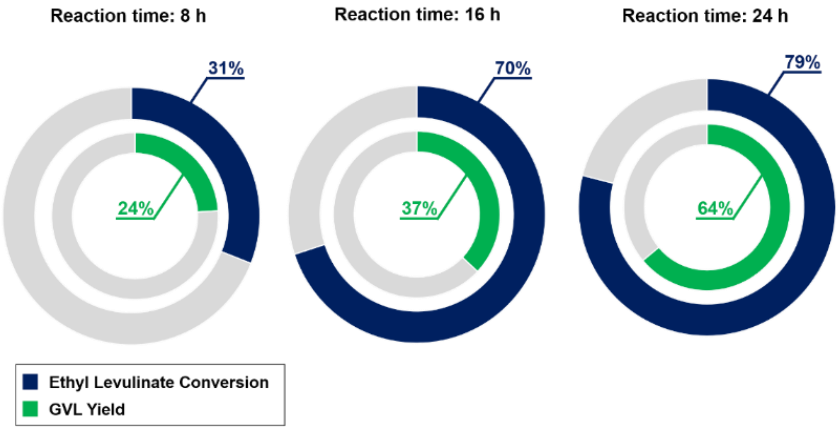

Figure 4.7. Reaction time effect in the CTH of EL at 250 °C.

The reusability and stability of the ZrO_2 catalysts were also assessed under batch conditions based on five consecutive recycling tests at 250 °C for 24 hours. As shown in Figure 4.8, no significant changes in the product selectivity were found, although a significant activity reduction was registered. However, when the used catalyst was regenerated (thermally treated at 400 °C for 2 hours under an air flow), its performance is comparable with the first run, with a conversion of 78% (66% yield of GVL) suggesting that the observed drop in its activity during recycling tests has to be attributed to the deposit of carbonaceous species.

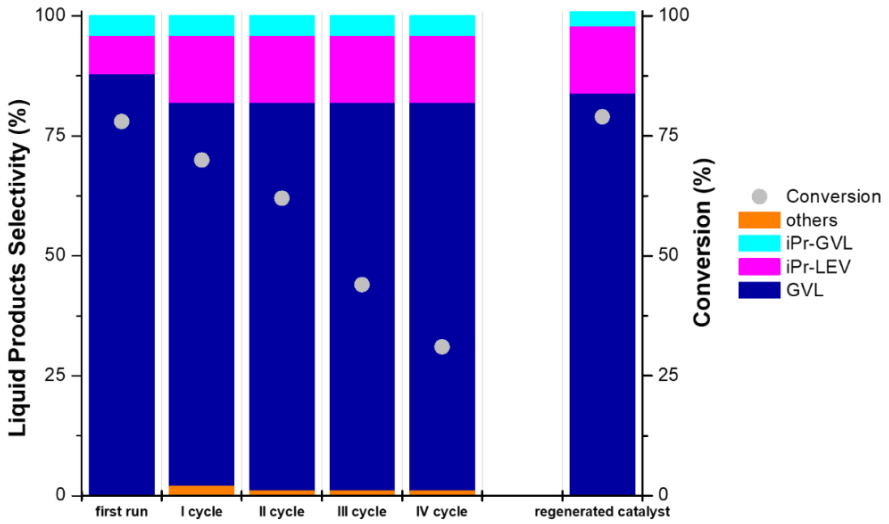

Figure 4.8. Reusability tests of ZrO_2 catalyst in the CTH of EL under batch conditions.

In order to confirm this hypothesis, the XRD analysis was performed on the spent ZrO_2 catalyst and no changes in the crystalline phase were observed (Figure 4.9). Moreover, the BET surface area was determined, obtaining just a slight decrease of the original value given the deposition of carbonaceous material on the surface of the catalysts during the catalytic activity, as confirmed by TGA (weight loss of 4%).

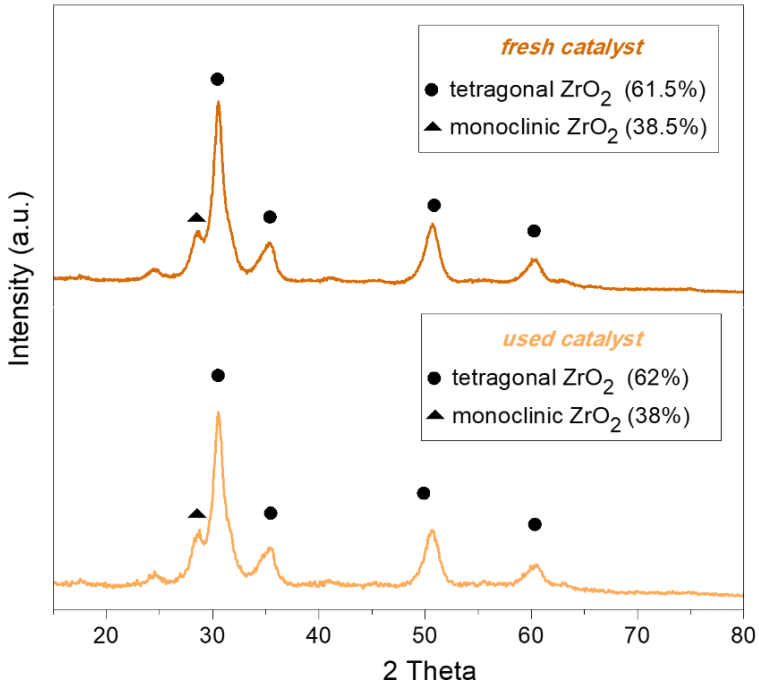

Figure 4.9. XRD of fresh (up) and used (down) ZrO_2 catalyst.

4.3.4 Catalytic upgrading of levulinates under continuous gas-flow conditions

The results of experiments conducted by feeding ML and EL in continuous gas-flow conditions are shown in Figure 4.10. Under the conditions used, ZrO_2 allows a complete ML conversion after more than 300 min time-on-stream, promoting the formation of GVL with a good-to-excellent yield, when EtOH and 2-PrOH are used as reducing agents (yield 70 and 80%,

respectively). EtOH in-situ not only transforms into acetaldehyde, behaving as a hydroxyalkylating agent of the formed GVL, finally yielding ethyl-GVL (the main side products at the beginning of the reaction), but also promotes catalyst deactivation, because of oligomerization leading to the deposition of heavy carbonaceous compounds on the catalytic surface. Indeed, when using a longer reaction time, the chemoselectivity of the reaction undergoes a change toward the formation of EL, which occurs by means of ML transesterification and/or the alcoholysis of the intermediates with EtOH.

Moreover, a low amount of ethyl pentanoate can also be produced by the alcoholysis of GVL itself. Some lighter compounds have also been detected, namely 1-butanol and ethyl acetate obtained from the Guerbet and Tishchenko reaction of EtOH and acetaldehyde, respectively. When 2-PrOH was used as the reducing agent, the GVL yield obtained was slightly higher than that with EtOH. However, GVL yield is limited by two consecutive reactions: i) GVL alcoholysis with the formation of propyl pentanoate (that can be further reduced to propyl pentanoate), and ii) the consecutive reduction/dehydration to 2-methyltetrahydrofuran (2-MTHF). Significantly, a more stable catalytic activity was achieved. This is probably due to both the lower reactivity of acetone during the formation of the coke precursors and the higher steric hindrance of the secondary alcohol that hinders the transesterification.

A completely different behavior was observed when using MeOH as H-donor. In this case, the conversion of ML drops from 90 to 30% in a 300 min time-on-stream, with both a very low average GVL yield (4%) and poor carbon balance. The poor reactivity showed in the CTH of ML with MeOH as H-donor can be explained considering that the catalytic test was conducted using EL as the starting substrate, where the presence of an equilibrium limitation in the intramolecular cyclization of ML to angelica lactones can be ruled out due to the presence of a MeOH excess.

Our results highlight the following:

1) EL shows a higher reactivity than does ML, albeit the conversion falls slightly from 99 to 86%. This phenomenon may be attributed, to a limited extent, to an increased efficiency of EtOH as the leaving group in the intramolecular cyclization of EL to angelica lactones and, to a greater extent, to the transesterification of EL with MeOH to yield ML;

2) MeOH is the least active alcohol for the CTH of alkyl levulinates; even though the GVL yield is greater than 30% at the beginning of the reaction (probably due to the easier formation of the intermediate angelica lactones), it rapidly decreases in favor of ML with prolonged reaction times;

3) The presence of ethyl pentanoate and ML clearly indicates that zirconia efficiently activates MeOH for the alcoholysis of both GVL and angelica lactones.

The higher reactivity of EL than ML and the absence of equilibrium limitation for the intramolecular cyclization are also confirmed by the results obtained by feeding EL and EtOH (Figure 4.10). Indeed, in this case, a trend similar to that of ML (Figure 4.10) was observed, with the complete conversion of the ester, and both GVL and ethyl-GVL as the main products. Moreover, the GVL yield increases from an average value of 68% up to 75% by changing the nature of the substrate from ML to EL. Significantly, a similar catalyst deactivation rate was detected in both cases; the decrease in EL conversion started after a 200 min time-on-stream.

In a similar way, the CTH of EL with i-PrOH (Figure 4.10) leads to the complete and stable conversion of the substrate, with GVL and propyl pentanoate as the main products. In this case, however, both the GVL yield and the carbon balance of the reaction are considerably lower if compared to the same test performed starting from ML.

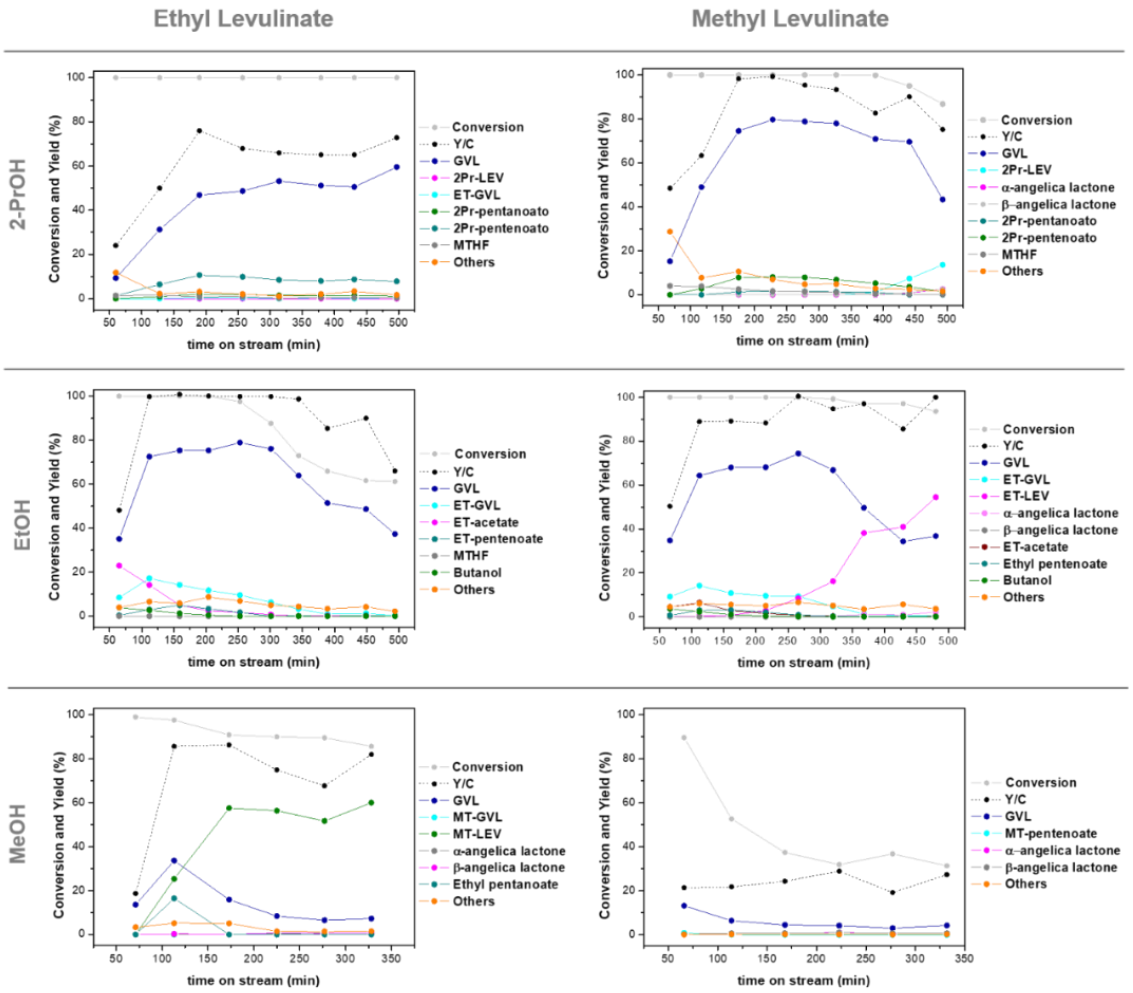

Figure 4.10. Catalytic results obtained in the EL and ML reduction via H-transfer using different alcohols as the H-donor over a ZrO_2 catalyst (Reaction conditions: molar ratio EL or ML: alcohol=1:10, T: 250°C, τ = 1 s, % mol N_2: EL or ML: alcohol = 90.1: 0.9: 9).

In order to understand the reasons for catalyst deactivation and worsening of the C balance, we characterized the spent catalysts by means of thermogravimetric analysis (Table 4.3).

TGA plots show similar behaviors for the reactions occurring with either EtOH or 2-PrOH, and confirm the detrimental effect of MeOH on the C balance, probably due to in-situ-formed formaldehyde which is able to promote the oligomerization of angelica lactones and other intermediates to heavier compounds, finally leading to catalyst deactivation.

Table 4.3. TGA analysis of the spent ZrO_2 catalysts in the CTH reactions occurring under continuous gas-flow conditions.

Entry	H-donor	Time-on-stream (min)	Weight lost (%)	Accumulation (mg/min)
EL	2-PrOH	314	3.03	0.00135
EL	EtOH	301	3.13	0.00164
EL	MeOH	328	4.00	0.00088
ML	2-PrOH	327	3.20	0.00098
ML	EtOH	320	3.05	0.00130
ML	MeOH	332	7.66	0.00246

On the other hand, the comparison of the TGA profiles of spent catalysts for reactions in which 2-PrOH was used as the H-donor with both ML and EL, do not show a substantially different weight loss. Nevertheless, the reaction between EL and 2-PrOH lead to a considerably worse carbon balance compared to that obtained with ML.

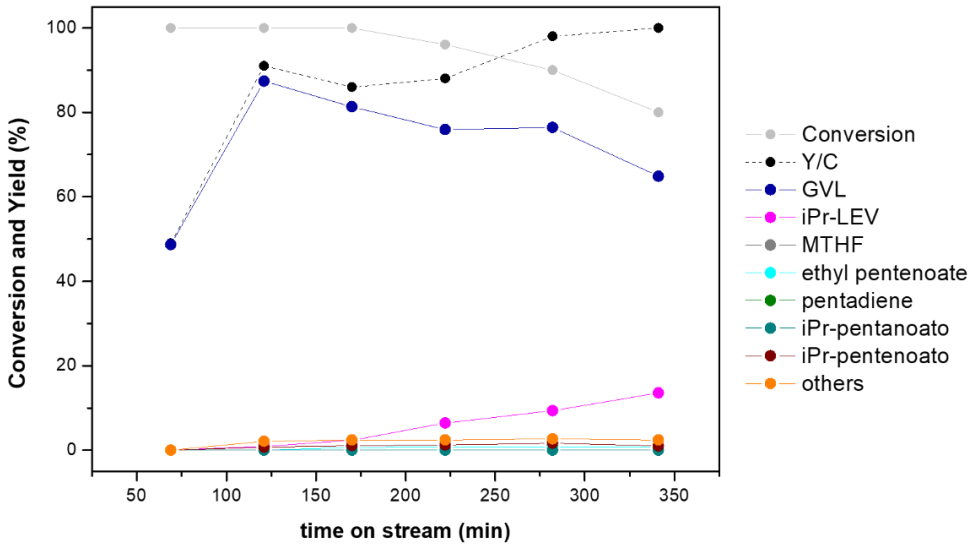

Figure 4.11. Catalytic results obtained in EL reduction via H-transfer using 2-PrOH as the reducing agent over ZrO_2. (Reaction conditions: molar ratio EL: 2-PrOH = 1:10, T = 200°C, τ = 1 s, %mol N_2: EL: alcohol = 90.1: 0.9: 9).

The latter may be attributed to a substrate over reduction to light compounds or alkenes which could not be detected with our off-line analysis setup, due to the highly reactive substrate and alcohol.

In order to evaluate this hypothesis, another test was performed by feeding the same reagent mixture at a lower temperature (200 °C) in order to slow down both the reaction rate and the extent of consecutive reactions (Figure 4.11).

The catalytic results obtained at 200 °C prove that, at a lower reaction temperature, it is possible to limit the extent of the consecutive reactions of GVL transformation into both propyl pentanoate and other lighter compounds. In particular, at the beginning of the reaction, the GVL yield was 87% with a good carbon balance. Unfortunately, a progressive catalyst deactivation was also observed, leading to the decrease in EL conversion from 100 down to 80% with the concomitant increase in isopropyl levulinate selectivity. The deactivation phenomenon occurres in parallel with a progressive shift of product distribution from the more reduced compounds (GVL and pentanoate) to the transesterification products. In order to obtain a better insight into the mechanism and to confirm the nature of reaction intermediates, tests were carried out by changing the contact time (Figure 4.12). The test performed at the lowest contact time (0.5 s) show a low EL conversion (around 37%) and the formation of angelica lactones, which disappear when a longer contact time is used, thus demonstrating their role as intermediates in the formation of GVL.

Surprisingly, isopropyl levulinate was also detected under these conditions, but it was completely converted with a longer contact time until catalyst deactivation occurres. This is probably ascribable to a complex reaction pathway in which the transesterification of the starting substrate and the alcoholysis of angelica lactones, to yield a different alkyl levulinate, are reversible equilibria.

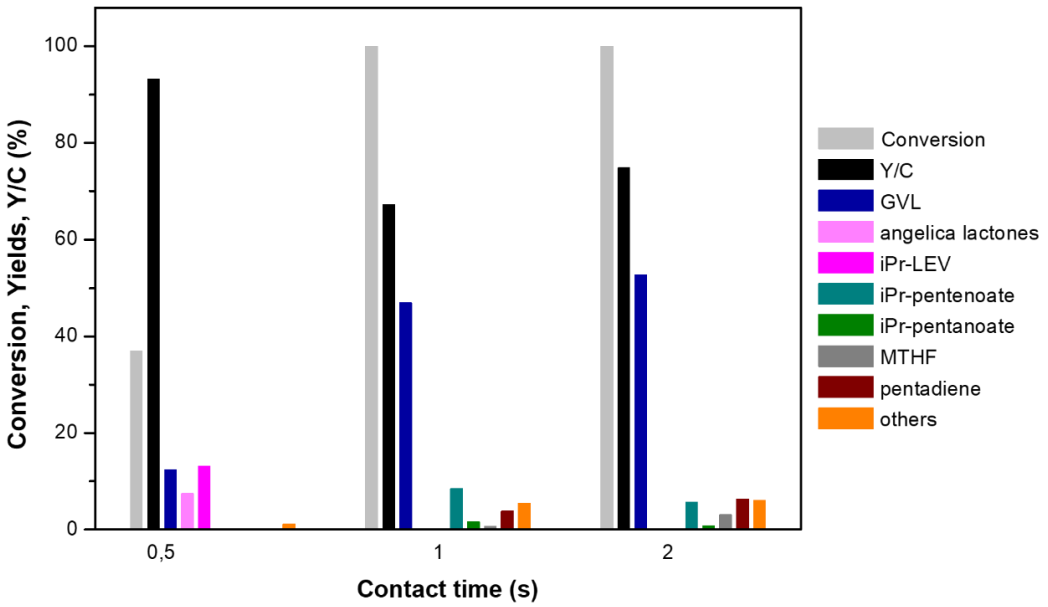

Figure 4.12. Catalytic results obtained in the EL reduction via H-transfer using 2-PrOH as the reducing agent over ZrO_2, varying the contact time over the catalytic bed (Reaction conditions: molar ratio EL: 2-PrOH = 1:10, T = 250 °C, τ = variable, %mol N_2: EL: alcohol = 90.1: 0.9: 9).

Moreover, depending on the nature of the alkyl group, this new ester could be characterized by a higher reactivity when compared to the parent levulinate. It is noteworthy that the increased contact time makes it possible to reach a complete EL conversion, with a parallel increase in GVL yield. However, the selectivity to propyl pentanoate, methyl tetrahydrofuran (2-MTHF), and other light compounds also increase as well, according to a consecutive reaction pathway starting from GVL.

Lastly, in order to test the long-term stability, the reaction between EL and 2-PrOH was performed for more than 750 min time-on-stream. The results are shown in Figure 4.13.

Our results confirm the stability of ZrO_2 for more than 10 hours reaction time; after that, however, deactivation leads to a parallel decrease in EL conversion, while the isopropyl levulinate yield increases. The possibility to perform the in-situ catalyst regeneration was also investigated. In particular, the reagent mixture flow was stopped, and the catalyst was kept for two hours

at 400 °C in an air flow (30 ml/min) in order to promote the combustion of carbonaceous residues. As it can be seen in Figure 4.13, after this treatment the catalytic activity was successfully restored, making it possible once again to obtain yields and conversion similar to the initial ones.

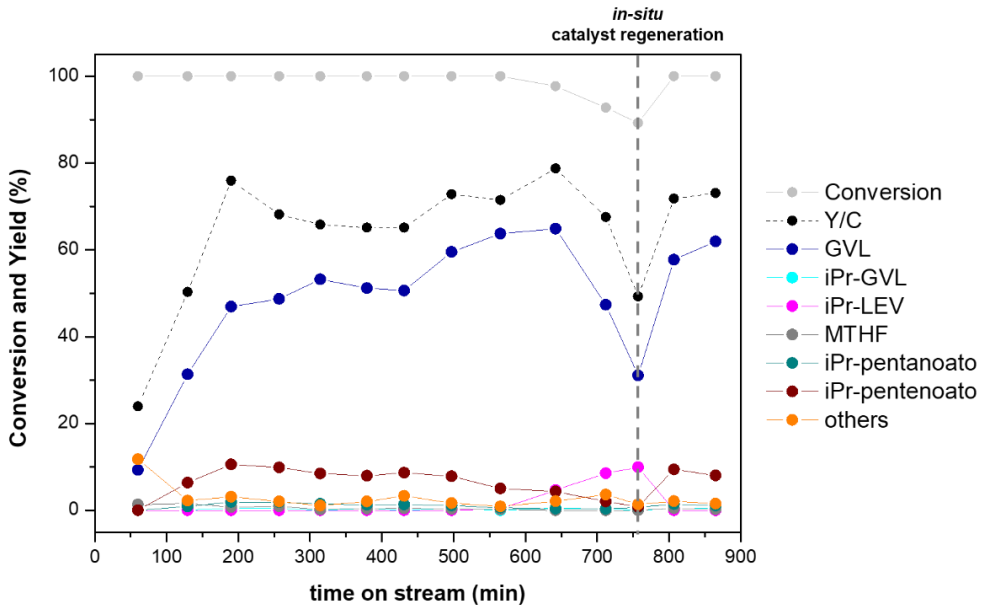

Figure 4.13. Catalytic results obtained in the EL reduction via H-transfer using 2-PrOH as the reducing agent over ZrO_2. The regeneration of the catalyst was performed in-situ after 760 minutes of time-on-stream (Reaction conditions: molar ratio EL: 2-PrOH = 1:10, T = 250 °C, τ = 1s, %mol N_2: EL: alcohol = 90.1: 0.9: 9).

Unraveling the reaction mechanism in the CTH of methyl and ethyl levulinate

Catalytic tests, as well as kinetic and thermodynamic factors, make it possible to interpret all results in both batch and gas flow conditions. The CTH ability of alcoholic solvents is the main factor driving the transformation of alkyl levulinates into GVL, changing in the order 2-PrOH > EtOH >> MeOH. Furthermore, it is also necessary to consider that, in the transesterification, the reactivity takes place in the order: MeOH> EtOH > 2-PrOH (this order is reversed if the leaving group is considered).

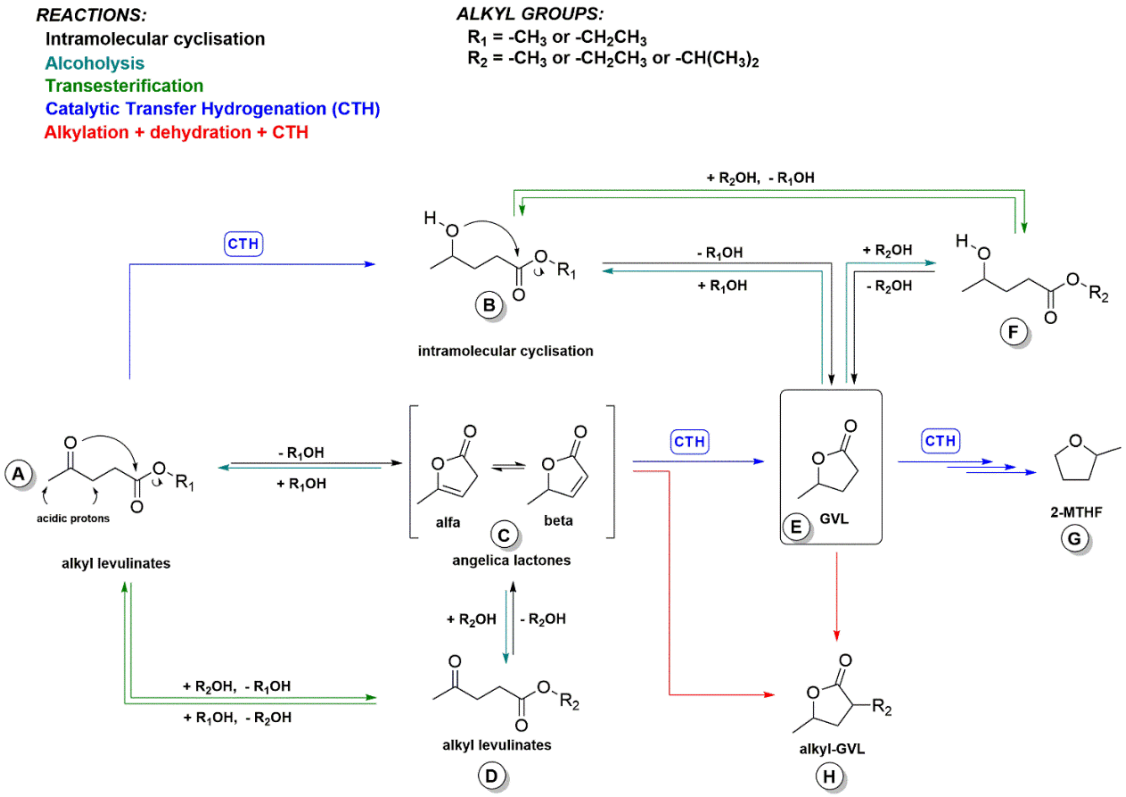

Scheme 4.2. Reaction pathways in the CTH of alkyl levulinates.

Therefore, the catalytic results obtained in batch and gas flow conditions support the reaction mechanism shown in Scheme 4.2. Under CTH conditions, alkyl levulinates (R = CH_3, CH_2CH_3) undergo a series of reactions: (i) carbonyl CTH hydrogenation resulting in B, which rapidly undergoes cyclization to GVL; (ii) transesterification leading to D. At the same time, GVL can also be formed via the CTH of α and β angelica lactones (the latter being formed by the cyclization of alkyl levulinates) which, in turn, may undergo alcoholysis leading to D. Formation of D and E from angelica lactones was confirmed by allowing the β-angelica lactone to react with different alcoholic solvents (results on of catalytic experiments on hydrogenation of β-angelica lactone in presence of 2-propanol as solvent/H-donor under both batch and continuous gas-flow conditions are reported in Table 4.4). F, G, and H are formed in minor amounts only.

Table 4.4. Catalytic transfer hydrogenation of β-angelica lactone promoted by a ZrO_2 catalyst in presence of 2-PrOH as solvent/H-donor under batch and continuous gas-flow conditions (reaction time: 8 hours).

Reaction conditions	Conversion [%]	Chemoselectivity [%]			
		LEV-2PrOH	GVL	GVL-2PrOH	O.P.
Batch	30	60	14	10	16
Continuous gas-flow conditions	100	-	75	-	25

The different peculiarities of H-donor/solvent alcohols (MeOH, EtOH, and 2-PrOH) explain the different amounts of products formed, as shown in Scheme 1. 2-Propanol – due to the greater tendency of secondary alcohols to release hydrogen and its poor entering group characteristics – promote CTH steps (A→B and C→E) while, at the same time, being less effective in transesterification (A→D). Conversely, methanol is poor as CTH agent and the most efficient entering group, thus better assisting the transesterification with little formation of GVL. Accordingly, EtOH showed an intermediate behavior between 2-PrOH and MeOH in both the CTH and transesterification.

In order to gain further insight into the mechanism of conversion of alkyl levulinates into GVL, DRIFT analyses of absorbed reactants (ML), intermediates (α-angelica lactone), and products (GVL) over the fresh ZrO_2 catalyst were performed (Figure 4.14).

Results obtained by feeding ML and α-angelica lactone show spectra characterized by the same bands. It follows that, also in absence of an H-donor molecule, ML rapidly undergoes an intramolecular cyclization, catalyzed by the basic sites of the catalyst. Nonetheless, in the absence of any H-donor, an important lack of the carbon balance was observed. This behavior can be ascribed to the oligomerization of the angelica lactones over the catalytic surface (the catalyst becomes black after the DRIFT experiment). It follows that bands observed could correspond to both angelica lactones and their oligomers. In addition, DRIFTs experiments coupled with a mass spectrometer

were performed feeding a mixture of ML and i-PrOH. The results obtained show the formation of a small amount of angelica lactones when the temperature starts to increase above 200 °C. However, it immediately starts to decrease upon a further increase in temperature, this occurs with the concomitant increase of the GVL production. Lastly, spectra obtained from this test shows the same characteristic bands similar to the ones obtained on feeding only GVL (in particular bands at 2868 and 2970 cm^{-1}, which were far less intense in the previous tests). Nonetheless, a complete and deepened investigation on the mechanism and the attribution of the IR bands of the intermediate species will be the scope of future studies.

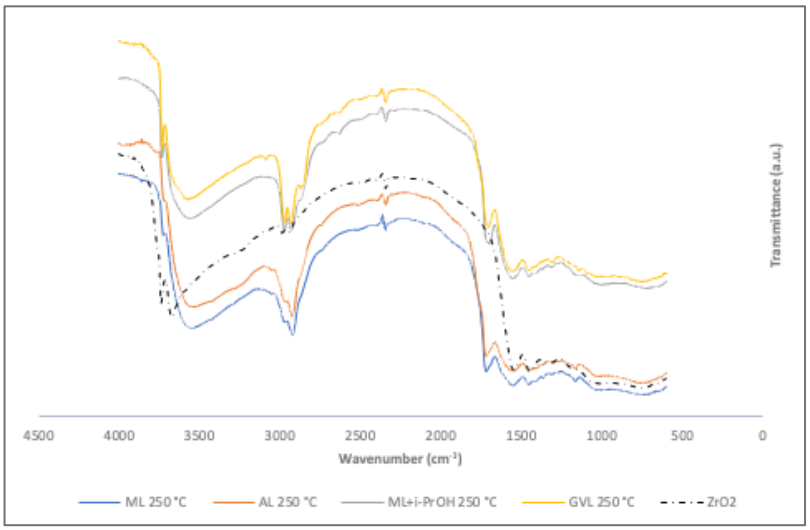

Figure 4.14. DRIFTs analysis of the adsorbed species obtained by feeding a pulse of ML (blue line), α-angelica lactone (orange line), GVL (yellow line) and the mixture of ML and isopropanol (grey line). The IR of fresh ZrO_2 is also reported for comparison (dotted line).

4.4 Conclusions

The conversion of limonene to p-cymene was carried out over Pd/C catalyst under both batch and gas-flow conditions, using different alcohols (EtOH and 2-PrOH) and reaction atmospheres (H_2 or N_2). Under batch conditions, it was observed that p-cymene selectivity increased with

increasing reaction temperature from 200 to 300 °C. In addition to this, p-menthane was found to be a significant reaction product both in ethanol and 2-propanol medium.

At the same time, it was demonstrated how the commercially available Pd/C catalyst can be efficiently used in the production of p-cymene under continuous gas-flow conditions.

The performance of the tetragonal ZrO_2 catalyst was investigated in the conversion of methyl levulinate and ethyl levulinate in transfer hydrogenation conditions, under both batch and continuous gas-flow conditions.

Under batch conditions, the product selectivity, in the liquid phase, was found to be dependent on the choice of the H source. On using 2-PrOH as H-donor, a very high selectivity to GVL was observed, whereas the reactions carried out in EtOH and MeOH were found to be much less efficient.

On the other hand, under continuous gas-flow conditions, high conversions and GVL yield can be obtained using 2-PrOH and EtOH, while poor reactivity with MeOH was observed. Moreover, the ZrO_2 catalyst shows excellent stability for more than 10 hours of time-on-stream and can be easily regenerated *in-situ* by feeding air at 400 °C for 2 h, thus permitting an almost total recovery of the initial catalytic performance.

Both the transfer hydrogenation, ruled by the ability of alcohols as reducing agents, and the transesterification, strongly influenced by the steric hindrance of the H-donor molecule, proved to be competitive procedures.

References

Buhl, D.; Roberge, D.M.; Hölderich, W.F. Production of p-cymene from α-limonene over silica supported Pd catalysts. *Appl. Catal. A Gen.* **1999**, *188*, 287-299.

Chuah, G.K.; Jaenicke, S.; Cheong, S.A.; Chan, K.S. The Influence of Preparation Conditions on the Surface Area of Zirconia. *Appl. Catal., A*. **1996**, *145(1-2)*, 267-284.

Espro, C.; Gumina, B.; Szumelda, T.; Paone, E.; Mauriello, F. Catalytic Transfer Hydrogenolysis as an Effective Tool for the Reductive Upgrading of Cellulose, Hemicellulose, Lignin, and Their Derived Molecules. *Catalysts* **2018**, *8(8)*, 313.

Lopez, E.F.; Sanchez Escribano, V.; Panizza, M.; Carnasciali, M.M.; Busca G. Vibrational and electronic spectroscopic properties of zirconia powders. *J. Mater. Chem*., **2001**, *11(7)*, 1891-1897.

Gazzoli, D.; Mattei, G.; Valigi, M. Raman and X-Ray Investigations of the Incorporation of Ca^{2+} and Cd^{2+} in the ZrO_2 Structure. *J. Raman Spectrosc.* **2007**, *38(7)*, 824-831.

Gilkey, M.J.; Bingjun, E.X. Heterogeneous Catalytic Transfer Hydrogenation as an Effective Pathway in Biomass Upgrading. *ACS Catal.* **2016**, *6(3)*, 1420-1436.

Gumina, B.; Mauriello, F.; Pietropaolo, R.; Galvagno, S.; Espro, C. Hydrogenolysis of sorbitol into valuable C3-C2 alcohols at low H_2 pressure promoted by the heterogeneous Pd/Fe_3O_4 catalyst. *Mol. Catal.* **2018**, *446*, 152-160.

Komanoya, T.; Nakajima, K.; Kitano, M.; Hara, M. Synergistic Catalysis by Lewis Acid and Base Sites on ZrO_2 for Meerwein-Ponndorf-Verley Reduction. *J. Phys. Chem. C* **2015**, *119(47)*, 26540-26546.

Kuwaharaa, Y.; Kaburagic, W.; Osadac, Y.; Fujitanic, T.; Yamashita, H.; Catalytic transfer hydrogenation of biomass-derived levulinic acid and its esters to γ-Valerolactone over ZrO_2 catalyst supported on SBA-15 silica. *Catal. Tod*. **2017**, *281*, 418-428.

Martin-Luengo, M.A.; Yates, M.; Rojoa, S.E.; Arribas, D.H.; Aguilar, D.; Hitzkya, R.E. Sustainable p-cymene and hydrogen from limonene. *Appl. Catal. A* **2010**, *387*, 141-146.

Mauriello, F.; Ariga, H.; Musolino, M.G.; Pietropaolo, R.; Takakusagi, S.; Asakura, K. Exploring the catalytic properties of supported palladium catalysts in the transfer hydrogenolysis of glycerol. A*ppl. Catal. B Environ*. **2015**, *166-167*, 121-131.

Mauriello, F.; Paone, E.; Pietropaolo. R.; Balu, A.M.; Luque, R. Catalytic Transfer Hydrogenolysis of Lignin-Derived Aromatic Ethers Promoted by Bimetallic Pd/Ni Systems. *ACS Sustain. Chem. Eng*., **2018**, *6(7)*, 9269-9276.

Omoruyi, U.; Page, S.; Hallett, J.; Miller, P.W. Homogeneous Catalyzed Reactions of Levulinic Acid: To γ-Valerolactone and beyond. *ChemSusChem* **2016**, *9(16)*, 2037-2047.

Rietveld, H.M. A profile refinement method for nuclear and magnetic structures. *J. Appl. Cryst.* **1969**, *2*, 65-71.

Tabanelli, T.; Paone, E.; Blair Vásquez, P.; Pietropaolo, R.; Cavani, F.; Mauriello, F. Transfer Hydrogenation of Methyl and Ethyl Levulinate Promoted by a ZrO_2 Catalyst: Comparison of Batch vs Continuous Gas-Flow Conditions. *ACS Sustain. Chem. Eng.* **2019**, *7*, 9937-9947.

Vásquez, P.B.; Tabanelli, T.; Monti, E.; Albonetti, S.; Dimitratos, N.; Cavani, F. Gas-phase catalytic transfer hydrogenation of alkyl levulinates with ethanol over ZrO_2. *ACS Sustain. Chem. Eng*. **2019**, *7(9)*, 8317-8330.

Wang, D.; Astruc, D. The Golden Age of Transfer Hydrogenation. *Chem. Rev.* **2015**, *115(13)*, 6621-6686.

Wragg, D.S.; O'Brien, M.G.; Di Michiel, M.; Lønstad-Bleken, F. Rietveld analysis of computed tomography and its application to methanol to olefin reactor beds. *J. Appl. Cryst.* **2015**, *48*, 1719-1728.

Wright, W.R.H.; Palkovits, R. Development of Heterogeneous Catalysts for the Conversion of Levulinic Acid to γ-Valerolactone. *ChemSusChem* **2012**, *5(9)*, 1657-1667.

Yan, K.; Jarvis, C.; Gu, J.; Yan, Y. Production and Catalytic Transformation of Levulinic Acid: A Platform for Speciality Chemicals and Fuels. *Renew. Sustain. Energy Rev.* **2015**, *51*, 986-997.

Young, R.A.; Prince, E.; Sparks, R.A. Suggested guidelines for the publication of Rietveld analyses and pattern decomposition studies. *J. Appl. Cryst.*, **1982**, *15*, 357-359.

Chapter 5

Conclusions

In this doctoral work, the hydrothermal carbonization process has been investigated for the complete upgrading of the orange peel waste into hydrochar and value-added chemicals. The main processing variables, reaction temperature, initial pH and residence time, affect the mass yield (MY), while the solid:liquid ratio was found insignificant for all L:S investigated. Indeed, there was a strong correlation between temperature and residence time, suggesting that the role of these two variables cannot be analyzed independently. The highest yield of hydrochar is obtained at a 210°C reaction temperature, 180 min residence time, 6:1 w/w orange peel waste to water ratio and a 3.6 initial pH. The results suggest that the conversion of the citrus waste occur during the hydrothermal carbonization process, due to a series of reactions such as decarboxylation, and dehydration, leading to an improvement of the chemical, structural and morphological characteristics of the optimized hydrochar, making it a carbonaceous material suitable for a wide range of applications, both in the chemical and energy fields.

The bio-products distribution strongly depends on the applied reaction conditions. 180 °C was found to be the best reaction temperature that maximizes the production of FU and 5-HMF in the presence of pure water as reaction medium. On the other hand, by using a sulfuric acid solution as reaction media, levulinic acid can be easily obtained as main product. Accordingly, a good production in methyl levulinate and ethyl levulinate can be achieved in the presence of methanol or ethanol, respectively, with the best yield obtained with methanol in the esterification reaction.

In addition, the electrical and electrochemical properties of the various hydrochar samples depend on the hydrothermal treatment temperature, as a consequence of the different surface characteristics observed. Hydrochar sample prepared at 300 °C (HC300) exhibited the best electrical properties and therefore was used for fabricating high performance conductometric sensors for the monitoring of NO_2. This report represents the first example of a hydrochar-based conductometric gas sensor that can successfully be utilized for the environmental monitoring of NO_2 pollutants. The electrochemical characteristics of HC300 hydrochar were also exploited for the fabrication of a high-performance screen-printed electrochemical sensor. The experiments have demonstrated that the hydrochar modified-SPCE presents an enhanced dopamine response compared to the SPCE reference one. The improved electroanalytical properties could be beneficial for other electrochemical sensing applications. We are then confident that this work might open up the opportunity to use the low-cost and waste material from the citrus industry for the green production of hydrochars with outstanding electrical and electrochemical properties and its utilization in chemical sensors.

The last part of the research concerns the possibility to use limonene as starting substrate for the preparation of p-cymene, which is an important intermediate in several industrial catalytic processes, via heterogeneous catalysis. The dehydroaromatization of limonene to p-cymene was carried out over Pd/C catalyst under both batch and gas-flow conditions, using different

alcohols (EtOH and 2-PrOH) and atmospheres (H_2 or N_2). Under batch conditions, it was observed that p-cymene selectivity increased with increasing reaction temperature from 200 to 300 °C. In addition to this, p-menthane was a significant compound both in ethanol and 2-propanol medium. The addition of hydrogen in the atmosphere would not change this reaction pathway, but leads to lower selectivity of p-cymene due to the accelerated hydrogenation rates on the double bonds. Furthermore, limonene conversion in ethanol medium was much better compared with 2-propanol for lower temperatures. The performance under continuous gas-flow conditions confirmed the potential of commercially available Pd/C catalyst for limonene dehydrogenation/disproportionation with the complete selectivity toward p-cymene.

Furthemore, the present investigation was focused also on the performance of the tetragonal ZrO_2 catalyst in the conversion of methyl levulinate and ethyl levulinate in transfer hydrogenation conditions, under both batch and continuous gas-flow conditions.

Under batch conditions, the product selectivity, in the liquid phase, was found to be dependent on the choice of the H source. On using 2-PrOH as H-donor, very high selectivity to GVL was observed, whereas the reactions carried out in EtOH and MeOH were found to be much less efficient.

On the other hand, under continuous gas-flow conditions, high conversions and GVL yield can be obtained using 2-PrOH and EtOH, while poor reactivity with MeOH was observed. Moreover, the ZrO_2 catalyst showed excellent stability for more than 10 hours of time-on-stream and can be easily regenerated *in-situ* by feeding air at 400 °C for 2 h, thus permitting an almost total recovery of the initial catalytic performance.

Both the transfer hydrogenation, ruled by the ability of alcohols as reducing agents, and the transesterification, strongly influenced by the steric hindrance of the H-donor molecule, proved to be competitive procedures.

Others Activities

SCIENTIFIC PRODUCTION

Reverse chronological order

Full paper

Satira, A.; Paone, E.; Bressi, V.; Iannazzo, D.; Marra, F.; Calabrò, P.S.; Mauriello, F.; Espro, C. **Hydrothermal Carbonization as Sustainable Process for the Complete Upgrading of Orange Peel Waste into Value-Added Chemicals and Bio-Carbon Materials**. *Applied Science* **2021**, *11(22)*, 10983.

Espro, C.; **Satira, A.**; Mauriello, F.; Anajafi, Z.; Moulaee, K.; Iannazzo, D.; Neri, G. **Orange peels-derived hydrochar for chemical sensing applications**. *Sensors & Actuators: B. Chemical* **2021**, 341, 130016.

Review

Satira, A.; Espro, C.; Paone, E.; Calabrò, P.S.; Pagliaro, M.; Ciriminna, R.; Mauriello, F. **The Limonene Biorefinery: From Extractive Technologies to Its Catalytic Upgrading into p-Cymene**. *Catalysts* **2021**, 11, 387.

Calabrò, P.S.; **Satira, A**. **Recent advancements toward resilient and sustainable municipal solid waste collection systems**. *Current Opinion in Green and Sustainable Chemistry* **2020**, 26, 100375.

SCIENTIFIC PRODUCTION

1ST PAGE

Reverse chronological order

applied sciences

MDPI

Article

Hydrothermal Carbonization as Sustainable Process for the Complete Upgrading of Orange Peel Waste into Value-Added Chemicals and Bio-Carbon Materials

Antonella Satira [1,2], Emilia Paone [1,3,*], Viviana Bressi [2], Daniela Iannazzo [2], Federica Marra [4], Paolo Salvatore Calabrò [1], Francesco Mauriello [1] and Claudia Espro [2,*]

[1] Dipartimento DICEAM, Università Mediterranea di Reggio Calabria, Loc. Feo di Vito, 89122 Reggio Calabria, Italy; antonella.satira@unirc.it (A.S.); paolo.calabro@unirc.it (P.S.C.); francesco.mauriello@unirc.it (F.M.)
[2] Dipartimento di Ingegneria, Università di Messina, Contrada di Dio—Vill. S. Agata, 98166 Messina, Italy; viviana.bressi@unime.it (V.B.); diannazzo@unime.it (D.I.)
[3] Consorzio Interuniversitario per la Scienza e la Tecnologia dei Materiali (INSTM), 50121 Firenze, Italy
[4] Dipartimento di Agraria, Università Mediterranea di Reggio Calabria, Loc. Feo di Vito, 89122 Reggio Calabria, Italy; fede.marra6@gmail.com
* Correspondence: emilia.paone@unirc.it (E.P.); espro@unime.it (C.E.)

Featured Application: Hydrothermal carbonization process can be efficiently used for the simultaneous production of value-added chemicals, including furans and levulinates, and carbon-based materials.

Abstract: In this study, a simple and green protocol to obtain hydrochar and high-added value products, mainly 5-hydroxymethylfurfural (5-HMF), furfural (FU), levulinic acid (LA) and alkyl levulinates, by using the hydrothermal carbonization (HTC) of orange peel waste (OPW) is presented. Process variables, such as reaction temperature (180–300 °C), reaction time (60–300 min), biomass:water ratio and initial pH were investigated in order to find the optimum conditions that maximize both the yields of solid hydrochar and 5-HMF and levulinates in the bio-oil. Data obtained evidence that the highest yield of hydrochar is obtained at a 210 °C reaction temperature, 180 min residence time, 6/1 w/w orange peel waste to water ratio and a 3.6 initial pH. The bio-products distribution strongly depends on the applied reaction conditions. Overall, 180 °C was found to be the best reaction temperature that maximizes the production of furfural and 5-HMF in the presence of pure water as a reaction medium.

Keywords: orange peel waste (OPW); hydrothermal carbonization; hydrochar; 5-hydroxymethylfurfural (5-HMF); furfural (FU); levulinic acid (LA)

check for updates

Citation: Satira, A.; Paone, E.; Bressi, V.; Iannazzo, D.; Marra, F.; Calabrò, P.S.; Mauriello, F.; Espro, C. Hydrothermal Carbonization as Sustainable Process for the Complete Upgrading of Orange Peel Waste into Value-Added Chemicals and Bio-Carbon Materials. *Appl. Sci.* **2021**, *11*, 10983. https://doi.org/10.3390/app112210983

Academic Editor: Luca Fiori

Received: 19 October 2021
Accepted: 17 November 2021
Published: 19 November 2021

1. Introduction

Citrus fruits are among the most cultivated and processed fruits worldwide, with an annual production of about 152 million tons [1]. The citrus processing industry generates huge amounts of residues mainly in the form of pulp and peels, with the latter accounting for almost 50% of the wet fruit mass [2]. With more than 50 million metric tons in 2020 [3], the juice industry alone generates a huge volume of orange peel waste (OPW) that requires suitable management, taking into consideration the high OPW biodegradability that causes its fast fermentation, which is often uncontrolled. Therefore, the direct disposal of this secondary product without previous proper processing, raises serious environmental issues and economic loss for the citrus industry since traditional disposal strategies, such as incineration or landfilling, are expensive and insufficient in terms of environmental protection and energy efficiency [4,5].

PAPER *Sensors & Actuators: B. Chemical* **2021**, 341, 130016.

Sensors & Actuators: B. Chemical 341 (2021) 130016

Contents lists available at ScienceDirect

Sensors and Actuators: B. Chemical

journal homepage: www.elsevier.com/locate/snb

Orange peels-derived hydrochar for chemical sensing applications

C. Espro [a,*], A. Satira [b], F. Mauriello [b], Z. Anajafi [a], K. Moulaee [a], D. Iannazzo [a], G. Neri [a]

[a] Dipartimento di Ingegneria, Università di Messina, Contrada di Dio–Vill, S. Agata, I-98166, Messina, Italy
[b] Dipartimento DICEAM, Università Mediterranea di Reggio Calabria, Loc. Feo di Vito, I-89122, Reggio Calabria, Italy

ARTICLE INFO

Keywords:
Orange peels
Hydrochar
Hydrothermal treatment
Chemical sensors. NO_2
Dopamine

ABSTRACT

Hydrochar (HC) samples were prepared from orange peels waste (OPW) via hydrothermal carbonization (HTC) at different temperatures, from 180 to 300 °C. The complete characterization of hydrochar samples, carried out by various complementary techniques such as TGA, XRD, SEM-EDX, FT-IR, and BET surface area, highlighted their different morphological and microstructural characteristics. These modifications were also accomplished by variations of the electrical and electrochemical properties, which have been here exploited, for the first time, for the development of high performances chemical sensors based on HC as sensing element. Hydrochar derived from OPW treatment at 300 °C (HC300) showed the best characteristics, and thereby was used for the fabrication of a conductometric NO_2 and electrochemical dopamine sensors. The conductometric HC300-based sensor was demonstrated to be sensitive up to a 50 ppb of NO_2 in air 100 °C. Dopamine at nanomolar concentration was detected with good performances (large linear detection range from 0 to 1000 μM, and low limit of detection (LOD) of 180 nM) on the HC300-based electrochemical sensor. This work might open up the opportunity to use the waste materials from the citrus industry for the green production of hydrochar with outstanding characteristics in advanced research fields so far no reported.

1. Introduction

Carbon- based materials, including active charcoal, carbon nanotubes, and graphene, quite comprise the excellent properties of all the materials on the earth such as lightweight, high porosity, high-temperature resistance, acid and alkali resistance, good structural stability, easy conductivity, easy heat transfer, and easy processing. They have extensively studied for their practical applications in numerous fields such as gas adsorption, electrocatalysts, gas sensors, electrochemical sensors and energy production [1–4]. At present, our society faces the identical tasks of dwindling supply oil resource depletion and waste accumulation, leading to quickly rising raw material costs and more and more expensive and pre-emptive waste disposal legislation, focusing the attention on the possible way to obtain building blocks, for chemicals and biofuels, from renewable lignocellulosic biomass wastes [5,6]. On this account, great efforts are devoted currently to the preparation of novel carbon materials with enhanced characteristics from low-cost and reproducible natural sources.

Biomass - derived carbon materials can be obtained by easy and suitable physical and chemical procedures and can be extensively used as functional materials, as long as a valid strategy for the effective utilization of biomass wastes [7]. In this respect, various organic wastes have been used as precursors to produce carbon-based materials through hydrothermal carbonization, HTC [8,9]. HTC is a type of thermochemical conversion technique, through which biomass can be converted into hydrochar. This process carried out in a water medium under autogenous pressure at a quite low temperature (typically 150 – 300 °C), represents a promising bio-waste treatment technique [10]. The final product, hydrochar, is a carbon solid form, rich in oxygenated functional groups, and shows attractive features attracting considerable attention for potential applications in substitution of carbon materials like carbon nanotubes, graphene, and others [7–10].

Despite the numerous properties and applications of biomass - derived carbon materials that have been thoroughly studied, remain still chances for their use in higher- value technologies not yet broadly explored, e.g., such as their use in the fields of electrochemical sensors. Here, we report an investigation on the preparation of hydrochar obtained from orange peels waste (OPW). Orange is among the most worldwide cultivated fruit. The global orange production is estimated over 55 million metric tons for 2020, and the processing industry yearly generates huge amounts of agricultural waste (peel, pulp, etc.). OPW alone accounts for almost 50 % of the wet fruit mass. The direct disposal

* Corresponding author.
E-mail address: espro@unime.it (C. Espro).

https://doi.org/10.1016/j.snb.2021.130016
Received 21 November 2020; Received in revised form 17 April 2021; Accepted 19 April 2021
Available online 22 April 2021

catalysts

MDPI

Review

The Limonene Biorefinery: From Extractive Technologies to Its Catalytic Upgrading into p-Cymene

Antonella Satira [1], Claudia Espro [2,*], Emilia Paone [3], Paolo Salvatore Calabrò [1], Mario Pagliaro [4], Rosaria Ciriminna [4,*] and Francesco Mauriello [1,*]

[1] Dipartimento di Ingegneria Civile, dell'Energia, dell'Ambiente e dei Materiali (DICEAM), Università Mediterranea di Reggio Calabria, Via Graziella, loc. Feo di Vito, I-89124 Reggio Calabria, Italy; antonella.satira@unirc.it (A.S.); paolo.calabro@unirc.it (P.S.C.)
[2] Dipartimento di Ingegneria, Università degli Studi di Messina, Contrada di dio, I-98158 Sant' Agata di Militello, Messina, Italy
[3] Dipartimento di Ingegneria Industriale (DIEF), Università degli Studi di Firenze, Via di S. Marta 3, I-50139 Firenze, Italy; emilia.paone@unifi.it
[4] Istituto per lo Studio dei Materiali Nanostrutturati, CNR, Via U. La Malfa 153, I-90146 Palermo, Italy; mario.pagliaro@cnr.it
* Correspondence: espro@unime.it (C.E.); rosaria.ciriminna@cnr.it (R.C.); francesco.mauriello@unirc.it (F.M.)

Abstract: Limonene is a renewable cyclic monoterpene that is easily obtainable from citrus peel and it is commonly used as a nutraceutical ingredient, antibacterial, biopesticide and green extraction solvent as well as additive in healthcare, fragrance and food and beverage industries for its characteristic lemon-like smell. Indeed, the lack of toxicity makes limonene a promising bio-alternative for the development of a wide range of effective products in modern biorefineries. As a consequence, industrial demand largely exceeds supply by now. Limonene can be also used as starting substrate for the preparation of building block chemicals, including p-cymene that is an important intermediate in several industrial catalytic processes. In this contribution, after reviewing recent advances in the recovery of limonene from citrus peel and residues with particular attention to benign-by-design extractive processes, we focus on the latest results in its dehydrogenation to p-cymene via heterogeneous catalysis. Indeed, the latest reports evidence that the selective production of p-cymene still remains a scientific and technological challenge since, in order to drive the isomerization and dehydrogenation of limonene, an optimal balance between the catalyst nature/content and the reaction conditions is needed.

Keywords: limonene; green extraction; essential oil; citrus processing waste; p-cymene

Citation: Satira, A.; Espro, C.; Paone, E.; Calabrò, P.S.; Pagliaro, M.; Ciriminna, R.; Mauriello, F. The Limonene Biorefinery: From Extractive Technologies to Its Catalytic Upgrading into p-Cymene. *Catalysts* **2021**, *11*, 387. https://doi.org/10.3390/catal11030387

Academic Editor: Diego Luna

Received: 15 February 2021
Accepted: 16 March 2021
Published: 18 March 2021

1. Introduction

The chemical conversion (upgrade) of lignocellulosic biomasses and wastes for the production of fuels and chemical building blocks, the so-called "biorefinery", has been widely explored in the last two decades [1,2]. Modern biorefineries already use cellulose, hemicellulose and lignin (the three-key components of lignocellulose) as starting feedstocks for the preparation of furans, polyols, acids and aromatics [3–5]. However, other important platform chemicals can be easily extracted from biomass-derived wastes and residues and used as biobased building blocks for the preparation of value-added intermediates, products, renewable energy and biofuels, supporting and slowly replacing the well-assessed technologies that gave a great contribution to these fields [6–10].

In this context, limonene (1-methyl-4-(1-methyl phenyl) cyclohexene), the main constituent of citrus essential oil (around 68–98% *w*/*w*) is industrially derived from the citrus industry from orange processing waste [11]. An optically active cyclic monoterpene that exists in two enantiomeric forms, *R*-limonene (the predominant isomeric form in citrus varieties, also known as *d*-limonene) and *S*-limonene (the less common isomer found in

Available online at www.sciencedirect.com

ScienceDirect

Current Opinion in Green and Sustainable Chemistry

Recent advancements toward resilient and sustainable municipal solid waste collection systems

P. S. Calabrò and A. Satira

The municipal solid waste (MSW) management is one of the major issues on the planet, but it is also a potential major source of resources for circular economy. This paper covers recent technical-scientific advancements related to (i) the choice of the MSW collection system between single stream and systems relying on separate collection; (ii) the customer engagement in advanced MSW collection systems; and (iii) the role of the informal sector for sustainable MSW management systems in developing countries. The current opinion on these issues is that separate collection gives superior results, but it needs a strong customer commitment that can be primarily obtained through information and educational campaigns. For countries that are still developing their MSW management systems, the inclusion of the informal sector is considered essential for obtaining resilient and sustainable systems.

Addresses
Department of Civil, Energy, Environmental and Materials Engineering, Università Mediterranea di Reggio Calabria, via Graziella – loc. Feo di Vito, 891 22, Reggio Calabria, Italy

Corresponding author: Calabrò, P.S (paolo.calabro@unirc.it)

Current Opinion in Green and Sustainable Chemistry 2020, **26**:100375

This review comes from a themed issue on **Recycling and reuse**

Edited by **Veena Sahajwalla, Samane Maroufi** and **Francesco Mauriello**

Available online 23 June 2020

For complete overview of the section, please refer the article collection - Recycling and reuse

https://doi.org/10.1016/j.cogsc.2020.100375

Introduction

According to the UN estimates, thanks to rapid technological and political improvements experienced in the 20th and 21st centuries, world population increased from $1.6 \cdot 10^9$ to about $7.5 \cdot 10^9$. In the same period, urban population increased from about 15% to more than 50% of the total; this fact caused a dramatic rise of municipal solid waste (MSW) generation. The efficient and timely management of MSW is imperative because of the inherent risk for human health and to the potential pollution of environmental matrices [1,2].

However, it is also clear that waste has a great potential for circular economy because the huge amount of raw materials and energy present in the MSW are essential for a successful application of this economic theory [3–6].

The waste management hierarchy [4], globally accepted and included in most of the environmental regulations worldwide, ranks the waste management options and establishes that the most preferable option is the source reduction of waste (avoidance), the second is reuse (goods are put on the market after refurbishment), followed by recycling (materials recovery) and energy recovery (through combustion mainly) while the least preferable option is landfilling. Waste collection is essential for waste that cannot be avoided or reused: through collection, waste enters in the waste management system and can be then correctly treated for valorization or disposal.

One of the most serious issues on global MSW management is still the coverage of the waste management service; it is esteemed that 3 billion people, especially in developing countries, are not served by an organized, 'formal' system but by 'informal systems' and local open dumps where waste are deposited by citizens without any control. In poorly serviced areas, the informal sector operation is the only effort for recovery of recyclables from waste [7–12].

Several systems have been implemented to collect MSW; the main options are drop-off centers, bins, and door-to-door (curbside) collection systems (Figure 1). These collection systems can be integrated together to develop advanced collection systems [13–16].

Drop-off centers (also called ecological islands) require the waste producer to carry the MSW to a fixed or mobile collection system according to local rules.

Bin collection (in some papers in the literature, it is called curbside/kerbside collection) is based on the positioning of containers (bins of various sizes and types) in streets. They are destined to the general public; customers can deposit their waste in the containers that are periodically emptied by dedicated trucks (compactors generally).

Door-to-door/curbside systems [13,17,18] differ from conventional bin collection systems basically because street bins are substituted by smaller containers managed by single customers (e.g. households, shops,

ATTENDANCE AT CONFERENCES

Reverse chronological order

XXVII SCI Congress
Virtual meeting
14th - 23th September **2021**
Oral Speech
Tandem Catalytic Upgrading of Limonene and Methyl Levulinate promoted by Pd-based Catalysts
A. Satira, E. Paone, C. Espro, T. Tabanelli, A. Allegri, S. Albonetti, F. Mauriello and F. Cavani

XII National Congress AICIng
Reggio Calabria,
Italy
5th - 8th September **2021**
Poster
Orange peels-derived hydrochar for chemical sensing applications
A. Satira, C. Espro, F. Mauriello, Z. Anajafi, K. Moulaee, D. Iannazzo and G. Neri

SCI Interdivisional Group of Catalysis
Reggio Calabria,
Italy
27rd –30th July **2021**
Scientific competition

SCI Abruzzo Workshop
Virtual meeting
5th –6th July **2021**
Oral Speech
Chemicals from biomass: the transformation of orange peel waste into high added value products by hydrothermal carbonization (HTC) process
A. Satira, C. Espro, F. Mauriello, Z. Anajafi, K. Moulaee, D. Iannazzo and G. Neri

SCI Gruppo Giovani Workshop
Rimini,
Italy
25th –27th November **2019**
Oral Speech
Catalytic conversion of levulinic acid into γ-valerolactone under transfer hydrogenation conditions
A. Satira, E. Paone, M. G. Musolino and F. Mauriello

XII National Congress AICIng
Reggio Calabria,
Italy
27th - 29th June **2019**
Poster
Produzione di γ-valerolattone a partire da acido levulinico e promossa da catalizzatori eterogeni a base di Pd e di Ru
A. Satira, E. Paone, M. G. Musolino and F. Mauriello

ATTENDANCE AT DOCTORAL SCHOOLS

6rd SINCHEM Doctorate Winter School
Bologna,
Italy
4th - 6th February **2020**